Fangfang Guo

Geochemistry of Archaean and Palaeoproterozoic mafic-ultramafic rocks in NE Fennoscandia and implications for their Ni-Cu-PGE prospectivity

Fangfang Guo

Geochemistry of Archaean and Palaeoproterozoic mafic-ultramafic rocks in
NE Fennoscandia and implications for their Ni-Cu-PGE prospectivity

Res Terrae, Ser. A, No. 50, OULU, 2024

Cover Figure:

A field photo of spinifex texture in a komatiitic lava flow of the Sovdozero area.

Fangfang Guo

Geochemistry of Archaean and Palaeoproterozoic mafic-ultramafic rocks in NE Fennoscandia and implications for their Ni-Cu-PGE prospectivity

Academic dissertation to be presented with the assent of the Doctoral Training Committee of Technology and Natural Sciences of the University of Oulu for public defence in auditorium L5, University of Oulu, on November 5th , 2024 at 12 o'clock.

University of Oulu

Oulu, 2024

Geochemistry of Archaean and Palaeoproterozoic mafic-ultramafic rocks in NE Fennoscandia and implications for their Ni-Cu-PGE prospectivity

Fangfang Guo

University of Oulu Graduate School; University of Oulu, Faculty of Technology, Oulu Mining School, Geoscience Research Unit
P.O.Box 3000, FI-910014 University of Oulu, Finland

Abstract

Northeastern Fennoscandia contains multiple generations of extrusive and intrusive mafic-ultramafic magmatism in the Archaean greenstone belts and Palaeoproterozoic rift-related basins, resulting in the formation of many mineral deposits. This study is focused on the geochemistry of the mafic-ultramafic rocks to constrain the petrogenesis and ore potential of different magmatic events and to identify key factors in ore formation which have potential implications for exploration. The study is sub-divided into three parts focusing on 1) Archaean komatiites in Russian Karelia, 2) Palaeoproterozoic dyke swarms in NE Fennoscandia, and 3) Palaeoproterozoic basaltic, komatiitic and picritic metavolcanites in several rift-related supracrustal belts in NE Fennoscandia.

Samples of Archaean komatiites and komatiitic basalts from the Vedlozero-Segozero and Tikshozero greenstone belts in Russian Karelia were analysed for their major, trace and chalcophile element contents. The results indicate a lack of both enrichment or depletion of chalcophile elements in the analysed samples. With the exception of localised mobility of Pd, Cu and Au during alteration and metamorphism, the behaviour of platinum-group elements (PGE) in these rocks is largely consistent with the fractionation of chromite and platinum-group minerals (PGM). The apparent paucity of dynamic lava channel environments, as indicated by the scarcity of olivine-rich adcumulates, and the lack of exposed sulphidic sedimentary rocks in the region lead to the conclusion that the potential of the Archaean greenstone belts in Russian Karelia to host Ni-Cu sulphide mineralisation is relatively low.

During the Palaeoproterozoic, the Karelian craton underwent several rifting events. In this study, they are divided into early (2.5−2.3 Ga), middle (2.3−2.06 Ga) and late (2.06−1.94 Ga) stages of rifting. During the early-stage rifting at 2.5–2.45 Ga, two main magma types were identified in a suite of dykes, siliceous high-magnesian basalt (SHMB) and tholeiitic basalt. The SHMB group shows large variation in trace element ratios (e.g., La/Sm, Th/Nb) and high initial $^{87}Sr/^{86}Sr$ ratios from 0.7028 to 0.7036. These features are consistent with crustal contamination of a mantle-derived magma, which was confirmed by thermodynamic modelling. The preferred model for the formation of SHMB-group dykes involves crustal contamination of a komatiitic magma in the deeper crust at a pressure of ca. 300 MPa followed by fractional crystallisation at a shallower depth, at a pressure of ca. 100 MPa. In contrast, the magma of the tholeiitic group mainly experienced fractional crystallization with less crustal contamination.

Based on trace element and isotope characteristics, the SHMB dykes are suitable candidates for the parental magmas to some of the Finnish PGE-mineralised layered intrusions (e.g., Penikat and Portimo), whereas the tholeiitic dykes may represent the parental magma to the Tsipringa layered intrusion in Russian Karelia. Both the SHMB and tholeiitic dyke types are fertile with respect to PGE, suggesting that the magmas remained sulphide undersaturated during mantle melting and *en route* to the upper crust. This interpretation is consistent with the fact that most of the ~2.45 Ga

Fennoscandian layered intrusions contain PGE mineralisation. Sulphide melt saturation in the dykes and layered intrusions was mostly attained after their final emplacement, likely due to crystal fractionation.

The mafic volcanic rocks of the middle-stage rifting (Jatulian stage, 2.3–2.06 Ga) are contemporaneous with wide-spread mafic dyke swarms across the Karelian craton. Volcanic rocks from different belts show variable depletion or enrichment in LREE. These features probably indicate diverse mantle sources, which have experienced variable extents of earlier melt extraction. New PGE data show that the magmas of this stage in both the Peräpohja and Kuusamo belts are clearly richer in Pt and Pd compared to global basaltic volcanic rocks. However, low Cu/Pd ratios together with high PGE contents and positive correlation between PGE and Cu with Zr, indicate that sulphide saturation did not widely occur at this stage.

In the late-stage rifting event (2.06–1.98 Ga), the magmas in the Central Lapland Greenstone Belt (CLGB) also show unusual high PGE contents, but with a higher Pt/Pd ratio than in the Jatulian stage. Sulphide saturation occurred widely in both primitive and evolved magmas in the CLGB, the Pechenga belt and the Kiiminki belt, reflected by high Cu/Pd ratios and PGE depletion, consistent with the formation of many significant Ni-Cu-(PGE) sulphide deposits in this stage. The oceanic plateau-related mafic volcanic rocks in the Kittilä belt in northern Finland show variable PGE contents and Cu/Pd ratios, indicating a PGE-rich primitive magma from which sulphide melt locally segregated. This also indicates some potential for exploration of Ni-Cu-PGE sulphide deposits in palaeo-oceanic environments, though the major deposits are generally considered to have formed in a continental environment.

The unusually high PGE contents (up to 32 ppb Pd and 24 ppb Pt at MgO of 10.8 wt.%) of mafic rocks in both the middle and late rifting stages in NE Fennoscandia is interpreted to be the result of a mantle source enriched in undissolved late veneer. The large variation of Pt/Pd ratio in these magmas could indicate the contribution of metals from diverse types of meteorites. If correct, the model would imply that the homogenization of late veneer materials in the Earth's mantle may have been operating until at least Palaeoproterozoic, i.e. much longer than the previously considered.

The differences in the ore-formation potential from the early to the late stage of rifting may be largely controlled by the lithospheric structure. During the early stage of rifting the lithosphere was still relatively thick, permissive to the formation of large, slowly cooling magma chambers in which magmas could fractionate extensively to form reef-type PGE sulphide deposits. Progressive extension during the middle stage of rifting weakened and thinned the lithosphere, preventing the formation of large magma chambers in the upper crust. During the late-stage rifting, interaction of magmas with sulphur-rich sediments deposited in deep rift basins allowed the formation of Ni-Cu-dominated sulphide deposits in magma conduits.

Arkeeisten ja Paleoproterotsooisten mafis-ultramafisten kivien geokemia Fennoskandian koillisosassa ja sen suhde kuparin, nikkelin ja platinametallien löytömahdollisuuksiin

Fangfang Guo

Oulun yliopiston tutkijakoulu, Oulun yliopisto, Teknillinen tiedekunta,
Kaivannaisalan yksikkö, Geotieteet
PL 3000, FI-90014 Oulun yliopisto, Suomi

Tiivistelmä

Koillisen Fennoskandian arkeeisissa vihreäkivivyöhykkeissä ja paleoproterotsooisissa repeämäaltaissa on useita generaatioita ekstrusiivista ja intrusiivista magmatismia, joihin liittyy useita malmiesiintymiä. Tämä tutkimus kohdistuu mafis-ultramafisten kivien geokemiaan tarkoituksena selvittää eri magmaattisten tapahtumien syntyä ja malmipotentiaalia ja identifioida malminmuodostuksen avaintekijöitä, joilla on malminetsinnällistä merkitystä. Tämä työ koostuu kolmesta osasta, jotka käsittelevät 1) arkeeisia komatiitteja Venäjän Karjalassa, 2) paleoproterotsooisia juoniparvia koillisessa Fennoskandiassa ja 3) paleoproterotsooisia basalttisia, komatiittisia ja pikriittisiä metavulkaniitteja useissa repeämiseen liittyvissä suprakrustisissa vyöhykkeissä koillisessa Fennoskandiassa.

Tässä tutkimuksessa määritettiin pää- ja hivenalkuainekoostumuksia sekä kalkofiilisten alkuaineiden pitoisuuksia komatiiteissa ja komatiittisissa basalteissa Vedlozero-Segozeron and Tikshozeron vihreäkivivyöhykkeiltä Venäjän Karjalasta. Tulokset osoittavat, että analysoiduissa näytteissä ei ole merkittävää kalkofiilisten alkuaineiden rikastumista tai köyhtymistä. Lukuun ottamatta paikallista Pd:n, Cu:n ja Au:n mobilisoitumista muuttumisprosesseissa ja metamorfoosissa platinaryhmän metallien käyttäytyminen näissä kivissä on selitettävissä kromiitin ja platinaryhmän mineraalien (PGM) kiteytymisen kautta. Dynaamisten laavakanavaympäristöjen vähäisyys päätellen oliviinirikkaiden adkumulaattien harvinaisuudesta sekä paljastuneiden sulfidirikkaiden sedimenttien puuttuminen tutkimusalueelta viittaa siihen, että Venäjän Karjalan arkeeisten vihreäkivivyöhykkeiden potentiaali sisältää Ni-Cu-mineralisaatioita on suhteellisen alhainen.

Karjalan kratoni koki useita repeämistapahtumia paleoproterotsooisena aikakautena. Tässä tutkimuksessa ne on jaettu varhaisen vaiheen (2,5−2,3 Ga), keskivaiheen (2,3−2,06 Ga) ja myöhäisen vaiheen (2,06−1,94 Ga) repeämisiin. Varhaisen vaiheen aikana 2,5–2,45 miljardia vuotta sitten syntyneissä juonikivissä on erotettu kaksi magman päätyyppiä: pii- ja magnesiumrikas basaltti (SHMB) ja tholeiittinen basaltti. SHMB-ryhmän juonilla on suuri vaihtelu hivenalkuainesuhteissa (esim. La/Sm, Th/Nb) ja korkeat initiaaliset $^{87}Sr/^{86}Sr$-suhteet vaihdellen välillä 0,7028−0,7036. Nämä piirteet ovat sopusoinnussa vaippaperäisen magman kuorellisen kontaminaation kanssa, mikä on myös vahvistettu termodynaamisen mallintamisen avulla. Parhaana mallina SHMB-ryhmän juonien synnylle pidetään komatiittisen magman syvällä kuoressa, 300 MPa:n paineessa tapahtunutta kuorellista kontaminaatiota, jota seurasi fraktioiva kiteytyminen ylempänä kuoressa noin 100 MPa:n paineessa. Sitä vastoin tholeiittisen ryhmän magma kävi läpi pääasiassa fraktioivaa kiteytymistä kuorellisen kontaminaation määrän ollessa vähäisempää.

Hivenalkuaine- ja isotooppikoostumusten perusteella SHMB-juonet ovat sopivia kandidaatteja kantamagmalle, joka tuotti joitakin suomalaisia PGE-mineralisoituneita kerrosintruusioita (esim. Penikat ja Portimo), kun taas tholeiittiset juonet voivat edustaa kantamagmaa Tsipringan

kerrosintruusiolle Venäjän Karjalassa. Sekä SHMB-juonet että tholeiittiset juonet ovat fertiilejä PGE:n suhteen, mikä viittaa siihen, että niiden magmat pysyivät sulfidin suhteen alikylläisinä niiden syntyessä vaipassa ja noustessa yläkuoreen. Tämä tulkinta on sopusoinnussa sen kanssa, että useimmat ~2,45 Ga:n ikäiset kerrosintruusiot Fennoskandiassa sisältävät PGE-mineralisaatioita. Sulfidikylläisyyden saavuttaminen juonissa ja kerrosintruusioissa tapahtui niiden lopullisen paikalleen asettumisen jälkeen todennäköisesti fraktioivan kiteytymisen kautta.

Keskivaiheen repeytymiseen (Jatulinen vaihe, 2,3–2,06 Ga) liittyvät mafiset vulkaaniset kivet ovat samanikäisiä laajalle levinneiden mafisten juoniparvien kanssa läpi Karjalan kratonin. Vulkaaniset kivet eri vyöhykkeillä osoittavat vaihtelevaa keveiden lantanidien (LREE) köyhtymistä tai rikastumista. Nämä piirteet todennäköisesti indikoivat erilaisia vaipan lähteitä, jotka olivat kokeneet aikaisempia, vaihtelevan asteisia sulamistapahtumia. Uudet PGE-analyysit osoittavat, että tämän vaiheen magmoissa Peräpohjan ja Kuusamon vyöhykkeillä on selvästi korkeammat Pt- ja Pd-pitoisuudet verrattuna globaaleihin basalttisiin vulkaanisiin kiviin. Alhaiset Cu-Pd-suhteet yhdessä korkeiden PGE-pitoisuuksien ja PGE:n, Cu:n ja Zr:n välillä olevan positiivisen korrelaation kanssa kuitenkin indikoivat, että kylläisyyttä sulfidin suhteen ei tapahtunut laajalti tässä vaiheessa.

Myöhäisen repeämistapahtuman aikana (2,06–1,98 Ga) syntyneillä Keski-Lapin vihreäkivivyöhykkeen (CLGB) magmoilla on myös epätavallisen korkeita PGE-pitoisuuksia, mutta niillä on korkeammat Pt/Pd-arvot kuin Jatuli-vaiheen vulkaniiteilla. Sulfidin kylläisyys saavutettiin laajalti sekä primitiivisissä että kehittyneissä magmoissa CLGB:ssä sekä Petsamon ja Kiimingin vyöhykkeissä, mikä heijastuu korkeissa Cu/Pd-suhteissa ja PGE:n köyhtymisenä, mikä on sopusoinnussa monien Ni-Cu-(PGE)-malmien muodostumisen kanssa tässä vaiheessa. Kittilän vyöhykkeessä Pohjois-Suomessa esiintyvillä, merelliseen tasankoon liittyvillä mafisilla vulkaniiteilla on vaihtelevia PGE-pitoisuuksia ja Cu/Pd-suhteita indikoiden PGE-rikasta magmaa, josta sulfidisula on paikallisesti erottunut. Tämä myös indikoi jonkinlaista potentiaalia Ni-Cu-PGE-sulfidiesiintymisen löytymiselle paleomerellisessä ympäristössä, vaikkakin suuret esiintymät ajatellaan yleisesti muodostuneen mantereisessa ympäristössä.

Mafisten kivien epätavallisen korkeat PGE-pitoisuudet (maksimissaan 32 ppb Pd ja 24 ppb Pt MgO-tasolla 10,8 p.-%) keski- ja myöhäisvaiheen repeämisen aikana koillisessa Fennoskandiassa ovat tulkittu johtuvaksi vaipan lähteen rikastumisesta metalleista, jotka tulivat maaplaneetalle sen ytimen muodostumisen jälkeen myöhäisen meteoriittipommituksen tuloksena (late veneer -hypoteesi). Näissä magmoissa todettu laaja vaihtelu Pt/Pd-suhteessa voisi johtua metalleista, jotka ovat peräisin erityyppisistä meteoriiteista. Jos näin on, tämä malli tarkoittaisi, että myöhäisessä pommituksessa tulleen materiaalin homogenisoituminen maan vaipassa olisi kestänyt ainakin paleoproterotsooiselle aikakaudella saakka eli paljon pitempään kuin on aikaisemmin ajateltu.

Erot varhais-, keski- ja myöhäisvaiheen malmipotentiaalissa voivat johtua litosfäärin rakenteesta. Varhaisen vaiheen repeämisen aikana litosfääri oli vielä suhteellisen paksu, mikä mahdollisti suurten, hitaasti jäähtyvien magmasäiliöiden synnyn, joissa magma saattoi fraktioitua pitkälle ja muodostaa reef-tyyppisiä PGE-sulfidiesiintymiä. Etenevä ekstensio keskivaiheen repeytymisessä heikensi ja ohensi litosfääriä estäen suurten magmasäiliöiden synnyn yläkuoreen. Myöhäisen vaiheen repeytymisessä magmojen vuorovaikutus sulfidirikkaiden sedimenttien kanssa syvissä repeämäaltaissa mahdollisti Ni-Cu-sulfidimalmien muodostumisen magman tulokanavissa.

Asiasanat: Arkeeinen, paleoproterotsooinen, platinaryhmän metallit, Ni-Cu-malmit, mafis-ultramafiset vulkaniitit, mafiset juonet, mantereinen repeytyminen, vaipan lähde, magman fertiliteetti, malminmuodostuskriteerit, Fennoscandia

Acknowledgements

Abbreviations

FTH   Fe-tholeiite

GBNO   Gabbronorite

IPGE   Iridium group elements

LTTH   Low-Ti tholeiite

MCS   Magma Chamber Simulator

PGE   Platinum-group elements

PGM   Platinum-group minerals

PM   Primitive mantle

PPGE   Palladium-group elements

SCLM   Subcontinental lithospheric mantle

SHMB   Siliceous high-magnesian basalt

Original publications

Paper I: Guo, F.F., Svetov, S., Maier, W.D., Hanski, E., Yang, S.H., Rybnikova, Z., 2020. Geochemistry of komatiites and basalts in Archean greenstone belts of Russian Karelia with emphasis on platinum-group elements. Mineralium Deposita 55, 971–990

Paper II: Guo, F.F., Maier, W.D., Heinonen J.S., Hanski, E., Vuollo J., Barnes S.-J., Lahaye, Y., Huhma, H., Yang, S.H., 2023. Geochemistry of 2.45 Ga mafic dykes in northern Finland: constraints on the petrogenesis and PGE prospectivity of coeval layered intrusions. Lithos 452–453, Article 107206

Paper III: Guo, F.F., Hanski, E., Maier, W.D., Yang, S.H., Barnes, S., manuscript. PGE geochemistry of Palaeoproterozoic mafic and ultramafic volcanic rocks from northern Finland: implications for exploration of magmatic sulphide deposits.

For papers I, II and manuscript III, F.F. Guo had the main responsibility for the manuscript preparation and interpretation of the results. The main scope of paper I, II and III was planned by F.F. Guo, W.D. Maier, E. Hanski and S.H. Yang. For paper I, samples were provided by S. Svetov and Z. Rybnikova and a field trip to Russia was guided by S. Svetov. In Paper II, the samples were the same used previously by J. Vuollo in his dyke research, and the samples and some thin sections were provided by the Geological Survey of Finland (GTK). The EPMA analyses of paper II were conducted mainly by F.F. Guo. The LA-ICP-MS analyses were done by F.F. Guo with help of Y. Lahaye. The thermodynamic modelling using Magma Chamber Simulator (MCS) received help from J. Heinonen. S.-J. Barnes's laboratory carried out the PGE analyses and contributed to the interpretation of the PGE data. H. Huhma conducted the Sm-Nd isotope analyses, and helped with the interpretation of data. For paper III, sampling was carried out by E. Hanski and W. Maier. All co-authors have contributed to the writing and revision of the three articles.

Contents

1. Introduction

Magmatic sulphide deposits hosted by mafic-ultramafic rocks are important raw material sources for the green energy transition (e.g., Ni, Co, Cu, PGE), including mainly komatiite-hosted, Ni-dominated sulphide deposits, Ni-Cu-dominated, conduit-type deposits, and layered intrusion-hosted PGE-dominated sulphide deposits (Naldrett, 2004). In NE Fennoscandia, there are multiple generations of mafic-ultramafic magmatism from the Archaean greenstone belts to Palaeoproterozoic rift-related basins, hosting several important mineral deposits, such as Kevitsa, Sakatti, Penikat, and Portimo in Finland (Barnes et al., 2001; Hanski et al., 2011; Maier and Hanski, 2017; Luolavirta et al., 2018; Iljina et al., 2015; Karinen, 2010) and Pechenga, Monchegorsk, and Fedorovo-Pana in the Russian part of the shield (Bayanova et al., 2009; Groshev et al., 2019; Mitrofanov et al., 2019; Pripachkin et al., 2023). However, poor exposure in many parts of this region has made exploration challenging. Moreover, the petrogenesis and key ore-formation criteria of these deposits remain uncertain, and as a result a clear exploration model is lacking. Thus, more efficient exploration targeting for this types of deposits is becoming important.

This research was designed to test whether one can constrain the regional prospectivity for Ni-Cu-PGE in NE Fennoscandia by using noble metals and other geochemical data from mafic-ultramafic volcanic rocks and dykes as pathfinder elements, as these rocks are potentially co-genetic with the ore deposits. The hypothesis is that for Ni-Cu-PGE deposits, the controlling factor is either association with, or proximity of fertile (noble metal rich) mafic-ultramafic magmas. It has been suggested that Ni-Cu-dominated deposits form when fertile mantle-derived magmas interact with S-rich crustal rocks, and PGE deposits form when fertile magmas pond and form large layered intrusions at certain geological conditions. Thus, I generated high-quality compositional data, including whole-rock major element, lithophile trace element and PGE concentrations, as well as mineral geochemistry and in-situ Sr isotope composition of plagioclase, which together with existing databases were used to constrain the mantle source, fertility and sulphide saturation history of the magmas and their potential to form magmatic sulphide deposits in different stages of the Archaean greenstones and Palaeoproterozoic rifting in NE Fennoscandia.

The dissertation consists of three main parts: 1) Using the platinum-group element geochemical features of Archaean komatiites in Russian Karelia to evaluate their prospectivity for Ni-Cu sulphide mineralisation prospectivity; 2) using the geochemical features of the 2.45 Ga mafic dykes in northern Finland to constrain their petrogenesis as well as PGE prospectivity of coeval layered intrusions; 3) By studying the geochemistry of the Palaeoproterozoic mafic-ultramafic

volcanic rocks from various belts in NE Fennoscandia to constrain the fertility and sulphide saturation history of the magmas and their potential to form magmatic sulphide deposits in different rifting stages.

2. Generation of magmatic Ni-Cu-PGE sulphide deposits

2.1 General information on magmatic Ni-Cu-PGE sulphide deposits

Mafic and ultramafic igneous rocks are important hosts to resources of many metals, such as Ni, Cu, Co, Cr, PGE, as well as Ti, V and Au. Magmatic sulphide ore deposits can be subdivided into two subgroups based on their sulphide content, metal association and geological occurrence. The first type includes sulphide-rich (>10%), Ni-Cu-dominated deposits with Co and PGE as by-products, as exemplified by Noril'sk in Russia, Jinchuan in China, Kevitsa and Sakatti in Finland, and Kambalda in Australia (Naldrett, 2004; Barnes et al., 2016; Smith and Maier, 2021). The second type consists of sulphide-poor (<5% sulphide), PGE-dominated deposits with Ni, Cu, Co and Au as by-products, such as Bushveld, Great Dyke, Stillwater, Skaergaard and Penikat (Naldrett, 2004; Barnes and Lightfoot, 2005). Both deposit types were formed from primitive, relatively magnesian, metal-rich mantle-derived magmas after a high degree of partial melting of mantle (Keays, 1995). One exception is the Sudbury Ni-Cu-PGE deposit, in which the magma is relatively less mafic and was generated by melting of crustal materials due to impact of an asteroid (Eckstrand, 1996; Naldrett, 2004).

The Ni-Cu-dominated sulphide deposits can be further divided into two subgroups including komatiite-related sulphide deposits (IA) occurring in a channelised lava flow environment on the Earth's surface, and basalt-related deposits (IB) normally occurring in magma feeder conduits (Barnes and Lightfoot, 2005). Komatiite-related deposits, such as Kambalda and Black Swan in the Yilgarn craton, Australia, and Alexo and Shebandowan in the Abitibi greenstone belt, Canada (Naldrett, 2004, and references therein), are characterised by a relatively high Ni/Cu ratio (up to 10), which is inherited from the chemical composition of the parental magma. These deposits have a high Ni grade and are important resources of Ni (Barnes and Lightfoot, 2005; Naldrett, 2010).

There are also occurrences of komatiite-hosted Ni sulphide deposits in Fennoscandia, though their size is normally relatively small, with only one ore body (Tainiovaara deposit 20,000 t at 1.4 wt.% Ni and 0.12 wt.% Cu, Puustinen et al., 1995) having been mined in the late 1980's (Vanne, 1981; Papunen, 1989). However, it is still controversial whether the large Sakatti deposit (44.4 Mt at

0.96 wt.% Cu and 1.90 wt.% Ni) is hosted by a komatiitic lava flow or an intrusive body (Makkonen et al., 2017). Basalt-related deposits display large variation in Ni/Cu, though this ratio is generally lower (<2) than in komatiite-related deposits due to a variable degree of differentiation of the magma, such as in the case of Noril'sk in Russia (Li et al., 2009), Jinchuan in China (Chai and Naldrett, 1992), and Nebo Babel in Australia (Seat et al., 2007). The parental magma of these deposits can be (ferro)picrite, high-magnesium basalt, or fractionated basalt.

The PGE-dominated deposits generally occur in large mafic layered intrusions representing fossilised large magma chambers. The intrusions are generally well layered and their sizes can vary from 10s of kms to 100s of kms along strike and thicknesses from hundreds of metersto >10 km. As mentioned previously, this deposit type is characterised by a relatively low abundance of sulphide minerals, normally less than 5%, or in some cases less than 1%. However, the PGE tenor tends to be very high, reaching 100s of ppm (Godel et al., 2007; Naldrett et al., 2009; Mansur et al., 2021). On the other hand, the bulk-rock Ni and Cu contents are not very high and therefore they are normally mined as by-products. PGE-dominated sulphide deposits can be further subdivided into three types: reef-type, contact-type (or marginal-type) and offset-type deposits. The reef-type PGE deposits are characterised by a thin mineralised interval (e.g., 1–2 meters) but can be traced along the whole strike of an intrusion. Based on the host rocks, reef-type deposits can be associated with chromitite (e.g., UG2 reef in Bushveld, Junge et al., 2015), pyroxenite or peridotite (e.g., Merensky reef in Bushveld, main sulphide zone in Great Dyke, Wilson et al., 1989), or magnetite cumulate (e.g., Stella, Maier et al., 2003, 2023; Skaergaard, Keays and Tegner, 2015). The silicate-hosted PGE reefs tend to be more sulphide rich (typically 1–5%) than reef-type PGE deposits hosted by chromitite or magnetite which have mostly very low sulphide contents (<0.1%), which some authors have interpreted to be the result of loss of sulphur due to subsolidus reactions between oxide and sulphide phases (Naldrett et al., 2012).

Contact-type PGE deposits occur in the contact zone between a mafic intrusion and basal country rocks. This type of PGE deposit is generally richer in sulphides than reef-type PGE deposits and the mineralised interval is normally thicker, but with a slightly lower metal grade (e.g., Platreef in Bushveld, McDonald and Holwell, 2011; Suhanko in the Portimo complex, Iljina et al., 2015). Offset-type PGE deposits occur in the country rocks to the mafic intrusions. This type of deposit is not very common, an example being the sulphide veins in the Archaean basement just below the Portimo complex in Finland (Iljina et al., 2015), and a number of deposits around the Sudbury igneous complex (Naldrett, 2004).

2.2 Ore-forming processes

The formation of magmatic sulphide deposits can be subdivided into several important stages (e.g., Naldrett, 2004; Barnes and Lightfoot, 2005): (1) generation of the magma in the source (mantle melting); (2) evolution of the magma during ascent into the crust; (3) sulphide saturation; (4) chalcophile metal enrichment in the sulphide melt; (5) accumulation, fractionation and cooling of metal-rich sulphide melt.

2.2.1 Generation of the magma in the source

It is generally thought that basaltic magmas are derived from the mantle, which can be broadly subdivided into three types: plume mantle, asthenospheric mantle, and subcontinental and suboceanic lithospheric mantle (SCLM and SOLM). There is still some controversy on the main mantle source of mafic-ultramafic magmas, particularly those forming magmatic ore deposits. It has been suggested that the SCLM is an important source for PGE in magmas (Zhang et al., 2008; Griffin et al., 2013; Ezad et al., 2024). However, the SCLM that is the result of a large degree of melt extraction is typically strongly depleted in PGE (Pearson et al., 2003; Lorand and Luguet, 2016, Maier et al. 2012). Most researchers suggest that the main source of metals and magma is a plume-type mantle (or asthenospheric mantle), and the crustal geochemical signature of many sulphide deposits is due to interaction of mantle-derived magma with crustal material (Puchtel et al., 1996, 1997; Hanski et al., 2001b; Arndt, 2013; Yang et al., 2016).

The estimated sulphur content of mantle rocks is relatively low, on the level of 250 ppm (Lorand et al., 2003). The base metal sulphide phases composed of monosulphide solid solution rich in iron and Ni and intermediate sulphide solid solution rich in Cu are important hosts of metals in the mantle, and can contribute considerably to the total budget of Cu, Ni, Co, PGE, and Au. Another important host of some chalcophile metals is olivine, which is the most abundant mantle mineral and controls the budget of Ni. Some minor platinum-group element-bearing phases (e.g., Pt-Fe alloy) may also contribute to the budget of some PGEs (Lorand et al., 2013, Alard et al., 2000).

15
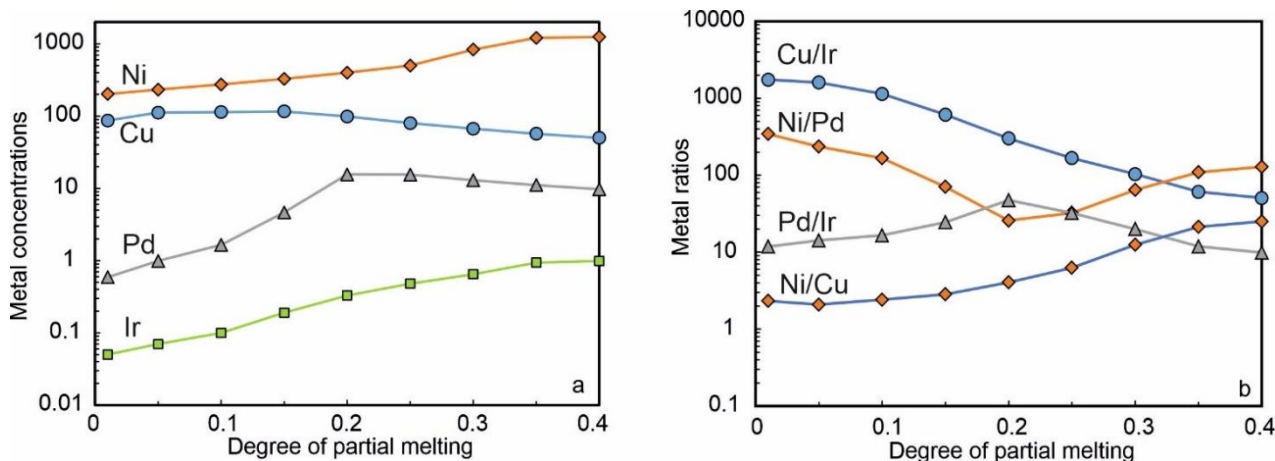
Fig. 1. a. Calculated concentration of metals in the melt vs. the degree of mantle melting; b. Calculated metal ratios in the melt vs. the degree of partial melting. Note the logarithmic scale on the Y-axis. Modified after Barnes and Lightfoot (2005).

To dissolve all sulphides and generate a metal-rich melt during mantle melting, a relatively high degree of melting is required. Otherwise, the chalcophile metals will be retained in the mantle sulphide phases, and the generated silicate magma will be depleted in chalcophile metals, especially those with extremely high sulphide-silicate melt partition coefficients (e.g., PGE). This effect is less important for base metals, which have lower partition coefficients with regard to sulphide melt. The exact degree of melting to exhaust all mantle sulphides has been estimated at roughly 15−25% (Keays, 1995, Naldrett, 2004; Barnes and Lightfoot 2005). Figure 1 shows chalcophile element concentrations in the melt as a function of the degree of mantle melting, as calculated by Barnes and Lightfoot (2005). The model calculations indicate that magmas generated by low degrees of partial melting (e.g., <10%) generally have low potential to form magmatic sulphide deposits due to low metal contents (Keays, 1995). If the degree of melting increases above 25%, most chalcophile elements will become progressively diluted in the magma (Fig. 1), with the exception of Ni, which is controlled by olivine, and IPGE, which may be controlled by PGE alloys. This explains why komatiites generally have the highest Ni and Ir contents, but relatively low content of Cu, Pd and Pt, and thus low Cu/Ir and Pd/Ir ratios and high Ni/Cu ratios (Fig. 1; Barnes and Lightfoot, 2005; Naldrett, 2010).

2.2.2 Transportation to the crust

To form an exploitable ore deposit, a fertile mantle-derived magma must be transported from the mantle to the crust without losing much of its metal content. This is facilitated by the presence of weak zones in the lithosphere, such as major fault structures, which provide channels for magma transportation (Barnes and Lightfoot, 2005; Barnes et al., 2016). Pressure release during magma

ascent will result in increasing sulphur solubility of magma (Wendlandt, 1982; Mavrogenes and O'Neill, 1999). Experimental studies indicate that the solubility of sulphur is ca. 1000 ppm at a pressure of 30 kbar, increasing to 2000 ppm at 12 kbar for a magma with ca. 11 wt.% FeO (Wendlandt, 1982). On the other hand, the temperature of the magma tends to decrease during its ascent, which could potentially result in lower sulphur solubilities. However, the pressure decrease has a much higher overall effect on the sulphur solubility (Mavrogenes and O'Neill, 1999). Because of these reasons, a magma that is undersaturated in sulphide when leaving the mantle tends to stay understaturated when ascending through the crust. Even a magma that is sulphur saturated under mantle conditions can potentially become sulphur undersaturated under crustal conditions. This is favourable for the formation of magmatic sulphide deposits, as the magma will retain a high metal budget on the way to shallower depths.

2.2.3 Sulphide saturation and metal enrichment

At shallow crustal levels, the magma needs to become saturated in sulphide liquid to be able to form a sulphide deposit. The formation mechanisms of Ni-Cu-dominated sulphide deposits and layered intrusion-hosted PGE deposits are different. Temperature is one of the important parameters that control the sulphide solubility. If temperature continues to decrease, a magma will finally reach sulphide saturation during fractionation. Extensive fractionation of magma will result in loss of metals, such as Ni and Co, to the earlier formed mafic silicate minerals. However, for PGE-dominated sulphide deposits, fractionation is less detrimental as Pt and Pd are incompatible in silicate and oxide minerals.

Another important process is the interaction of mafic-ultramafic magma with crustal rocks. Experimental studies show that addition of silica to the magma could potentially decrease the sulphur solubility. This is consistent, for example, with the coupled occurrence of elevated siliceous crustal contamination in the basaltic Nadezhdinsky Formation in the Siberian Traps and their clear depletion in chalcophile metals (Lightfoot and Keays, 2005). Alternatively, the addition of sulphur-bearing material to the magma could be more efficient to elevate the sulphur content of magma. This explains why many Ni-Cu sulphide deposits are located is areas where sulphur-rich country rocks are available (Barnes and Lightfoot, 2005), including sulphide-bearing black shales (e.g., Pechenga, Hanski et al., 2011; Duluth Complex, Samalens et al., 2017), sulphide-bearing VMS-type proto-ores (Yilgarn craton, Fiorentini et al., 2008), or sulphate-bearing sediments, such as anhydrite (e.g., Noril'sk, Iacono-Marziano et al., 2017). In the former two cases, sulphur is in a reduced form and can form sulphide melt directly. In the case of anhydrite, sulphur is in an oxidised

form, and thus a reducing agent (e.g., coal, or graphite) is required to reduce S^{6+} to S^{2-}. In the Noril'sk region, it was first suggested that coal was the reducing material (Naldrett, 1992). However, in later studies, it was found that the coal mainly occurs above the mineralised intrusions, and thus the reducing agent must be some other material. Li et al. (2009) suggests that Fe^{2+} in the mafic magma itself can be oxidised to Fe^{3+}, and thus serving as a reduction agent to reduce S^{6+} to S^{2-} to form sulphide.

The general ore-forming processes in conduit-type and komatiite-hosted Ni-Cu sulphide deposits are similar, with the difference being that the former occur in intrusive environments, whereas the latter generally occur in volcanic and subvolcanic environments. As komatiitic magma is very hot and has a high-density, lava flows can potentially erode the underlying substrate, being able to dissolve footwall material, which can trigger sulphide saturation, especially when the footwall contains sulphur (e.g., Naldrett, 2004).

For layered intrusion-hosted PGE deposits, the marginal-type PGE deposits may share some similarities with conduit-type sulphide deposits in terms of sulphide saturation mechanism. This is because there is normally intensive interaction between mafic magma and country rocks, as in the case of the Suhanko intrusion marginal series in Finland (Iljina et al., 2015) and Platreef in the northern Bushveld complex (Maier et al., 2013a). This is evidenced by the abundance of floor xenoliths and a high abundance of sulphide (ca. 5%) in the mineralised zones. On the other hand, reef-type PGE deposits are characterised by a relatively low sulphide abundance (1% or 0.1% level), such as in the UG2 chromitite and Merensky PGE reef in Bushveld (Godel, 2015; Maier et al., 2013), the Stella deposit in South Africa (Maier et al., 2003; 2023), and the three reefs in the Penikat intrusion (Maier et al., 2018). It is generally thought that external sulphur is not necessarily required to reach sulphide saturation to form these deposits (Maier et al., 2013a).

Naldrett (1994) suggests that mixing of a primitive and an evolved magma can form a mixture of magma lying above the sulphur solubility curve and thus form a sulphide melt. This process could occur when a new replenishing magma enters a magma chamber and mixes with a more evolved early-stage magma. However, Li and Ripley (2005) found that mixing can only trigger sulphide saturation if the mixing partners are close to S saturation. Alternatively, Maier et al. (2013a) suggest that crystal fractionation of silicate magma can increase the sulphur content of the residual magma and eventually lead to sulphide saturation. As most reef-type PGE deposits occur some distance above the floor of their host intrusions, some fractionation of magma is required before sulphide saturation takes place. In some cases where the host rocks are rich in oxide, such as

chromitite (e.g., UG2) or magnetite rock (e.g., Stella; Maier et al., 2023), the sulphide abundance in the PGE reef is extremely low (<0.1 wt.%). One possible explanation is that a magmatic sulphide melt became unstable due to the loss of Fe to the oxide minerals (Naldrett et al., 2009).

2.2.4 Chalcophile metal enrichment

Chalcophile elements partition into the sulphide liquid. According to experimental studies, the sulphide-silicate melt partition coefficients can be several hundreds for base metals and reach >1M for PGE (Mungall and Brenan 2014; Naldrett, 1989; Barnes and Francis, 1995; Tredoux et al., 1995). Hence, when a silicate liquid equilibrates with a sulphide melt, the bulk of the metals will be scavenged by the sulphide melt. To calculate the dependence of the metal content of the sulphide liquid (metal tenor) on the metal content of silicate melt and the R-factor, i.e., the mass ratio of silicate to sulphide liquid, Campbell and Naldrett (1979) developed the following equation:

$$C_{sulphide} = C_{silicate} \times D \times (R+1)/(R+D)$$

where $C_{sulphide}$, $C_{silicate}$, and D indicate metal content in sulphide melt, metal content in silicate melt, and partition coefficient of metal between sulphide melt and silicate melt, respectively. Based on studies of numerous deposits, the R factor in conduit-type Ni-Cu sulphide deposits is generally lower than that in layered intrusion-hosted sulphide deposits, with the former typically showing values on the level of several hundreds to a few 1000 and the latter more than 10000. The R factor tends to be particularly small in the case of massive sulphides whereas it is usually larger for disseminated sulphide deposits. Under some conditions, when R is much higher than D, the metal tenor can reach a maximum value when (R+1)/(R+D) approaches 1, and this maximum value is $C_{silicate} \times D$. Hence, the maximum metal enrichment efficiency $C_{sulphide}/C_{silicate}$ in sulphide melt is directly proportional to the partition coefficient.

An application of the equation of Campbell and Naldrett (1979) is shown in Figure 2, which illustrates Pd contents and Cu/Pd ratios of sulphide melt that equilibrated with silicate melt at different R values. Three silicate melt compositions are considered: a fertile mantle-derived melt and two fractionated melts produced by S-saturated crystallization of the primary melt. Due to the extremely high partition coefficients of Pd into sulphide, the concentration of Pd in the sulphide melt can reach 100 ppm. On the other hand, the maximum relative enrichment of base metals (e.g., Cu) in sulphide melt tends to be much lower than that of PGE resulting in lower Cu/Pd ratios with increasing R-factor. If there was earlier sulphide removal at depth, the residual silicate melt tends to be more depleted in Pd than Cu, obtaining a higher Cu/Pd ratio than the primitive mantle value at about 7000 (depleted field). If sulphide saturation occurs again later, the formed sulphide melt

19

will show enrichment in chalcophile metals, but clearly less so than in the sulphides derived from a fertile magma. If the magma has undergone an earlier sulphide segregation event prior to final emplacement, the residual silicate melt tends to be depleted in chalcophile metals resulting in elevated Cu/Pd ratio above the level of primitive mantle, and any sulphide subsequently forming will have relatively low PGE contents (Fig. 2).
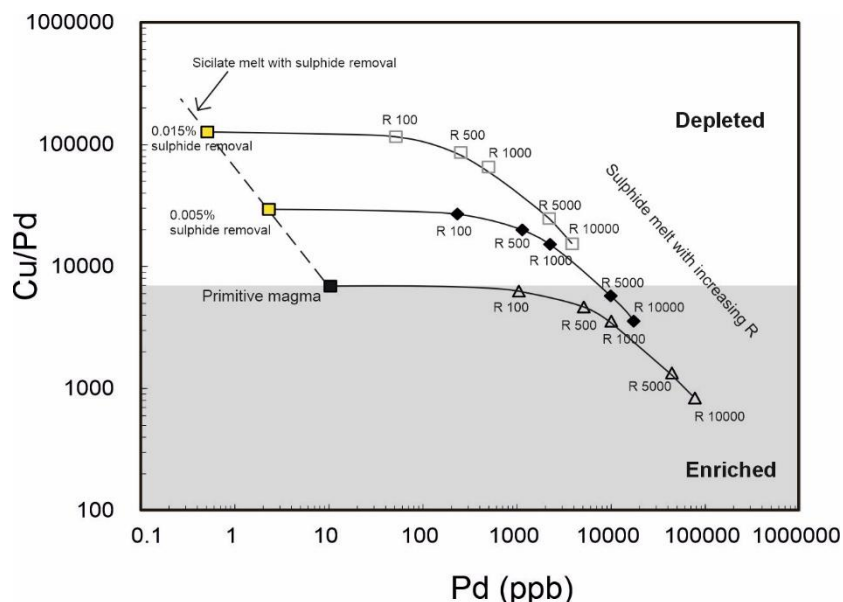
Fig. 2. Calculated Cu/Pd ratios and Pd concentrations in the sulphide melt derived with variable R values from a primitive metal-rich silicate melt and two more fractionated melts that have undergone earlier sulphide removal. If a primitive magma with fertile chalcophile element content reaches sulphide saturation, the sulphide melt will be enriched in chalcophile metals (open triangles) at different R-factors (100, 500, 1000, 30000), with a Pd content varying from 1 ppm up to more than 100 ppm. However, as the partition coefficient of Cu for sulphide melt is much lower than that of Pd, the Cu/Pd ratio of the sulphide melt tends to be lower than the primitive mantle value of about 7000. In the case where there was earlier sulphide removal at depth, the residual silicate melt tends to be more depleted in Pd than Cu, and therefore will have elevated Cu/Pd ratios (yellow squares in the depleted field). If sulphide saturation occurs again, the formed sulphide melt (open squares and black diamond) will show enrichment in chalcophile metals, but clearly less so than in the sulphides derived from a fertile magma. The concentrations of the metals in the primary mantle melt are from Barnes and Lightfoot (2005). The sulphide melt compositions were calculated using the equation of Campbell and Naldrett (1979) and sulphide melt/silicate melt D values of 30000 for Pd and 1000 for Cu. The calculation of silicate melt compositions after sulphide + silicate removal (1% sulphide, 99% olivine) is based on the Rayleigh fractionation equation.

2.2.5 Accumulation, fractionation and cooling of metal-rich sulphide melt

After interaction between sulphide melt and silicate melt, the metal-rich sulphide melt needs to be physically concentrated to form a deposit with an economic grade. The original sulphide melt occurs as fine-grained droplets, which could be transported by the host magma. The sulphide droplets tend to adhere to each other to form larger droplets (Barnes and Lightfoot, 2005).

20

For Ni-Cu sulphide deposits, the sulphide melt tends to accumulate at the bottom of magma conduits or komatiitic lava flows, due to its high density compared to that of silicate melt (Barnes and Lightfoot, 2005). Where there are flow dynamic traps such as embayments in the base of the magma chamber, the sulphide droplets can form massive or semi-massive sulphide bodies. One example is the contact-type sulphide ore at Sudbury concentrated in so-called embayments, or the massive sulphides in komatiite-hosted deposits in Western Australia (Naldrett, 2004). At Voisey's Bay, sulphides are concentrated at the exit of a conduit into a larger magma chamber, due to a decreasing transportation velocity of sulphides (Li and Naldrett, 1999).

In layered intrusion-hosted sulphide deposits, the sulphide melt tends to be concentrated in thin reefs having thicknesses of centimetres to a few meters. 3D computational tomography imaging has revealed that the abundance of sulphide minerals increases towards the base of the Merensky reef (Godel et al., 2007), which is interpreted as evidence for gravitational control on sulphide melt concentration. The porosity of the cumulus pile likely affects the efficiency of sulphide accumulation: In the case of Merensky reef, the thin basal chromitite layer trapped the percolating sulphide melt and prevented it from percolating into the footwall cumulates. As a result, the highest PGE grade is found at the top of the chromitite (Godel et al., 2007). Another model suggests that sulphides are derived from the cumulate pile below the reefs or the floor rocks of the magma chamber. The sulphur would have been transported in a volatile phase or a volatile-rich evolved silicate melt (Boudreau and McCallum, 1992).

When a magmatic sulphide melt cools down, the first phase to crystallise is monosulphide solid solution (MSS), FeS_{1-x} (Kullerud et al., 1969). In MSS, IPGE (e.g., Ir, Ru) are compatible, and Ni is moderately incompatible with partition coefficients between MSS and silicate melt of ca. 0.4–0.6 at high temperature (>1150ºC, Kullerud et al., 1969; Barnes and Lightfoot, 2005), whereas at <1,000°C, Ni is moderately compatible with MSS (D_{Ni} mss = 1–1.5) (Fleet et al., 1993; Barnes et al., 1997; Ballhaus et al., 2001). On the other hand, Cu, Pd and Pt are highly incompatible with regard to MSS. With decreasing temperature (<900ºC), the residual copper-rich sulphide melt will crystallise intermediate solid solution (ISS). When the temperature falls to below 600°C, MSS and ISS are not stable, with MSS exsolving pyrite under sulphur-rich condition, or pyrrhotite and pentlandite in sulphur poor conditions. ISS will exsolve to form chalcopyrite and pyrrhotite at low temperature (Kullerud et al., 1969; Cabri, 1973; Naldrett, 2004; Barnes and Lightfoot, 2005). Palladium and Pt are incompatible in MSS, but a considerable amount of Pd is hosted in pentlandite, interpreted as a result of diffusion of Pd from ISS to MSS. The remainder of Pd is hosted in platinum-group minerals (PGM) together with some semimetals (e.g., Se, As, Sb, Te). Platinum

tends to form discrete minerals, but has a very low content in base metal sulphides (Godel et al., 2007; Godel, 2015). The PGMs tend to occur as small grains either inside base metal sulphide or at the boundary between sulphide minerals and silicates, though PGM can also be associated with silicates (e.g., hydrous minerals, such as mica and amphibole) if experiencing later fluid-induced alteration processes (Godel, 2015).

2.3. Assessment of the ore potential

From an exploration point of view, it is critical to evaluate the sulphide saturation potential of mafic-ultramafic rocks in the areas under exploration. This can be done 1) using chemical and isotopic indicators that can reveal the effects of sulphide saturation in rocks that were potentially involved in ore formation processes and 2) recognising suitable geological environments for ore formation, such as the presence S-bearing country rocks.

The addition of sulphur from external sources, such as sulphide- or sulphate-bearing sedimentary rocks, has often been regarded as an essential requirement for formation of magmatic Ni-Cu deposits (Naldrett, 2004). To assess whether there has been addition of external crustal sulphur, sulphur isotope compositions can be used to constrain the source of sulphur, because mantle-derived sulphur tends to have δS^{34} around 0 with a small variation from -2 to +2‰ and sulphur derived from crustal source tends to show a large variation in δS^{34} from -20‰ to higher than +20‰ (Ripley and Li, 2003). In Archaean rocks, the variation in δS^{34} is limited, but the sedimentary sulphur tends to have a mass-independent sulphur isotope anomaly (non-zero ΔS^{33}) (Farquhar et al., 2000; Fiorentini et al., 2012; Konnunaho et al., 2013).

Where no sulphur-bearing country rocks exist, interaction between magma and crustal rocks can still change the magma composition (e.g., increasing silica content, increasing oxygen fugacity) and consequently decrease the sulphur solubility (Li and Naldrett, 1993). In such cases, the degree of siliceous crustal contamination is useful for evaluating the ore potential. There are many geochemical parameters for constraining crustal contamination, such as mantle-normalised rare earth element (REE) patterns, primitive mantle-normalised trace element spider diagrams, and Sm-Nd, Rb-Sr, Lu-Hf, and Re-Os isotope systematics. For example, a high degree of crustal contamination tends to result in enrichment in LREE and large-ion lithophile elements (LILE), depletion in Nb-Ta, negative initial εNd and εHf values, and high initial $^{87}Sr/^{86}Sr$ and $^{187}Os/^{186}Os$ ratios, though caution must be used as magmas with some of these chemical characteristics can also be formed from enriched mantle sources. Other important assessment criteria for crustal

contamination include physical features, such as the presence of abundant xenoliths of country rock in igneous bodies.

Constraining the sulphide saturation history of magma provides another tool for ore potential assessment. The general concept is that sulphide-saturated magma tends to show depletion in chalcophile metals. During the fractionation of a mafic-ultramafic magma, Cu and Zr behave incompatibly when sulphide saturation has not taken place, and the Cu/Zr ratio tends to be at the level of the primitive mantle (Li and Naldrett, 1999). On the other hand, if sulphide saturation occurs, Cu will become depleted relative to Zr, resulting in Cu/Zr_{PM} below 1. This concept has been applied in the study of the Voisey's Bay deposit (Li and Naldrett, 1999), for example. Similarly, Cu/Pd and Ni/Pt ratios are sensitive to sulphide saturation. Because the sulphide melt/silicate melt partition coefficients of Pt and Pd are much higher than those of Cu and Ni, Pt and Pd tend to be more concentrated in sulphide melt resulting in more depletion in residual silicate melt. Consequently, sulphide-saturated residual magma will show elevated Cu/Pd ratios (up to 10s to 100s of thousands) compared with the primitive mantle value of ca. 7000.

The Ni content in olivine provides another tool to detect metal depletion and is widely used in the study of mineral deposits related to mafic-ultramafic rocks. Because of the compatibility of Ni in olivine with partition coefficients at the level of 5 to 10 depending on the magma composition (Li and Ripley, 2010), olivine crystallised from primitive magmas generally contains high Ni, up to 3000 to 4000 ppm. Under sulphide-undersaturated conditions, crystal fractionation tends to generate decreasing Ni in olivine with decreasing MgO in magma. On the other hand, sulphide saturation will result in a sharp decrease in the Ni content of the magma without a concomitant decrease in MgO. This decrease in Ni can potentially be detected from a decrease in the abundance of Ni in olivine (Arndt et al., 2003; Li et al., 2003, 2004; Brownscombe et al., 2015; Barnes et al., 2023).

One example is the Siberian flood basalts and related Noril'sk-Talnakh sulphide deposits. One of the stratigraphic units of the flood basalt sequence, the Nadezhdinsky Formation, shows high $(La/Sm)_{CN}$ ratios, negative εNd values, and high $^{87}Sr/^{86}Sr$ ratios, which are coupled with low chalcophile element contents, especially those of PGE, and high Ni/Pt ratios (Lightfoot and Keays, 2005). It has been interpreted that this basaltic formation experienced extensive crustal contamination, which resulted in sulphide precipitation. The sulphide melt scavenged the chalcophile metals and accumulated at depth forming the giant Ni-Cu-PGE sulphide ores in the Noril'sk and Talnakh magma conduit system and the residual silicate magma erupted through the

magma conduit to form the metal-depleted basalt formation (Lightfoot et al., 1990; Naldrett, 1992; Hawkesworth et al., 1995).

Geochemical methods to assess ore potential have also been applied to several other large igneous provinces (LIP), such as the Emeishan LIP (Wang et al., 2007, 2011; Qi et al., 2008), the Paraná Magmatic Province (Mansur et al., 2021), and the Canadian High Arctic Large Igneous Province (HALIP) (Jowitt et al., 2014). Jowitt et al. (2014) suggested that the lower tholeiitic magma suite in the HALIP has a high Ni-Cu prospectivity because this magma shows significant crustal contamination and also a signature of chalcophile metal depletion. The authors argue that the crustal contamination resulted in a Ni-Cu sulphide deposit at depth.

For komatiite-related Ni-Cu sulphide exploration, a similar lithogeochemical assessment is applicable, but volcanology should also be considered as the rocks formed in an extrusive environment (Lesher and Stone, 1996; Lesher and Keays, 2002; Arndt, 2008).All types of komatiite (e.g., Al-depleted or Al-undepleted) have potential to produce sulphide deposits. As komatiitic magma is generally highly sulphur undersaturated, interaction with crustal materials, especially sulphur-bearing rocks is required to trigger sulphide melts saturation. All komatiitic sulphide deposits occur in lava conduits or channelised sheet flows, represented by the lower olivine cumulate zone in komatiitic lava flows. Hence, understanding the stratigraphy of komatiitic lava flows is important. A high magma flux may result in significant erosion of the footwall rocks. Hence, in a thick komatiitic sequence, thick olivine-rich cumulate zones should have a higher priority for detailed exploration. Komatiite lava flows with signs of strong crustal contamination (e.g., LREE enrichment, depletion in Nb) and sulphide segregation (e.g., PGE depletion) have the highest potential for ore deposits.

Some layered intrusions host PGE mineralisation, but others are barren. Empirical data suggest that well-mineralised intrusions are undepleted in PGE, with mantle-like Cu/Pd ratios in the lower portions, indicating a PGE-rich parental magma derived by a high degree of mantle melting. On the other hand, if high Cu/Pd ratios and low PGE contents are recorded in the upper stratigraphy, this indicates that sulphide saturation occurred at some stage of magma evolution. PGE-bearing reefs generally occur in the transitional zone between a stratigraphical interval with mantle-like Cu/Pd and an interval with higher Cu/Pd. These reefs generally show lower Cu/Pd ratios than the mantle values and also large variations in Cu/Pd. The low Cu/Pd ratio in the reefs is due to accumulation of PGE-rich sulphides enriching the reef in PGE relative to Cu (Maier and Barnes, 2005). On the other hand, if a layered intrusion shows a fertile PGE content and mantle-like Cu/Pd

ratios across the entire stratigraphy, it may not be a prospective target as sulphide saturation likely did not occur at any time of the magma evolution (Maier and Barnes, 2005). Where the whole stratigraphic section is depleted in PGE (resulting in high Cu/Pd ratios), the magma has already lost most of its chalcophile metals before its emplacement to the current magma chamber (Maier and Barnes, 2005), resulting in a low ore potential. In the case of contact-type deposits in layered intrusions, interaction of magma with footwall rocks may have played some role in sulphide saturation and ore formation, and the lower contact zone could then be an important research target. These principles has been applied to assess the PGE mineralisation potential of layered intrusions (e.g., Sonju Lake, Miller et al., 2002; Bushveld, Maier et al., 2003; Barnes et al., 2004; Kalka, Maier et al 2023).

3. Previous studies on mafic-ultramafic magmatism in NE Fennoscandia and motivation of this study

Archaean komatiites of the Karelian craton have been studied in a considerable detail, both in Russia (e.g., Puchtel et al., 1998, 1999, 2001, 2007; Svetov et al., 2001; 2010; Svetov and Smolkin, 2003; Svetov, 2005) and Finland (e.g., Hanski, 1980; Jahn et al., 1980; Papunen et al., 2009; Hölttä et al., 2012; Maier et al., 2013b). The komatiites in eastern Finland, including those in the Tipasjärvi-Kuhmo-Suomussalmi greenstone complex (TKS) and the Ilomantsi and Tulppio greenstone belts, have been dated at ca. 2.75–2.82 Ga (Huhma et al., 2012) and are thought to have formed in variable tectonic settings (Papunen et al., 2009; Hölttä et al., 2012; Maier et al., 2013b). Maier et al. (2013b) studied the platinum-group element (PGE) systematics of komatiitic rocks in the greenstone belts in eastern Finland. Based on their relatively evolved compositions, the lack of dynamic lava channel environments and PGE-enriched samples in most lava flows, the authors concluded that, compared to Archaean komatiite-bearing belts globally, they may have a relatively low Ni sulphide mineralisation potential. In Russian Karelia, Puchtel et al. (1998, 2001, 2005) and Puchtel and Humayun (2000) determined PGE concentrations in the 2.8 Ga Kostomuksha komatiites, and Puchtel et al. (2007) reported PGE data for the 2.8 Ga komatiites in the Volotsk suite. The PGE levels of both these belts seem to be similar to those of the Finnish belts. In the present study, I have determined the PGE contents of komatiites in two Archaean greenstone belts in Russian Karelia, Vedlozero-Segozero and Tikshozero, in order to evaluate their prospectivity for Ni-Cu sulphide ore deposits.

The 2.45 Ga magmatism is related to the initiation of long-lived rifting in Fennoscandia and generated a number of mafic layered intrusions, with many of them hosting significant

mineralisation (PGE, Cr or V) (Maier and Hanski, 2017). These mafic layered intrusions are spatially and temporally associated with abundant mafic dykes, which likely belong to the same magmatic event (Vuollo and Huhma, 2005; Iljina et al., 2015; Maier and Hanski, 2017; Maier et al., 2018). In the present study, I provide new compositional data for 37 dykes from the Karelian craton to constrain the petrogenesis of the dykes and evaluate the ore formation potential of correlated layered intrusions.

In the long-lived rifting history, one interesting feature is that the major mineralisation stage occurred in the initial and late stages of rifting. Similar types of magmatism and mineralisation also occur in other cratons (e.g., Superior in Canada). The early-stage magmatism either represents a crustally contaminated plume-derived komatiitic magma or melting of metasomatised subcontinental lithospheric mantle (SCLM). Magmas related to the middle-stage rifting generally show low degrees of crustal contamination and are clearly derived from asthenospheric mantle without significant interaction with SCLM and crust (Stepanova et al., 2014). In the late stage, plume-related magmatism occurred in both Finland and Russia, resulting in many significant Ni-Cu-dominated sulphide deposits. In this study, I focus on multiple generations of mafic-ultramafic volcanic rocks in several rifted basins across NE Fennoscandia, spanning in age from ca. 2.45 to 2.0 Ga. They represent Karelian magmatism, which occurred at various stages of rifting and disruption of the Archaean Karelian craton. In addition, this work integrates platinum-group element geochemistry and petrogenesis to constrain the key factors that affect the diversity of mineralisation styles in these magmatic events, which will have significant implications for exploration of critical raw materials.

4. Geological background

4.1 Archaean greenstone belts

Archaean rocks are widely distributed in the NE Fennoscandia in different cratons (Kola, Karelian, Belomorian and Norrbotten) that are mainly composed of different types of granitoids including tonalite-trondhjemite-granodiorite suite rocks (TTG), sanukitoid, quartz diorite-quartz monzodiorite (Huhma et al., 2012), and greenstone belts, which host some occurrences of Ni-Cu sulphide mineralisation (Konnunaho et al., 2015). Our research targets are located in Russian Karelia including the Vedlozero-Segozero greenstone belt in the Karelian craton and the Tikshozero greenstone belt at the boundary between the Karelian craton and the Belomorian mobile belt.

The Mesoarchaean Vedlozero-Segozero greenstone belt is located at the western margin of the Vodlozero terrane (Figs. 1, 2). It extends approximately in N-S direction over a distance of ca. 300 km from Lake Vedlozero to Lake Segozero and has a width of 50–60 km (Fig. 3). The underlying rocks are Archaean granite-gneisses and granites of the South Segozero block. The greenstone belt rocks are unconformably overlain by Palaeoproterozoic Jatulian supracrustal rocks composed of quartz conglomerates, quartzites, quartzitic sandstones, and basaltic lava flows. All the komatiitic rocks in the Vedlozero-Segozero greenstone belts have undergone seafloor alteration and regional metamorphism, with the latter varying from greenschist to amphibolite facies. During these processes, the primary textures have been preserved, but almost all the primary minerals have been completely replaced by secondary minerals.

In this belt, Mesoarchaean volcano-sedimentary rocks occur in several areas, including Hautavaara, Koikary, Palaselga, Sovdozero, and Semch, which likely represent fragments of an originally larger belt (Svetov et al., 2001) (Fig. 3). In plan view, these areas form subparallel zones separated by gneissose granites. This study was focused on the first four areas listed above (see Fig. 3). The exposed greenstone belts in these areas extend in N-S direction for approximately 10 to 30 km, with a width of between 1–2 km and up to 12 km. The greenstone belts are mainly composed of komatiitic-basaltic volcanic rocks from several hundreds of meters up to 2 kilometres in thickness, and interbedded tuffs, tuffites, and minor amounts of volcano-sedimentary and sedimentary rocks in the upper stratigraphy (Fig. 4). Detailed geochronological studies of felsic dykes and volcanic rocks confirm that the age of the volcanism is slightly older than 2.9 Ga (Bibikova and Krylov, 1983; Svetov et al., 2010; Arestova et al., 2012).
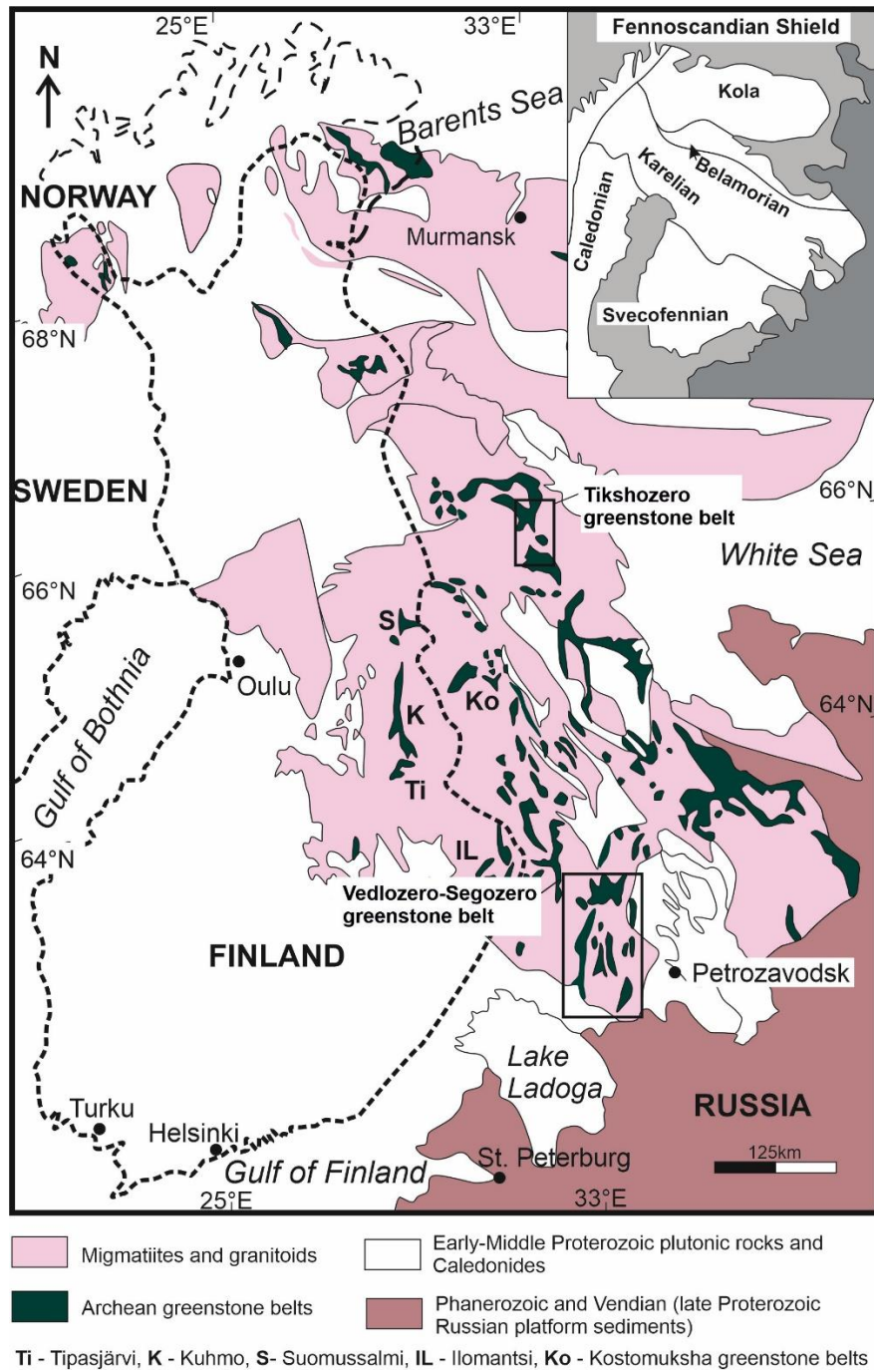
Fig. 3 Regional geological map showing Archaean greenstone belts in the eastern part of the Fennoscandian Shield (modified after Maier et al., 2013b).
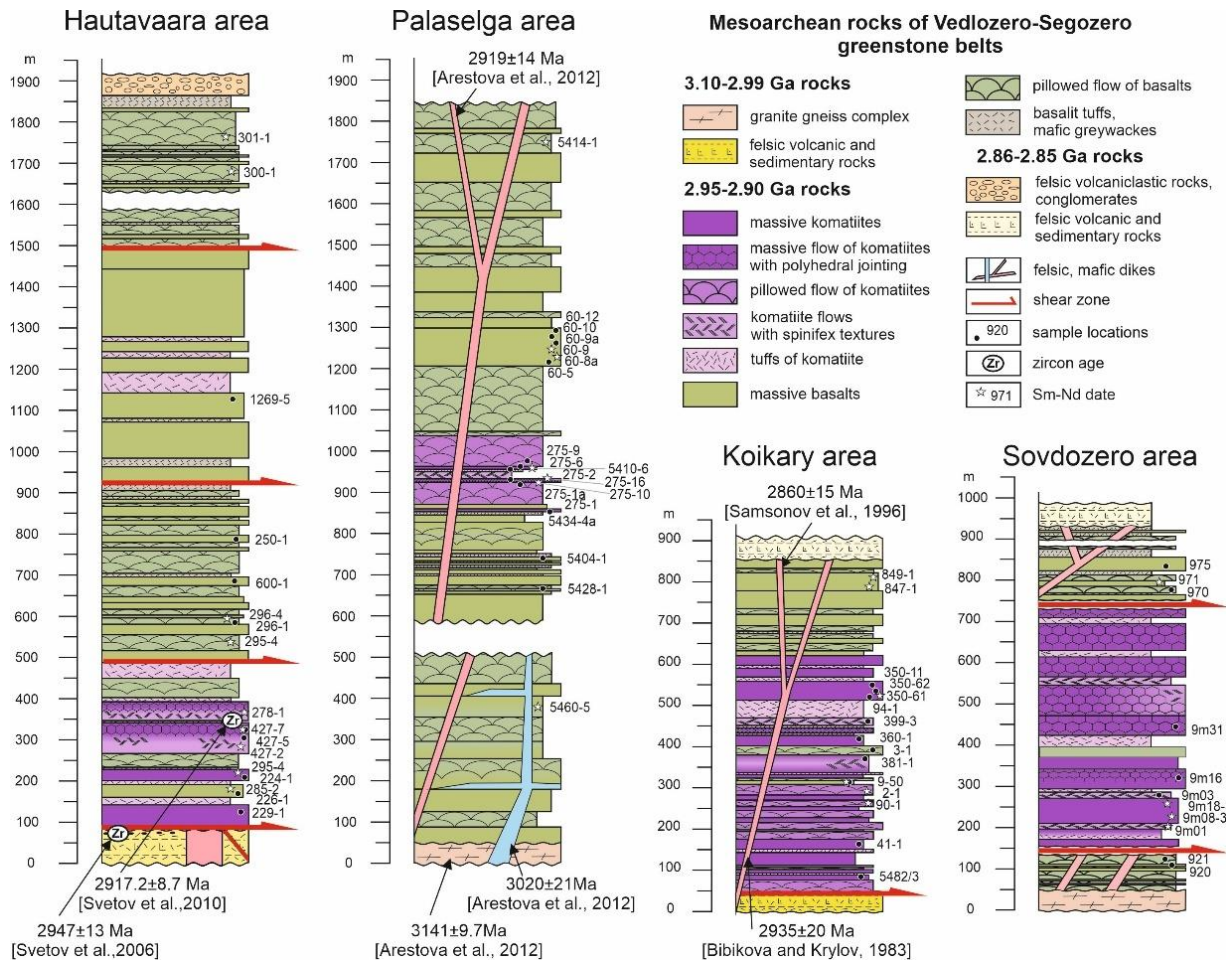
Fig. 4 Simplified stratigraphic sections of komatiite-bearing volcanic successions in the four study areas (Palaselga, Hautavaara, Sovdozero, and Koikary) of the Vedlozero-Segozero greenstone belt.

The Tikshozero greenstone belt extends for around 300 km along the boundary between the Karelian granite-greenstone terrain and the Belomorian mobile belt (Figs. 3). It comprises several sub-belts, which are separated from each other by granitoids. All the sub-belts contain similar lithologies and structural styles and have undergone amphibolite facies regional metamorphism. Thus, they likely represent fragments of a single Neoarchaean greenstone belt (Kozhevnikov, 1992, 2000). The Koizovaara and Irinozero areas are the research targets of this study. The volcanic sequences are mainly composed of komatiites, komatiitic basalts and basalts, and lesser amounts of felsic volcanic rocks. Peridotite is also identified in the Koizovaara area, and a gabbroic sill in the Irinozero area. Geochronological studies of felsic volcanic rocks suggest an age of ca. 2.8 Ga (Bibikova et al., 2003), being thus slightly younger than the age of the Vedlozero-Segozero greenstone belt.

4.2 Palaeoproterozoic long-lived rifting in NE Fennoscandia

4.2.1 2.45 Ga mafic dyke swarms

Several Mesoarchaean microcratons accreted together in the Neoarchaean, forming the Kenorland supercontinent (Enrst and Bleeker, 2010). In Finland, the Karelia craton is divided into four major blocks: Kuhmo, Taivalkoski, Pudasjärvi, and Iisalmi (Vuollo and Huhma, 2005; Hölttä et al., 2012) (Fig. 5). Across much of the NE Fennoscandian Shield, including the Karelian craton and the adjacent Belomorian mobile belt and Kola craton, widespread mafic-ultramafic magmatism occurred at ~2.5–2.45 Ga (Vuollo and Huhma, 2005).

The ~2.5–2.45 Ga Fennoscandian magmatism is composed of numerous mafic layered intrusions, mafic dyke swarms, mafic-ultramafic volcanic rocks, and minor felsic intrusive and volcanic rocks (Alapieti, 1982; Puchtel et al., 1997, 1998; Hanski et al., 2001b; Iljina and Hanski, 2005; Huhma et al., 2018; Maier et al., 2018). The 2.5 Ga magmatism is restricted to the Kola Peninsula, including the Monchegorsk, Fedorovo-Pansky and Mt. Generalskaya intrusions and the Olenogorsk dyke, while the ~2.45 Ga igneous rocks occur both in the Kola craton (e.g., Imandra) and the Karelian craton. The Karelian craton contains the Kemi, Penikat, Portimo, Koillismaa, Näränkävaara, Lukkulaisvaara, Tsipringa, and Kivakka intrusions or intrusion complexes in the Tornio–Näränkävaara intrusive belt in Finland and its continuation in Russia, and the Koitelainen and Akanvaara intrusions in Finnish Lapland (Amelin et al., 1995; Hanski et al., 2001b; Iljina and Hanski, 2005; Bayanova et al., 2019; Köykkä et al., 2022) (Figs. 5).

Several of the 2.5–2.45 Ga mafic layered intrusions in the Fennoscandian Shield host significant mineralisation of PGE (Penikat, Portimo, Koillismaa, Fedorova Pansky), Ni, Cu and Co (Monchegorsk, Fedorova Pansky), chromium (Kemi, Monchegorsk, Koitelainen, Akanvaara,), and vanadium (Koitelainen, Koillismaa, Akanvaara, Monchegorsk) (Alapieti et al., 1990; Halkoaho et al., 1990; Mutanen, 1997; Hanski et al., 2001b; Schissel et al., 2002; Karinen, 2010; Huhma et al., 2012; Karinen et al., 2015; Karykowski et al., 2018a, 2018b; Maier et al., 2018; Mokrushin and Smol'kin, 2021; Järvinen et al., 2022). At present, only one deposit (Kemi Cr) is under production (Huhtelin, 2015), but mining has occurred previously at Koillismaa (for V) and Monchegorsk (Cr, PGE, Cu-Ni), and many exploration projects are under development (Vuollo and Huhma, 2005) (Fig. 5).

The ~2.45 Ga dyke swarms, which form the focus of this study, are present in all the blocks of the Karelia craton with the exception of the Iisalmi block. Based on their geochemistry and mineralogy, Vuollo and Huhma (2005) subdivided these dykes into five major groups: 1) boninites, 2)

gabbronorites GBNO), 3) low-Ti tholeiites (LTTH), 4) Fe-tholeiites (FTH), and 5) orthopyroxene-plagioclase-phyric dykes, with the latest type being restricted to a few localities in the Kuhmo block. Since boninite is a term that is nowadays mainly applied to high-Mg, low-Ti volcanic rocks in fore-arc settings (Hickey and Frey, 1982), I replace it with the term siliceous high-magnesium basalt (SHMB) in this study.


Fig. 5. Geological map showing the distribution of 2.45 Ga mafic dyke swarms in the Karelian craton. Modified after Vuollo and Huhma (2005). Age data taken from Vuollo et al. (2005) and Huhma et al. (2018).

31

### 4.2.2 2.5–1.98 Ga mafic-ultramafic volcanic rocks in supracrustal belts

In the Palaeoproterozoic, the Fennoscandian shield experienced long-lasting rifting from 2.5 Ga to 1.95 Ga. We divide the repeated magmatism into three stages: an early stage (2.5–2.3 Ga), a middle stage (2.3–2.1 Ga), and a late stage (2.06–1.98 Ga). In the eastern part of the Fennoscandian Shield, there is a sedimentary interval with an unusual positive carbon isotope anomaly, with an age roughly ranging from 2.3 to 2.06 Ga, corresponding to the Great Oxygenation Event. This interval is termed the Jatuli-Lomagundi period in Fennoscandia (Karhu, 1993; Melezhik et al., 2013). Hence, we also define the different stages of volcanic rocks as pre-Jatulian, Jatulian, and post-Jatulian.

Evidence for magmatism related to long-lived rifting has been reported from several cratons including Superior in Canada, Wyoming in the USA, as well as Karelia and Kola in Fennoscandia (Ernst and Bleeker, 2010). It is suggested that these cratons are linked together and were part of the Kenorland supercontinent before its breakup. In this study, we collected samples of mafic to ultramafic volcanic rocks from different supracrustal belts of the Karelian and Kola cratons. These belts include, from south to north, the Kainuu belt, Kiiminki belt, Kuusamo belt, Peräpohja belt, Salla belt, and Central Lapland greenstone belt in northern Finland, and the Pechenga belt located in the Kola Peninsula, NW Russia (Fig. 6). Figure 7 displays simplified stratigraphic columns of the corresponding supracrustal belts and their correlation. It should be noted that some rock units non-essential for this study have been ignored in Fig. 7. Also note that because of the deformed nature of the bedrock in most areas, the stratigraphic thicknesses of the units are only indicative.

The early-stage rift magmatism (2.5–2.45 Ga) is mainly composed of mafic-ultramafic volcanic rocks with a minor amount of intermediate and felsic volcanic rocks lying directly on Archaean basement rocks. In the Peräpohja belt the sequence begins with conglomerates which must be younger than 2.45 Ga because they contain fragments of 2.45 Ga intrusive rocks. Younger mafic volcanic rocks occur above the conglomerates, followed by a sequence of quartzites, mafic volcanic rocks and dolomites deposited in the middle rifting stage (Jatulian stage, 2.3–2.1 Ga). These rocks can be observed the Jouttiaapa Formation of the Peräpohja belt as well as the Petäjävaara and Ruukinvaara Formations of the Kuusamo belt, and ending with deep-water sediments including graywackes and black schists as well as ultramafic volcanic rocks represented by the Sattasvaara Formation (2.06 Ga) in the CLGB (Hanski et al., 2001a), the Pilgujärvi Formation (1.98 Ga) of the Pechenga belt (Melezhik and Hanski, 2012), and the Kiiminki and Haukipudas Formations in SW Karelia.
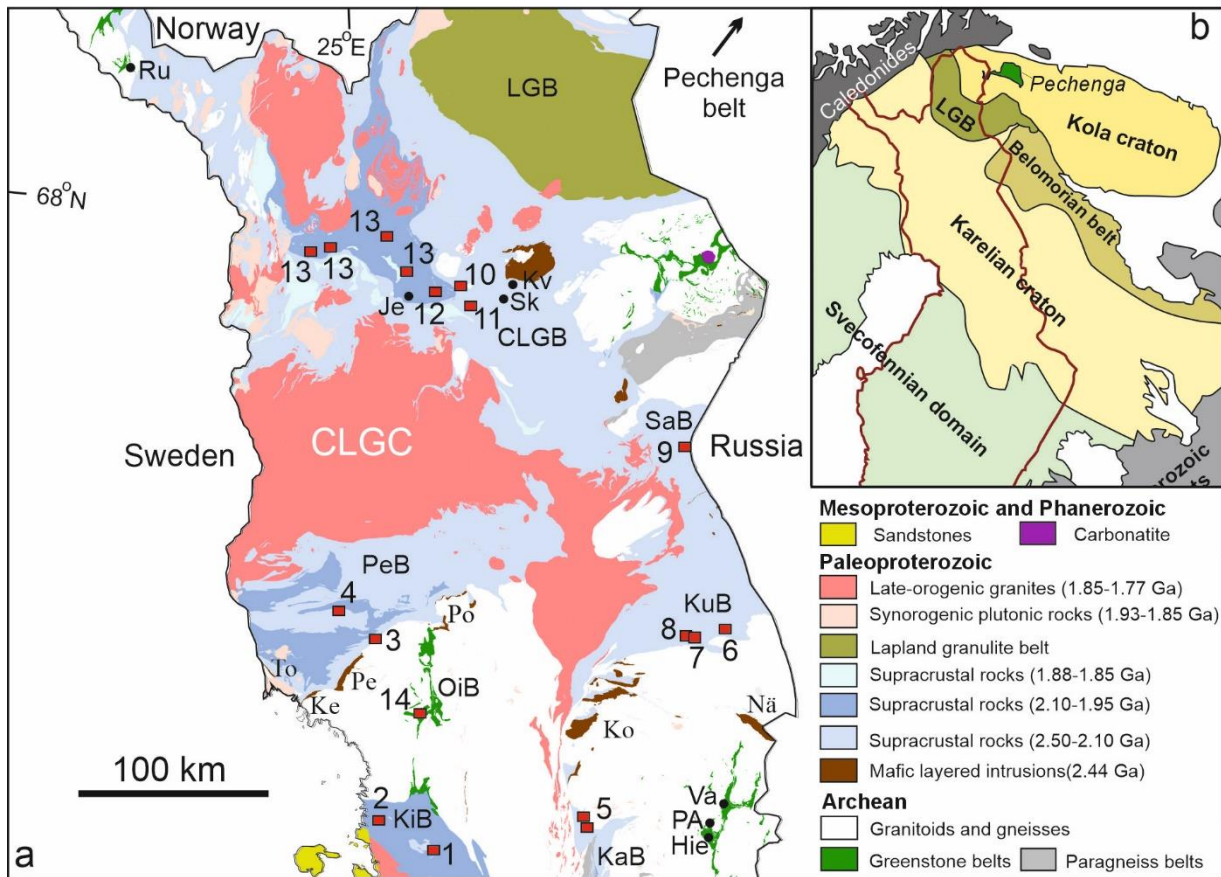
Fig. 6. Sampled volcanic formations shown by red squares on a simplified geological map of northern Finland (based on DigiKP, the digital map database of the Geological Survey of Finland, Version 1.0; available at: www.geo.fi/en/bedrock.html). 1 = Kiiminki Formation, 2 = Haukipudas Formation, 3 = Runkaus Formation, 4 = Jouttiaapa Formation, 5 = Vihantaselkä and Matinvaara Formations, 6 = Kuntijärvi Formation, 7 = Petäjävaara Formation, 8 = Ruukinvaara Formation, 9 = Mäntyvaara Formation, 10 = Möykkelmä Formation, 11 = Sattasvaara Formation, 12 = Kautoselkä Formation, 13 = Vesmajärvi Formation. Abbreviations for geological units: CLGB = Central Lapland greenstone belt, CLGC = Central Lapland Granitoid Complex, KaB = Kainuu belt, KiB = Kiiminki belt, KuB = Kuusamo belt, LGB = Lapland granulite belt, PeB = Peräpohja belt, SaB = Salla belt, OiB= Oijärvi green stone belt. The Pechenga belt is located outside the map in the Kola Peninsula, NW Russia. Locality name abbreviations: Hie-Hietaharju, PA-Peura-aho, Va-Vaara, To-Tornio, Ke-Kemi, Pe-Penikat, Po-Portimo, Ko-Koillismaa, Nä-Näränkävaara, Je-Jeesiörova, Kv-Kevitsa, Ru-Ruossakero.

33
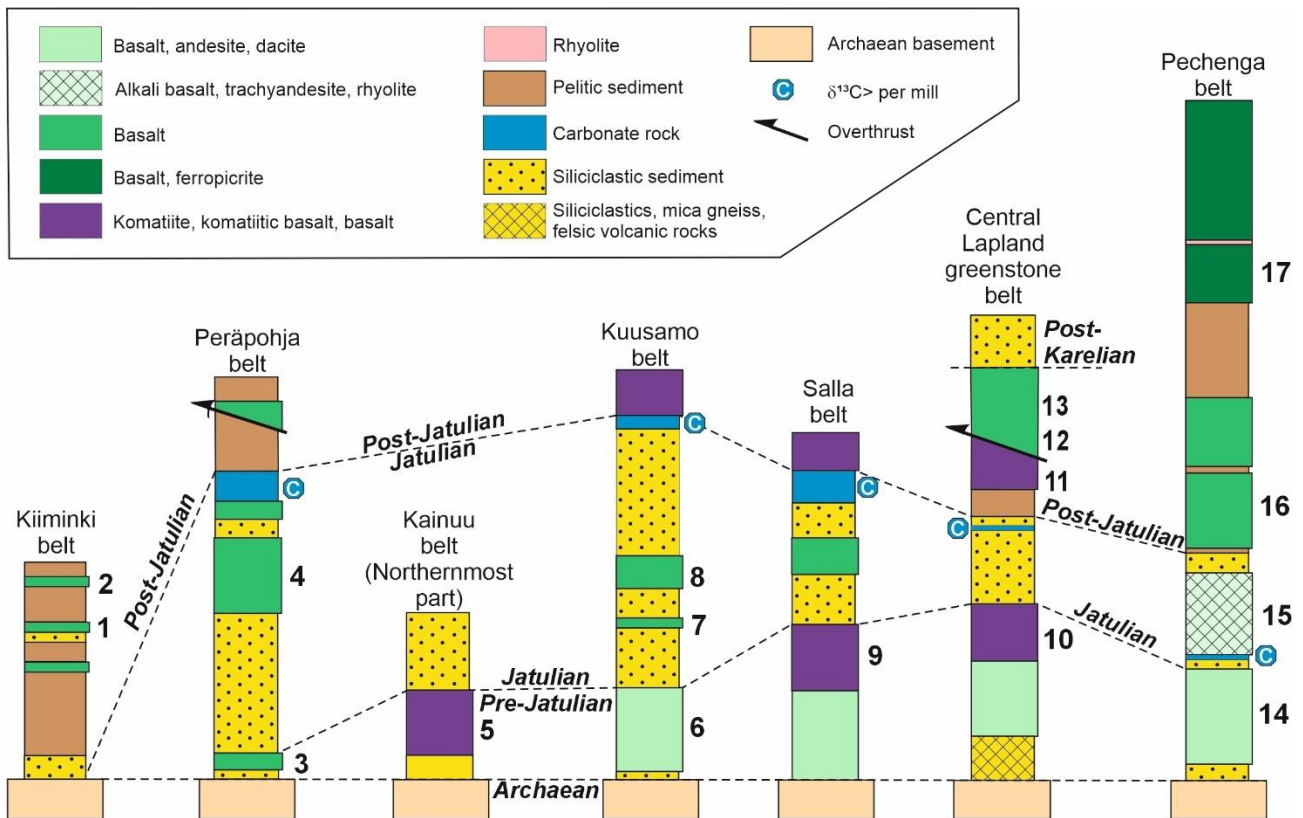
Fig. 7. Simplified stratigraphic columns of the study areas and their correlation (Honkamo, 1987; Manninen, 1991; Kyläkoski et al., 2012; Melezhik and Hanski, 2012; Huhma et al., 2018). Numbers refer to the studied volcanic Formations: 1 = Kiiminki Formation, 2 = Haukipudas Formation, 3 = Runkaus Formation, 4 = Jouttiaapa Formation, 5 = Vihantaselkä and Matinvaara Formations, 6 = Kuntijärvi Formation, 7 = Petäjävaara Formation, 8 = Ruukinvaara Formation, 9 = Mäntyvaara Formation, 10 = Möykkelmä Formation, 11 = Sattasvaara Formation, 12 = Kautoselkä Formation, 13 = Vesmajärvi Formation, 14 = Ahmalahti Formation, 15 = Kuetsjärvi Volcanic Formation, 16 = Kolosjoki Volcanic Formation, 17 = Pilgujärvi Volcanic Formation.

5. Sampling and analytical methods

Field work for komatiites was carried out in 2013, and additional samples were collected by S. Svetov. The mafic dyke samples were collected in a previous projects by GTK and the University of Oulu. The mafic-ultramafic volcanic rock samples were collected by Eero Hanski from various belts, partly utilizing samples of the Lapland Volcanite Project of GTK carried out in the 1980's.

Microscope analyses of silicate minerals were conducted at the University of Oulu, using a polarised light microscope with transmitted and reflected light. The compositions of olivine, clinopyroxene, orthopyroxene and plagioclase of the mafic dyke samples were determined using a JEOL JXA-8200 electron microprobe at the Centre of Microscopy and Nanotechnology, University of Oulu.

For the komatiite samples, major elements were determined using ICP-OES at Cardiff University and by XRF at the Institute of Geology of the Karelian Research Center of the Russian Academy of Sciences (IG KRC RAS; Petrozavodsk, Russia). Selected trace elements (Sc, V, Cr, Co, Ni, Cu, Zn, Sr, Y, Zr, Ba) were determined by ICP-OES at Cardiff University. Additional trace elements were determined by ICP-MS (Perkin-Elmer Sciex Elan 5000) at Cardiff University and IG KRC RAS.

For the mafic dyke samples, whole-rock geochemical analyses were carried out in two batches. In the first batch including a small group of samples, the major elements and selected trace elements (Cr, Ni, Cu, Zr) were determined by XRF at the Geological Survey of Finland (GTK), analytical methods were described in Vuollo and Salmirinne (2011). Most of our samples were analysed in the second batch, using ICP-OES and a full spectrum of trace elements were determined using ICP-MS (Perkin-Elmer Sciex Elan 5000) at Cardiff University, UK.

For the mafic-ultramafic volcanic rock samples, whole-rock major elements and a full spectrum of trace elements of samples from the Suurikuusikko area and two samples from the Jouttiaapa Formation were determined at Cardiff University, UK, using ICP-OES and ICP-MS, respectively. The analytical methods of the rest samples of the Jouttiaapa Formation were described in Hanski (2012). For other mafic-ultramafic volcanic rock samples, the major elements and selected trace elements (Cr, Ni, Cu, Zr) were determined by XRF mostly at the GTK and partly at ALS Scandinavia AB.

For the komatiite samples, mafic dyke samples and samples from the Suurikuusikko area and the Jouttiaapa Formation, platinum-group elements and Au were determined by ICP-MS after Ni-sulphide fire assay and tellurium co-precipitation in the analytical laboratory of the University of Quebec at Chicoutimi (Laboratoire d'Analyses Géochimiques de l'UQAC) (for analytical details, see Savard et al., 2010).

The in-situ analysis of Sr isotope compositions of pristine plagioclase grains of mafic dyke samples on thick sections (200 μm) was conducted on a Photon Machine Analyte G2 laser microprobe coupled to a Nu Plasma HR multicollector inductively coupled plasma mass spectrometer (LA-MC-ICP-MS) at the Geological Survey of Finland, Espoo. More detailed descriptions of the methods can be found in Papers I, II and III (Guo et al., 2020, 2023, and Guo et al., manuscript).

6. Review of original publications

6.1 Paper I

Guo, F.F., Svetov, S., Maier, W.D., Hanski, E., Yang, S.H., Rybnikova, Z., 2019. Geochemistry of komatiites and basalts in Archean greenstone belts of Russian Karelia with emphasis on platinum-group elements. Mineralium Deposita 55, 971–990.

In paper I, I have studied two Archaean greenstone belts, namely the Vedlozero-Segozero and Tikshozero belts in Russian Karelia (Fig 3), for their field geology, major, trace and chalcophile elements geochemistry, and evaluated their prospectivity for Ni-Cu sulphide ore deposits. Samples were analysed from four areas of the Vedlozero-Segozero belt, Hautavaara, Koikary, Palaselga, and Sovdozero, and two areas of the Tikshozero belt, Khizovaara and Irinozero. Stratigraphic columns from four areas are illustrated in Fig. 4.

The samples from six areas of both belts are divided into two groups, with one representing komatiites (MgO >18 wt.%) and the other komatiitic basalts (MgO 10–18 wt.%) and basalts (MgO 5–10 wt.%). The komatiitic samples from different areas show average Al_2O_3/TiO_2 ratios of 21.1 (Irinozero), 21.1 (Khizovaara), 18.7 (Koikary), 21.0 (Hautavaara), 21.3 (Sovdozero), and 26.3 (Palaselga), and thus belong to the Al-undepleted komatiite series (Nesbitt et al., 1979). Samples from both greenstone belts show negative correlations between MgO and SiO_2, TiO_2, Al_2O_3, and CaO (Figs. 8A–D), forming continuous trends from komatiites to komatiitic basalts and basalts and suggesting that these rocks form a differentiation series related to olivine accumulation and fractionation. Samples from both greenstone belts show a well-defined positive correlation on the Ni vs. MgO diagram (Fig. 8E), consistent with olivine-control trends. Notably, a few samples from the Khizovaara area and one sample from the Irinozero area have slightly higher Ni contents plotting above the main trend (Fig. 8E). However, the Cu contents of our samples show significant scatter when plotted against MgO (Fig. 8F). Most of the samples have a Cu content of less than 200 ppm, with 3 exceptions that have higher Cu contents between 284 to 491 ppm. The scatter is likely due to secondary mobility caused by regional metamorphism. On the Cr vs. MgO plot (Fig. 8G), our komatiitic samples display two different trends: a negative correlation for samples with MgO greater than 25 wt.%, indicating mixing of olivine with chromite-undersaturated komatiitic liquid, and a positive linear trend for samples with <25 wt.% MgO, reflecting co-accumulation and fractionation of olivine and chromite. The Zr contents in samples from the Sovdozero-Veldozero and Tikshozero greenstone belts plot at the lower
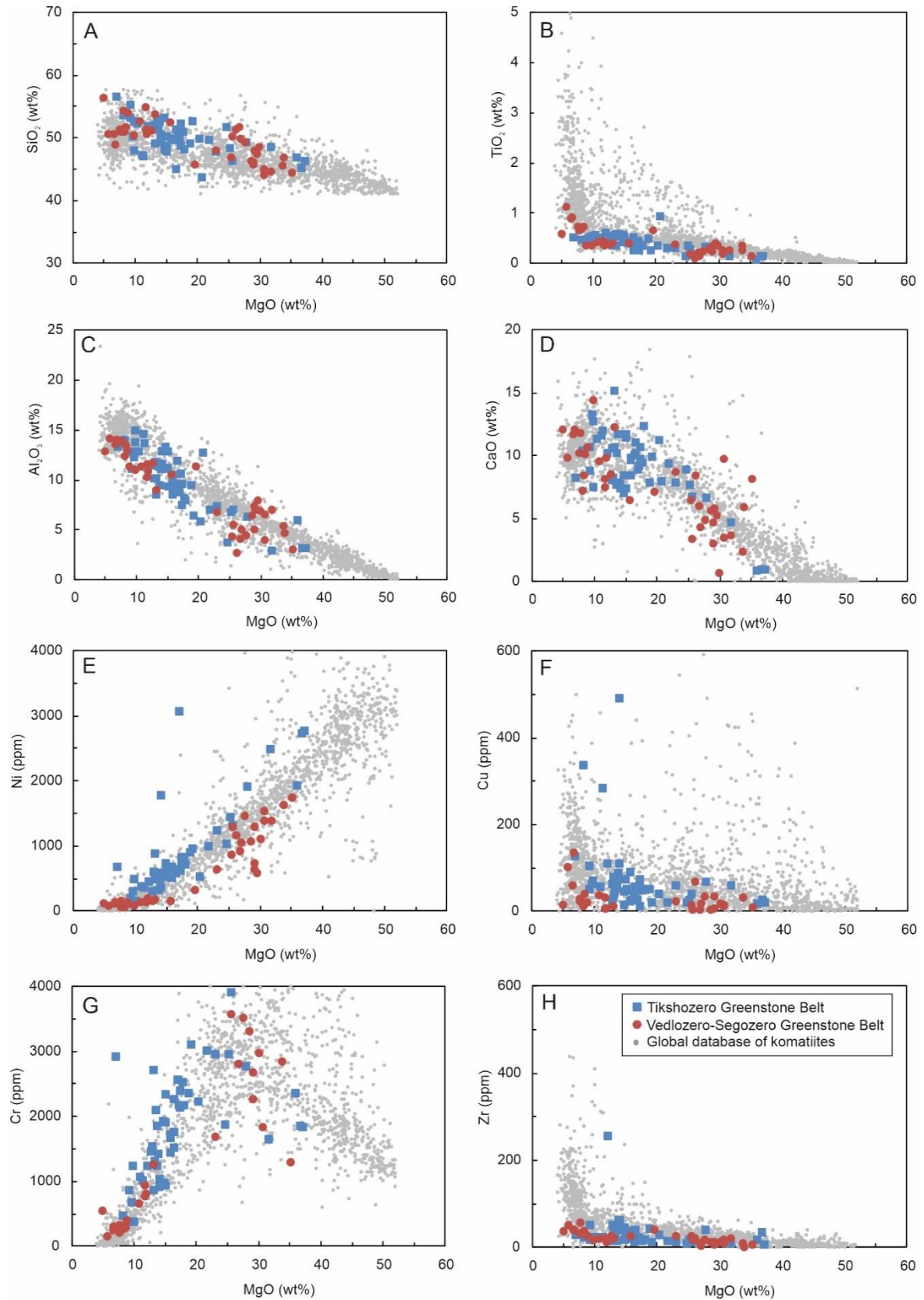
Fig. 8. Variation of TiO₂, Al₂O₃, CaO, Ni, Cu, Zr and Cr as a function of MgO in komatiites from the Vedlozero-Segozero and Tikshozero greenstone belts. TiO₂ data of 'boninitic rocks' are from Shchipansky et al. (2004). For comparison, analytical data from a global komatiite data base are also shown (Barnes and Fiorentini, 2012).

end of a global database (Fig. 8H), indicating a lower degree of crustal contamination compared to other greenstone belts globally.

Most samples from the Hautavaara area have flat REE patterns, with two komatiite samples showing slightly enriched light rare-earth element (LREE) patterns. All the samples in this area have weak negative Nb-Ta anomalies (Figs. 9A–B). Samples from the Koikary and Palaselga areas are moderately depleted in the LREE but have generally flat heavy rare-earth element (HREE) patterns. However, some samples have flat LREE or slightly LREE-enriched patterns as well as weak negative Nb-Ta anomalies (Figs. 9C–F). All the komatiite samples from the Sovdozero area show a slight enrichment in LREE, while all the komatiitic basalt and basalt samples show flat or slightly depleted LREE patterns, but generally, samples from this area have no negative Nb-Ta anomalies (Fig. 9G–H).

In terms of REE, the samples from the Khizovaara area can be divided into two sub-groups. One group is slightly depleted in LREE but has generally flat HREE patterns (Fig. 9I–J), while the other group shows a LREE enrichment and significant negative Nb-Ta anomalies (Fig. 9I–J). Notably, all the LREE-enriched samples are komatiitic basalts from the central part of the Khizovaara area, while the LREE-depleted samples are from the northern part of the Khizovaara area, including cumulates, komatiites and komatiitic basalts. Samples from the Irinozero area show similar REE patterns as the LREE-depleted groups of the Khizovaara area, with most samples having weak Nb-Ta anomalies (Fig. 9K–L).

In Fig. 10, Th/Nb, Th/Yb, and Nb/La ratios are plotted against La/Sm. Samples both from the Vedlozero-Segozero and Tikshozero greenstone belts fall within the trend of the global database and show a weak positive correlation between Th/Nb and La/Sm, a relatively good positive correlation between Th/Yb and La/Sm, and a negative correlation between Nb/La and La/Sm.

The PGE contents of most of the komatiite samples are in the global range of Al-undepleted komatiites, with up to 15.1 ppb Pt, 20.9 ppb Pd, 8.99 ppb Ir, 6.35 ppb Ru, 6.71 ppb Os, and 27.7 ppb Au. Three samples from the Vedlozero-Sovdozero belt show higher Pd concentration than the others, but their Pt content is in the range of the other samples, and thus the higher Pd contents may be result of mobility of Pd during metamorphism. Iridium and Ru have generally positive correlations with MgO, but some samples with a high MgO content have very low Ir and Ru concentrations (Fig. 11). Platinum, Pd and Au contents generally increase with falling MgO contents, but there is a sharp decrease when the MgO content falls below 10 wt.% (Fig. 11). Rhodium shows a slight increase with decreasing MgO. Due to the different compatibility of IPGE

38

(Iridium group Ir, Ru, Os) and PPGE (Palladium group, Pt, Pd, Rh), the Pd/Ir ratio broadly increases with decreasing MgO (Fig. 11).

The PGE concentrations in these Munro-type komatiitic rocks are at the level of other similar S-undersaturated komatiites and komatiitic basalts globally, with Pt and Pd falling in the range of 5–20 ppb and Pd/Ir varying from <10 (komatiites) to >15 (komatiitic basalts and basalts). Generally, the metals of the iridium group platinum-group elements (IPGE, Ir, Ru, Os) show a compatible behaviour, decreasing in abundance with falling MgO, whereas the metals of the platinum-group (Pt, Pd, Rh) exhibit an incompatible behaviour (Fig. 11). The poor correlation between Ir and MgO suggests that olivine is not the main control on IPGE contents. In contrast, Ir, Ru show positive correlation with Cr (Fig. 12), consistent with the compatibility of IPGEs in chromite or during the co-precipitation of chromite and platinum-group minerals (PGM).
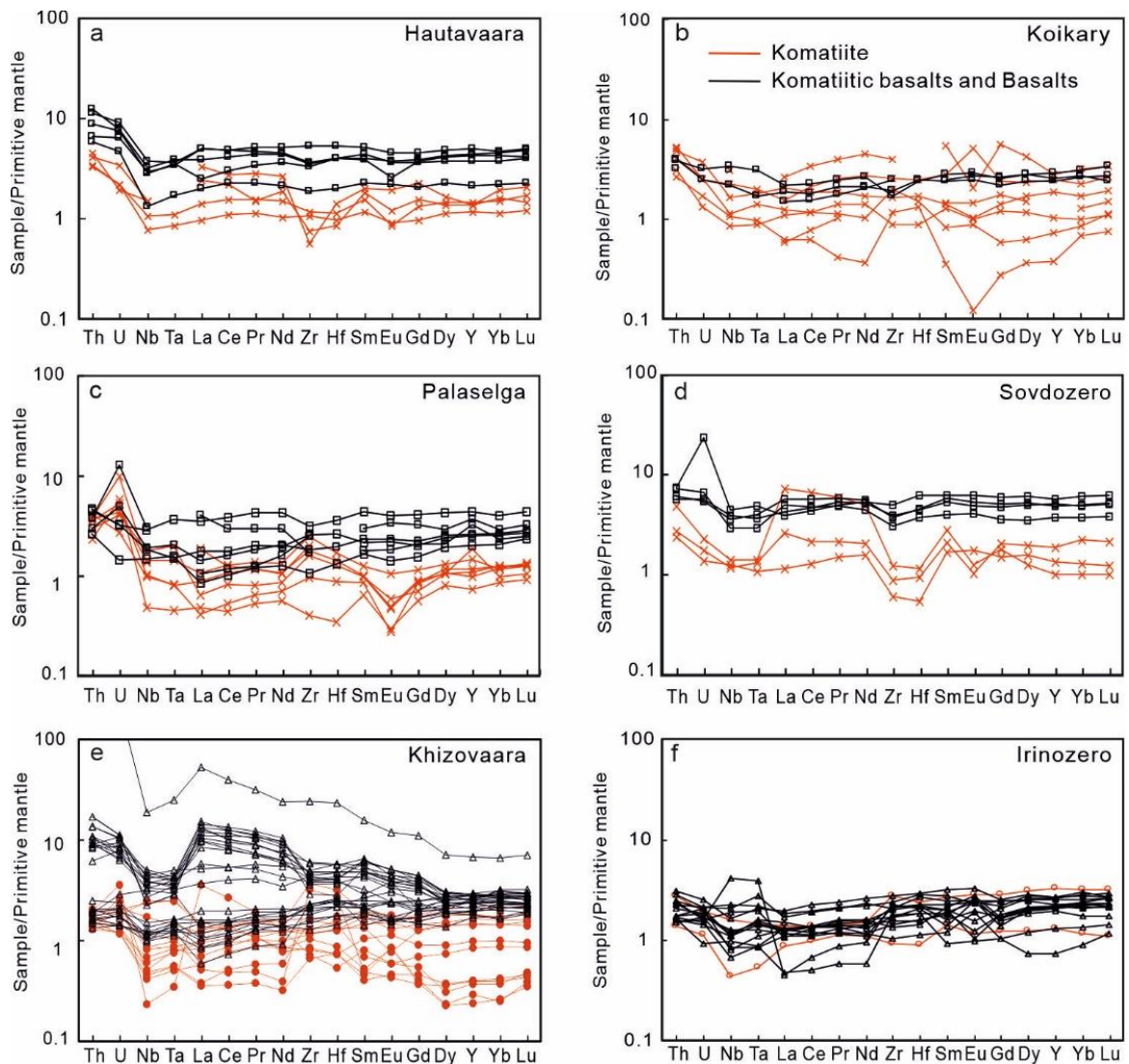
Fig. 9. Primitive mantle-normalised chalcophile element diagram for komatiites in the Vedlozero-Segozero and Tikshozero greenstone belts. Normalisation values are from McDonough and Sun (1995).
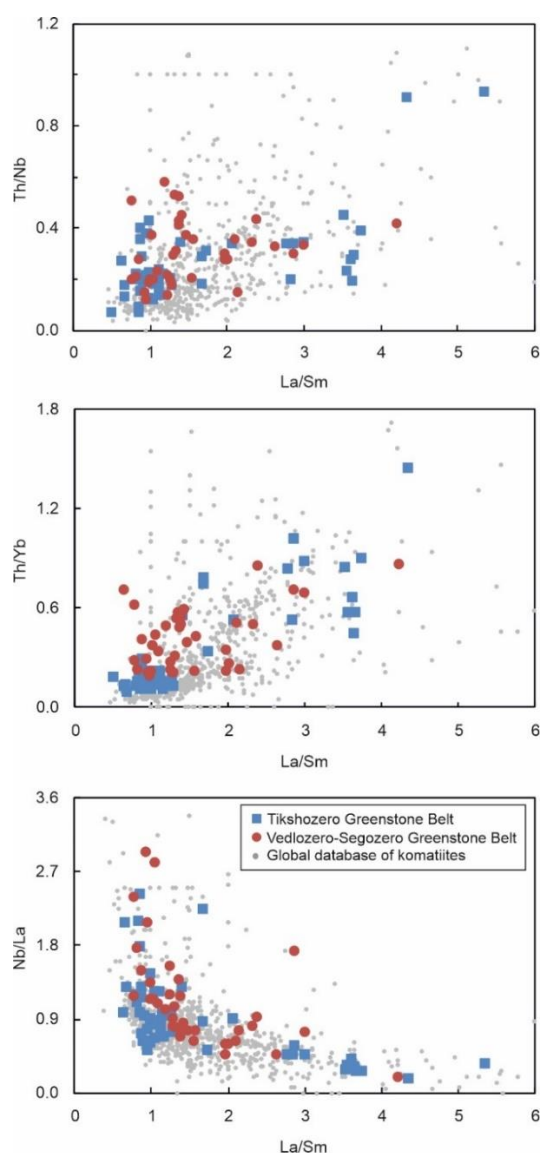
Fig. 10. Correlation between Th/Nb, Th/Yb, Nb/La and La/Sm in komatiites from the Vedlozero-Segozero and Tikshozero greenstone belts. For comparison, analytical data from a global komatiite database are also shown (Barnes and Fiorentini, 2012).

Palladium, Cu and Au have been variably mobile during alteration and metamorphism whereas Pt appears to have been less mobile. Some samples from the Khizovaara area show low $(Pt/Ti)_N$ ratios, low Ni, and high La/Sm and La/Nb, suggesting localised sulphide saturation in response to crustal contamination. However, the potential of the Russian Karelian greenstone belts for Ni-Cu sulphide mineralisation is considered relatively low due to the lack of both enrichment or depletion of chalcophile elements in any of the analysed samples (Fig. 11), and the paucity of dynamic lava channel environments as indicated by the scarcity of olivine-rich adcumulates. In addition, there appears to be a lack of exposed sulphidic sedimentary rocks in the region.

40
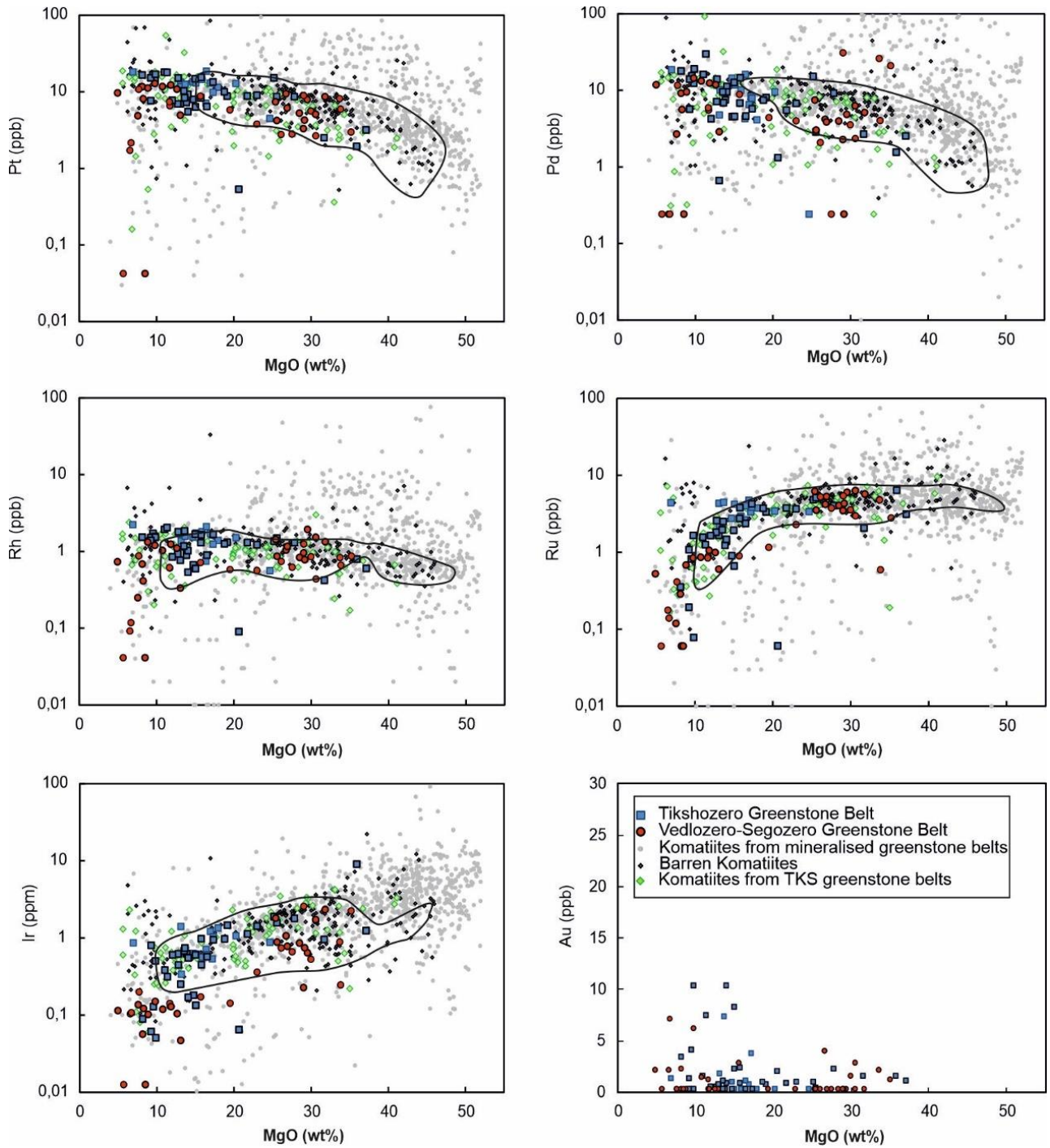
Fig. 11. Pt, Pd and Rh contents in komatiites in the Vedlozero-Segozero and Tikshozero greenstone belts compared to analytical data from a global komatiite database, with the outline representing the field of komatiites from unmineralised greenstone terrane (Barnes and Fiorentini, 2012).
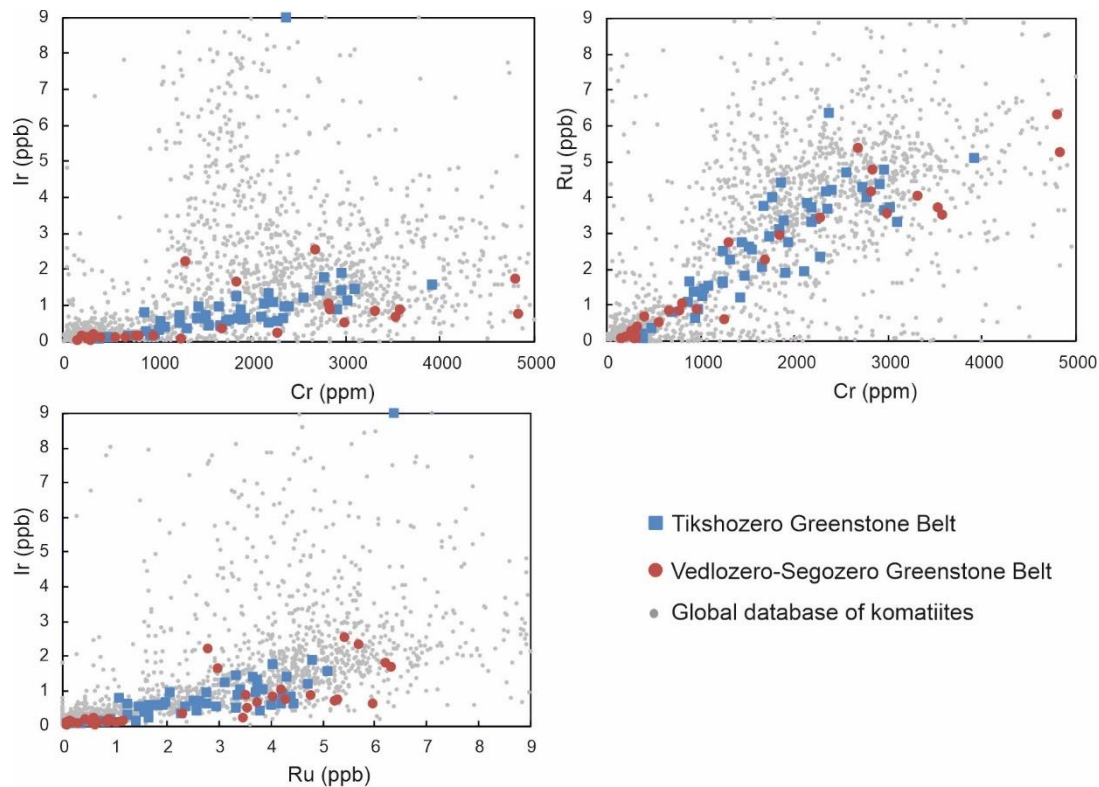
Fig. 12. Plots of IPGE vs. Cr, and Ir vs. Ru for komatiites in the Vedlozero-Segozero and Tikshozero greenstone belts. For comparison, analytical data from a global komatiite database are also shown (Barnes and Fiorentini, 2012).

6.2 Paper II

Guo, F.F., Maier, W.D., Heinonen J.S., Hanski, E., Vuollo J., Barnes S.-J., Lahaye Y., Huhma H., Yang, S.H., 2023. Geochemistry of 2.45 Ga mafic dykes in northern Finland: constraints on the petrogenesis and PGE prospectivity of coeval layered intrusions. Lithos 452−453, Article 107206

In this paper, I studied the ~2.45 Ga mafic dykes that are compositionally, temporally and, in some cases, spatially related to PGE-mineralised mafic-ultramafic layered intrusions in the Karelian craton. The dykes can be subdivided into four groups:1) siliceous high-magnesian basalts (SHMB), 2) gabbronorites (GBNO), 3) low-Ti tholeiites, and 4) Fe-rich tholeiites (Fig. 11). In this study, the SHMB and GBNO dykes are considered together as the SHMB group and the two tholeiitic group dykes as the tholeiite group, based on their similar geochemical and mineralogical features.
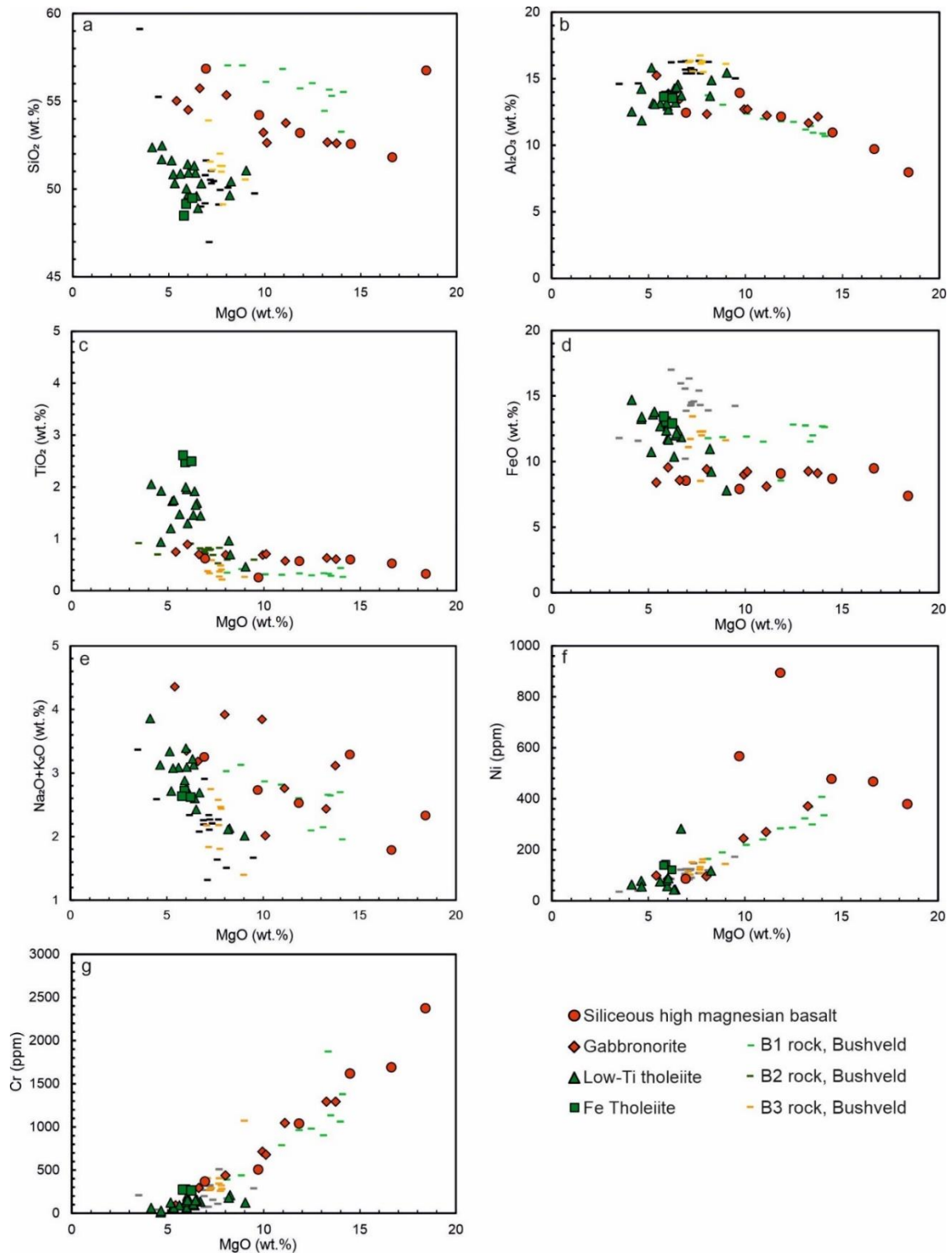
Fig. 13. Selected major element oxides plotted against MgO for the studied dykes. Bushveld data taken from Barnes et al. (2010).

The SHMB and GBNO dykes have broadly similar major element compositions, displaying a good overlap on binary variation diagrams (Fig. 13). The SHMB dykes display a somewhat wider compositional range than the GBNO dykes. The former has 4.6–18.4 wt.% MgO, 52–57 wt.%

SiO$_2$, 2–4.5 wt.% Na$_2$O+K$_2$O, while the latter have 5.41–13.7 wt.% MgO, 51–56 wt.% SiO$_2$, 1.5–3.2 wt.%, 1.5–3.2 wt.% Na$_2$O+K$_2$O. One striking feature of these two dyke groups is the relatively high SiO$_2$ and alkali (Na$_2$O+K$_2$O) contents at a given MgO content (Fig. 13). The LTTH dykes have 4–9 wt.% MgO, 47–53 wt.% SiO$_2$, and 2.01–3.86 wt.% Na$_2$O+K$_2$O. Due to the relatively small number of samples, the FTH dykes show a limited variation in the binary variation diagrams. The samples contain 48.5–49.5 wt.% SiO$_2$, 5.79–6.23 wt.% MgO, 2.6–2.7 wt.% Na$_2$O+K$_2$O, and plot broadly together with the LTTH dykes (Fig. 13). The two groups of tholeiite dykes show clearly lower SiO$_2$ and alkali contents, and also lower Cr and Ni contents, but slightly higher TiO$_2$ and FeO contents than the SHMB and GBNO groups (Figs. 13c, 14a). However, all dykes mainly plot in the field of the low-Ti series of other LIPs, though the FTH group plots near the lower range of the high-Ti series (e.g., Emeishan, Paraná, Fig. 14a) (Arguin et al., 2016; Mansur et al., 2021). This is consistent with the observation that all mafic dyke groups in Fennoscandia show lower Ti/Y ratios than the high-Ti series in other LIPs (Fig. 14b). Compared with high-Ti series of the Emeishan and Paraná flood basalts, the dykes in Fennoscandia show lower Sm/Yb and La/Yb ratios (Figs. 14c, d).
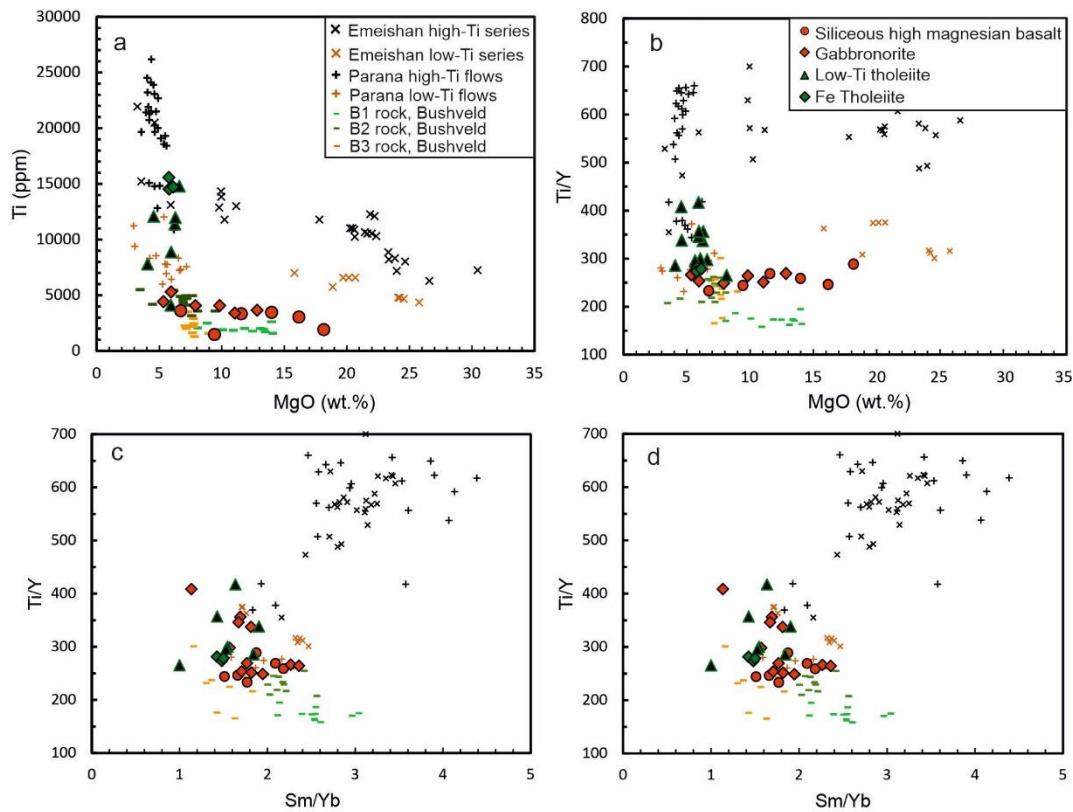
Fig. 14. Binary plots of MgO (wt.%) vs Ti (ppm), MgO (wt.%) vs. Ti/Y, Sm/Yb vs. Ti/Y, La/Yb vs. Ti/Y for our studies samples, high-Ti and Low-Ti basalts from the Paraná Magma Provice (Mansur et al., 2021) and the Emeishan Large Igneous Province (Arguin et al., 2016). Bushveld data are taken from Barnes et al. (2010).

The SHMB and GBNO dykes display fractionated chondrite-normalised REE patterns with a clear enrichment in LREE compared to HREE (Figs. 15a, b). One of the tholeiitic dykes shows a flat REE pattern, whereas the majority of the tholeiitic samples show enrichment in LREE but with less fractionated LREE/HREE compared to the SHMB and GBNO dykes (Figs. 15c, d). Notably, amongst the tholeiites, the Fe tholeiites show small negative Eu anomalies, but this is not a characteristic feature of all LTTH dykes.

In primitive mantle-normalised incompatible trace element plots, both SHMB and GBNO dykes show strong negative Ta-Nb and P anomalies, and relative enrichments in Rb, Ba, Th, U and Pb, whereas the tholeiitic dykes display weak negative Ta-Nb anomalies and generally rather flat patterns, albeit with minor enrichment in Pb and depletions in K, Sr and P (Figs. 15e, h). The FTH group shows strong negative Sr anomalies, which is consistent with the negative Eu anomalies of this dyke type. All dyke samples show a negative correlation between Nb/La and La/Sm ratios and a positive correlation between Ce/Yb and La/Sm ratios (Fig. 16), suggesting the presence of a crustal component, especially in the SHMB and GBNO suites.
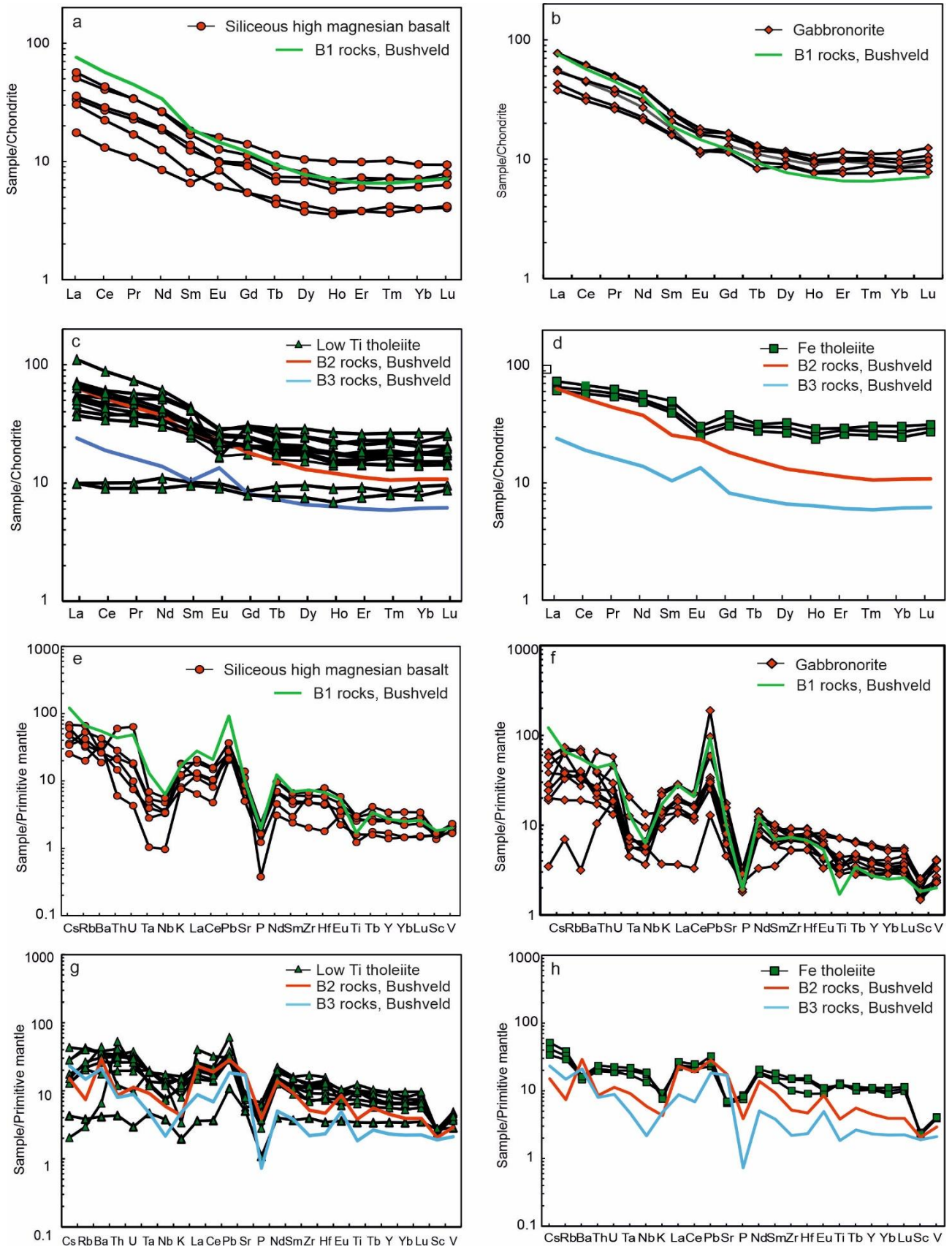
Fig. 15. Chondrite-normalised rare earth element (REE) patterns and primitive mantle-normalised lithophile trace element patterns for different dyke groups. Bushveld data are taken from Barnes et al. (2010) and normalisation values from McDonough and Sun (1995).

46
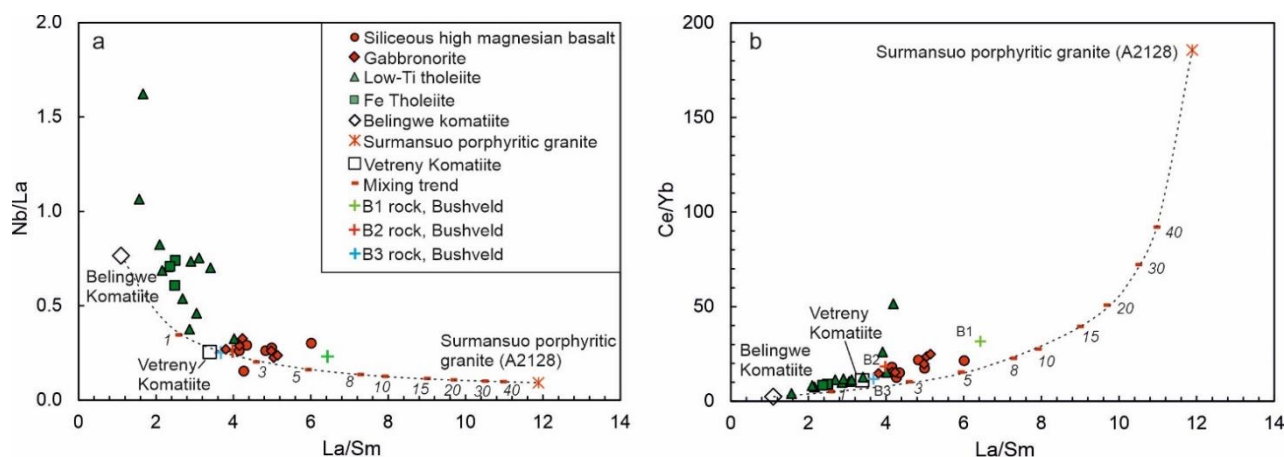
Fig. 16. a. Trace element ratios in the studied dykes showing a negative correlation between Nb/Th and La/Sm and a positive correlation between Ce/Yb and La/Sm. b. Simplified two component mixing calculation with komatiite and trondhjemite as end-members indicating <10% contamination for the tholeiite group and 5–20% for SHMB and GBNO. Primitive mantle values are from McDonough and Sun (1995). Comparative data for komatiite from Belingwe are from Shimizu et al. (2005), Vetreny komatiite from Puchtel et al. (1997), and Surmansuo porphyritic granite (A2128) from Mikkola et al., (2014).

In the SHMB group dykes, plagioclase has initial $^{87}Sr/^{86}Sr$ ratios of 0.7028 to 0.7036 and initial bulk-rock εNd values vary from -2.5 to -1.0 (Fig. 17), indicating moderate degrees of contamination with Archaean basement. The tholeiitic dykes show less-radiogenic Sr isotope compositions with an average initial $^{87}Sr/^{86}Sr$ ratio of 0.7024 and higher initial εNd values ranging from +0.3 to +1.7 (Fig. 17).
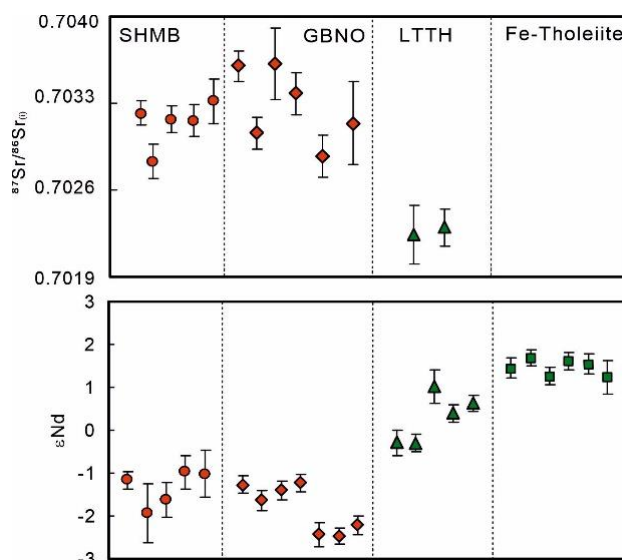
Fig. 17. In-situ Sr isotope compositions of plagioclase and bulk-rock Nd isotope compositions of the studied dyke samples. Nd isotope data taken from Vuollo and Huhma (2005).
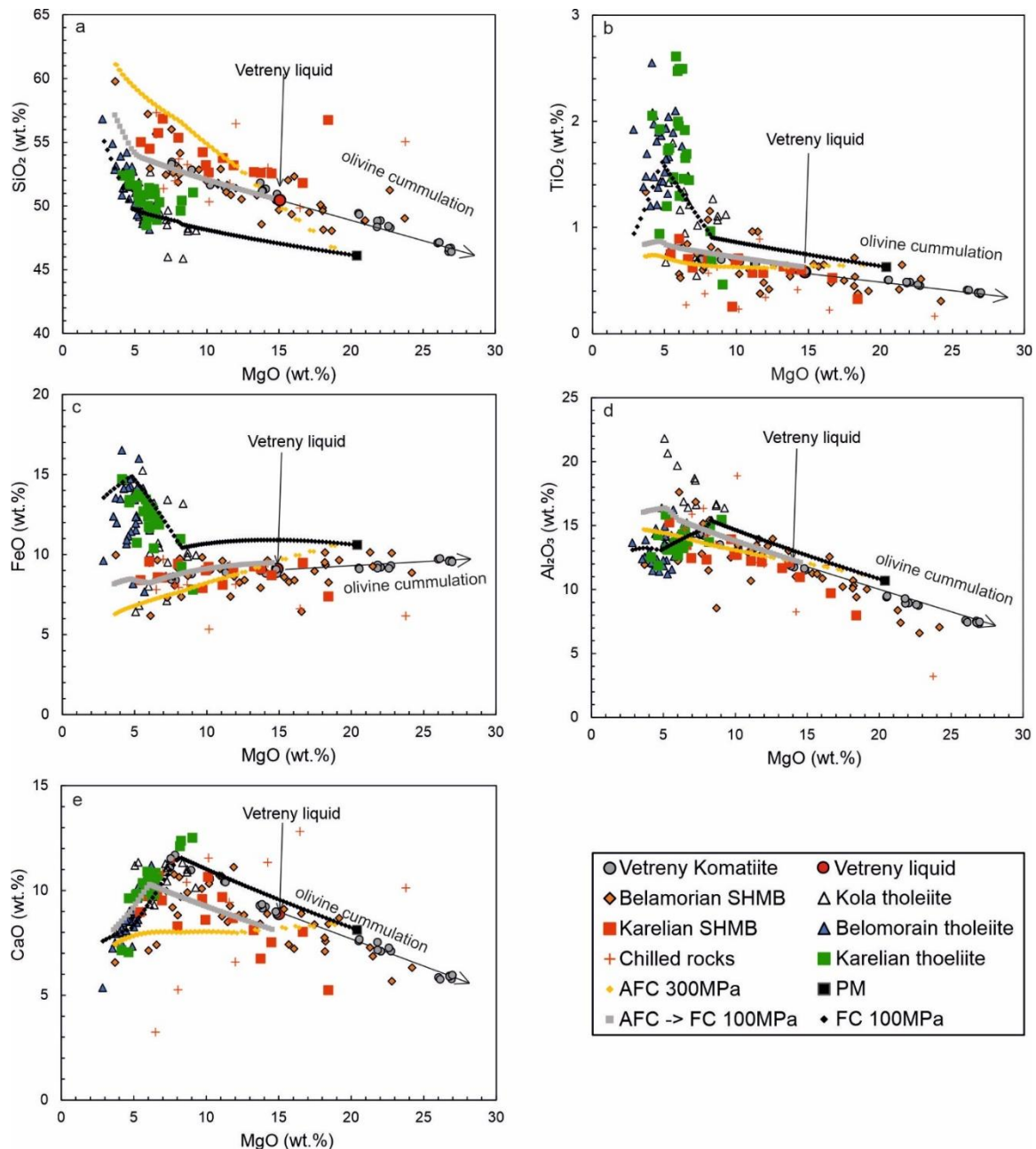
Fig. 18. MCS (Magma Chamber Simulator) major element modelling for different types of mafic dykes in Karelian, Belomorian and Kola regions at different pressures.

Thermodynamic and geochemical modelling suggests that the SHMB group dykes could have formed by crustal contamination of a komatiitic magma in relatively deep crust followed by fractional crystallisation at shallower depth, whereas the tholeiitic group mainly experienced fractional crystallisation with less crustal contamination (Fig. 18). Based on trace element and isotope characteristics, the SHMB dykes are suitable candidates for the parental magmas to some of the Finnish PGE-mineralised intrusions (e.g., Penikat and Portimo), whereas the tholeiitic dykes may represent the parental magma of the Tsipringa layered intrusion in Russia.
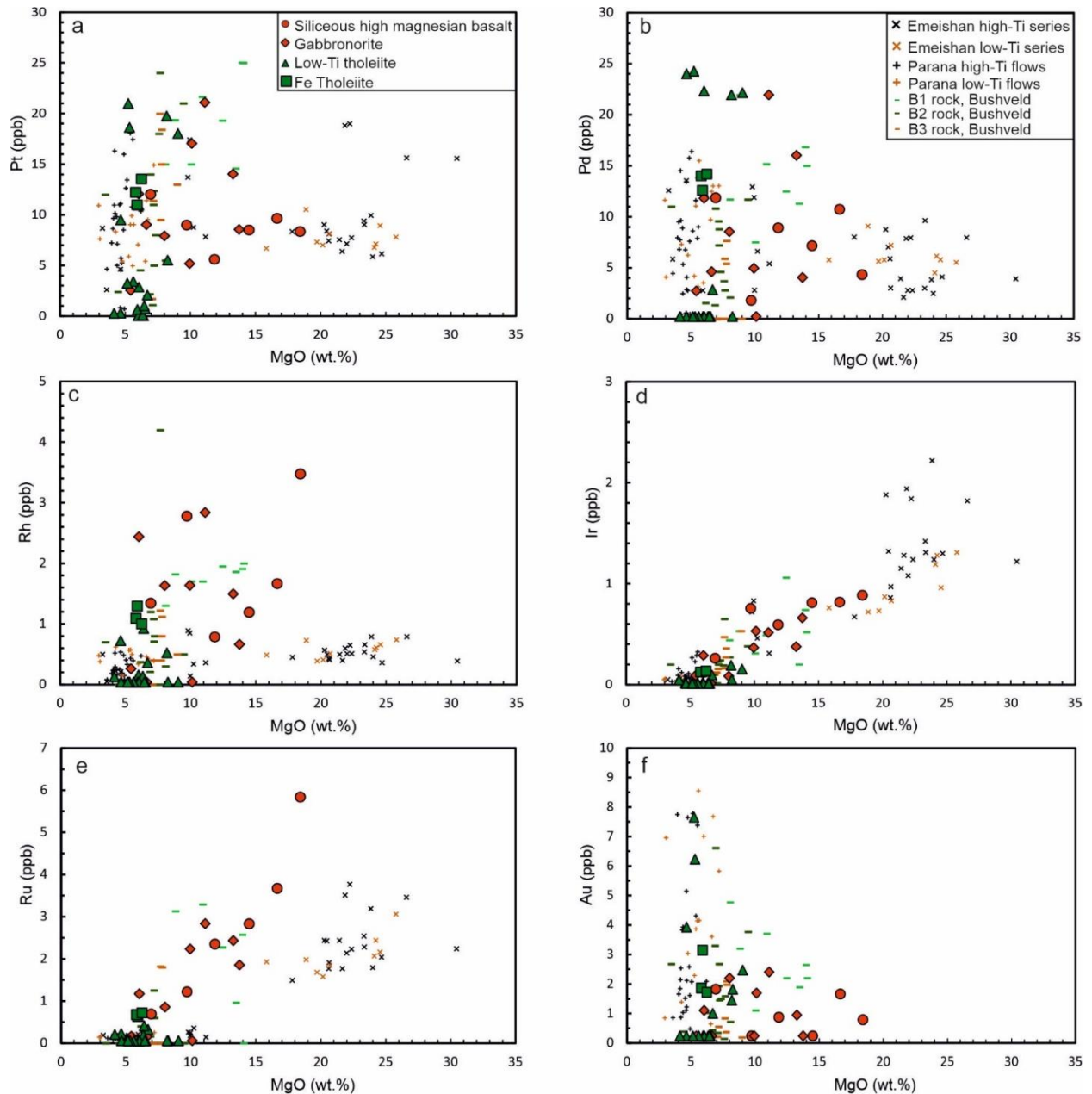
Fig. 19. Plots of Pt, Pd, Rh, Ru, Ir and Au vs. MgO diagrams for the studied dykes.

The SHMB dykes have rather variable Pt and Pd contents, ranging from 0.24 to 12.0 ppb, and contain 0.02–0.89 ppb Ir, and 22–152 ppm Cu. The GBNO samples have broadly similar chalcophile element concentrations to those of the SHMB samples. In the SHMB and GBNO groups, MgO shows good positive correlations with Ir, Ru and Rh, but a poor correlation with Pt, Pd, Au. However, the most primitive samples with MgO from 15–20 wt.% show moderate Pt and Pd contents ranging from 5 to 10 ppb, and the highest Pt and Pd contents occur in samples with moderate MgO of about 10 wt.% (Fig. 19). Samples with low MgO contents (4–7 wt.%) display a

large variation in Pt and Pd contents, varying from values below the detection limit to the highest values found in the entire dyke population (Fig. 19).

The LTTH dykes also have variable Pt and Pd contents ranging from 0.24 to 24.3 ppb, and very low Ir and Ru contents from below detection limit to 0.21 ppb, 81.2–254 ppm Cu and 0.24–7.66 ppb Au. The FTH dykes have a narrow range of 11.0–14.2 ppb for Pt and Pd, low Ir contents from 0.12 to 0.14 ppb, and 13–76 ppm Cu, and 0.89–2.7 ppb Au. Some samples of the LTTH group with moderate MgO contents (5–9 wt.%) show the highest Pd and Pt contents of up to 24 ppb and 20 ppb, respectively, being higher than in the SHMB and GBNO groups. Other samples with lower MgO contents (4–7 wt.%) have very low Pd and Pt contents falling below the detection limit. In contrast, the LTTH dykes show relatively low IPGE and Rh contents (Fig. 19). The FTH group with a limited number of samples (3) has moderate Pd and Pt contents, similar to those of the SHMB and GBNO dykes, and low but detectable IPGE contents, overlapping with the positive trend between IPGE and MgO displayed by the SHMB and GBNO groups. However, the FTH dykes show the highest Cu content of about 300 ppm among all dyke groups (Fig. 19). For all four dyke groups, the variation in Au is similar to that of Pd and Pt, though more scattered (Fig. 19). Platinum shows a positive correlation with Pd, plotting broadly on the 1:1 trend line, although some LTTH samples show higher Pd than Pt (2:1) (Fig. 20). This trend is somewhat different from the Bushveld magma compositions (B1, B2, B3), which have higher Pt/Pd ratios (Fig. 20). On the plot of Ir vs. Pt, the SHMB and GBNO dykes show relatively high Ir and moderate Pt contents, and some LTTH and FTH dykes show low Ir but high Pt contents, whereas the other samples display very low Pt and Ir contents. In this plot, the B1 marginal rocks from Bushveld display a lot of overlap with the SHMB and GBNO group dykes, and the B2 and B3 rocks with the LTTH and FTH groups.
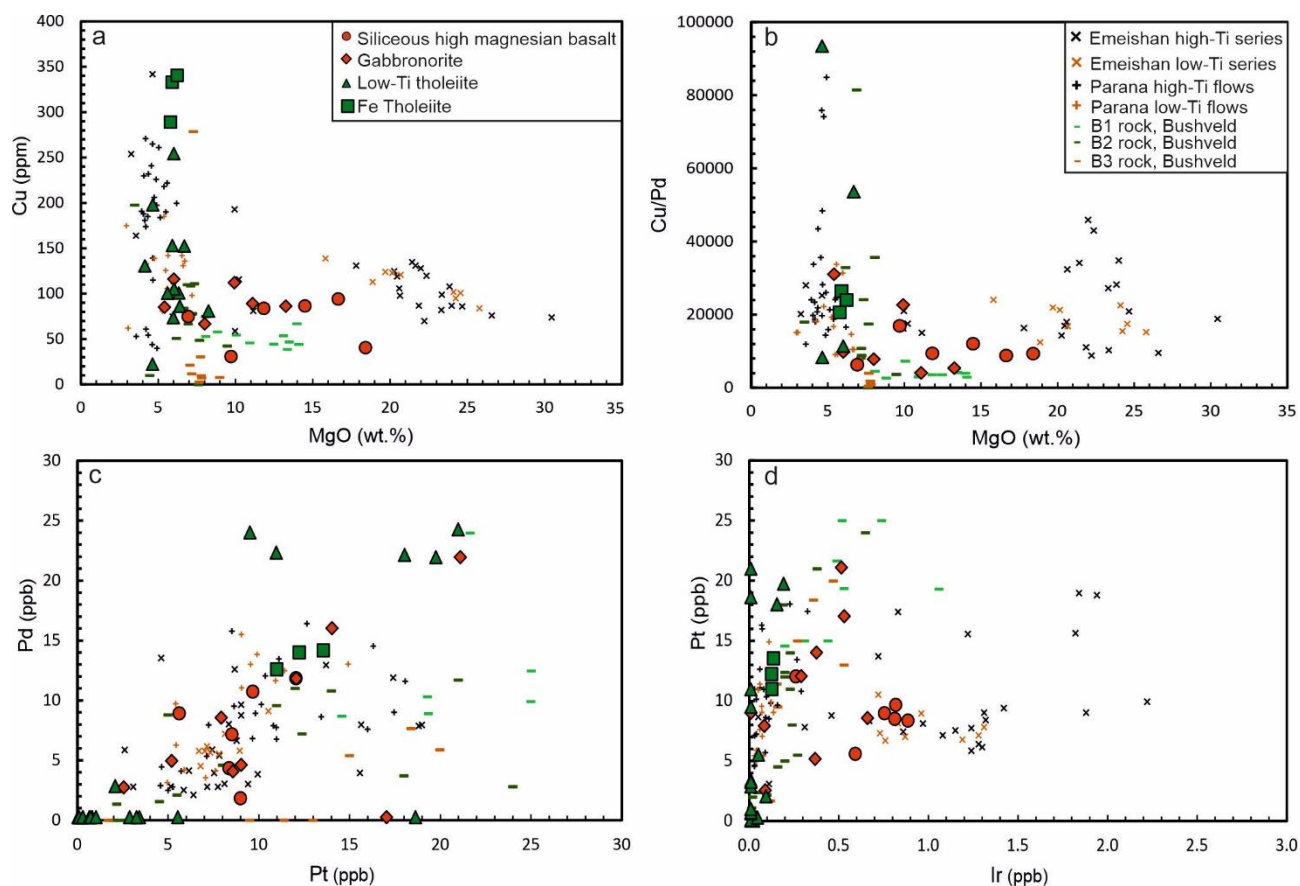
Fig. 20. Cu, Cu/Pd vs. MgO, Pd vs. Pt and Pt vs. Ir diagrams for the studied dykes.

The samples of all four dyke groups show mostly PGE-undepleted primitive mantle-normalised chalcophile element patterns, except that the IPGE are generally depleted relative to Ni, and Au is depleted relative to Pd and Cu (Fig. 21). In terms of chalcophile element patterns, the SHMB and GBNO groups are similar to Bushveld B1, and the LTTH and FTH groups similar to Bushveld B2 and B3. Accordingly, the FTH samples typically have very high Cu/Pd >20000 whereas most samples from the other groups have Cu/Pd <15000, with the exception of a couple of LTTH and GBNO samples with low Pd contents below the detection limit showing the highest Cu/Pd ratios (Fig. 20).

Both the SHMB and tholeiitic dyke types are fertile with regard to PGE, with up to 10–20 ppb Pt and Pd and mantle-like Cu/Pd ratios in their least evolved members (Fig. 14), suggesting that the magmas remained sulphide undersaturated during mantle melting and *en route* to the upper crust. This interpretation is consistent with the fact that most of the ~2.45 Ga Fennoscandian layered intrusions contain PGE mineralisation. Sulphide melt saturation in the dykes and layered intrusions was mostly attained after their final emplacement, likely due to crystal fractionation.

51
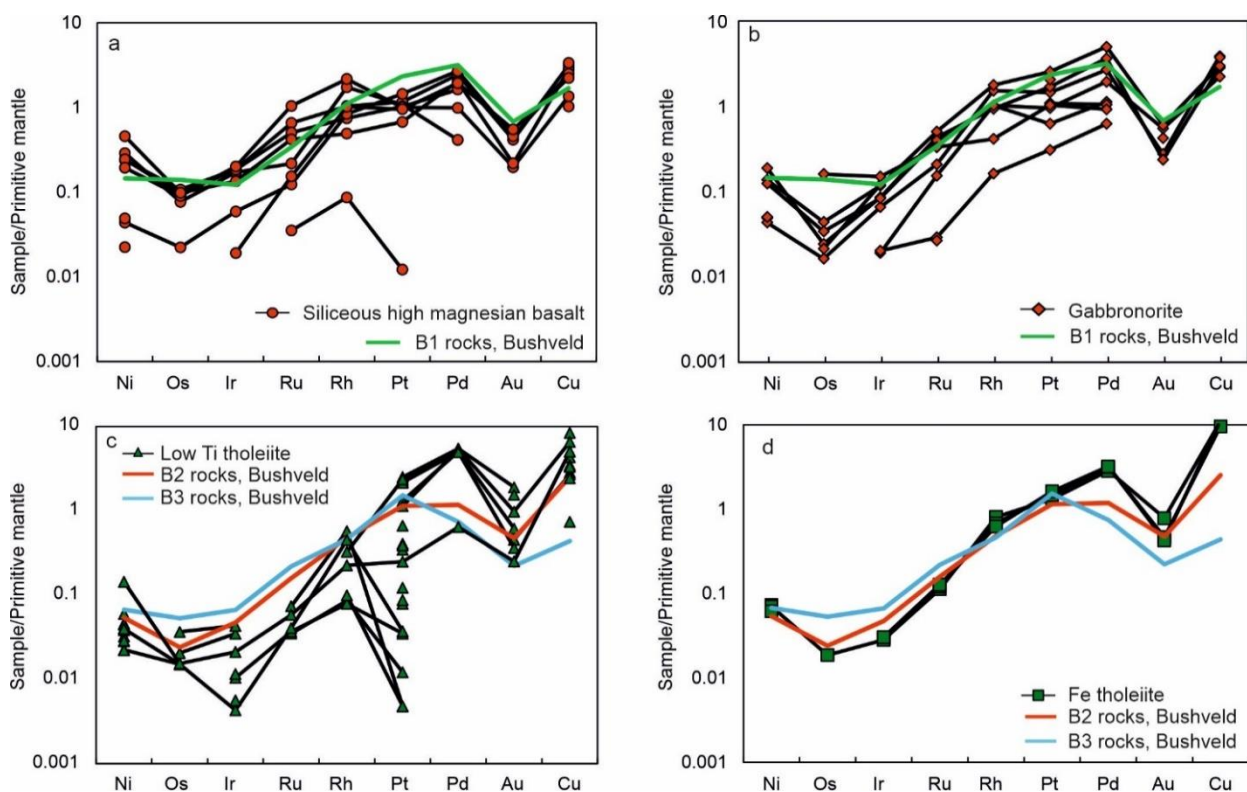
Fig. 21. Primitive mantle-normalised siderophile element patterns for the studied dykes. Normalisation values taken from (McDonough and Sun, 1995).

6.3 Paper III

Guo, F.F., Hanski, E., Maier, W.D., Yang, S.H., Barnes, S., manuscript. PGE geochemistry of Palaeoproterozoic mafic and ultramafic volcanic rocks from northern Finland: implications for exploration of magmatic sulphide deposits.

Multiple stages of Palaeoproterozoic rifting related magmatism have resulted in the break-up of the Kenorland supercontinent. These extensional tectonic events were associated with wide-spread mafic-ultramafic magmatism producing important ore deposits of Cr, Ti, V, Ni, Cu and PGE. I studied the geochemistry of Palaeoproterozoic mafic-ultramafic volcanic rocks from several Palaeoproterozoic supracrustal belts in NE Fennoscandia (Fig. 6, 7) to constrain the fertility and sulphide saturation history of the magmas and their potential to form magmatic sulphide deposits. The evolution of the belts has been divided in this work into three rifting stages, early, middle and late, with the boundary between the 1st and 2nd stage being set at the appearance of Jatulian siliciclastic sediments and that between the 2nd and 3rd stages at the disappearance of the Jatuli-Lomagundi carbon isotope anomaly in carbonate rocks. Thus, the three stages and corresponding

volcanic rocks can also be called pre-Jatulian (2.5–2.3 Ga), Jatulian (2.3–2.1 Ga) and post-Jatulian (2.06–1.98 Ga).

Early rifting stage (2.45-2.3 Ga, pre-Jatulian)

Figure 22 shows selected major element plots for our samples from different belts of the pre-Jatulian stage. Among the analysed pre-Jatulian volcanic rocks, there are samples from three belts, Kainuu (Vihantaselkä and Matinvaara Formations), Salla (Mäntyvaara Formation) and CLGB (Möykkelmä Formation). The three additional pre-Jatulian volcanic formations that represent a more restricted major element compositional range without any highly magnesian samples are the Ahmalahti Formation in the Pechenga belt, the Runkaus Formation in the Peräpohja belt, and the Kuntijärvi Formation in the Kuusamo belt. These volcanic rocks represent a magmatic suite varying from komatiites with MgO up to 20.8 wt.% to evolved basaltic rocks with MgO down to 3.8 wt.%. It is worth noting that in the 2.45 Ga group, almost all the volcanic formations show relatively high SiO_2 contents at a given MgO content, and high alkali and low TiO_2 contents, plotting in the field of the 2.45 Ga silicious high-magnesium basalt (SHMB) dykes (Guo et al. 2023). These rocks also display enrichment in LREE, large-ion lithophile elements (LILE, e.g., Th, U) and depletion in Nb and Ta in primitive mantle-normalised trace element spider diagrams (Fig. 23).

The 2.44 Ga volcanic rocks from the Kainuu and Salla belts and the CLGB have relatively primitive compositions with high concentrations of MgO (up to about 20 wt.%) as well as Ir and Ru, and following the same fractionation trend (Figs. 22, 24). The somewhat younger (2.3 Ga) Runkaus Formation also shows relatively evolved composition with MgO ranging from 5 to 7 wt.%, and Os, Ir, and Ru generally lower than 0.1 ppb. The concentrations of the PPGE range from about 5 to 12 ppb for Pt, 5 to 12 ppb for Pd, and 0.8 to 1.5 ppb for Rh (Fig. 24). The Pd/Ir ratios of the rocks show negative correlation with MgO contents. Relatively low values of about 5 to 10 occur in the primitive samples having MgO from 20 to 8 wt.%. Pd/Ir increases to about 120 at MgO of about 3-5 wt.% (Fig. 25). The mafic-ultramafic volcanic rocks from all pre-Jatulian belts (including the Vetreny belt) show similar variation that the PPGE show negative correlations with MgO consistent with the incompatibility of these elements during early-stage fractionation of sulphur-undersaturated silicate melt (Fig. 24). However, the lowest PPGE levels typically occur in the most evolved samples. The Cu/Pd ratios vary a lot from 150 to 123600, with the lowest values occurring in the Kainuu belt and the CLGB associated with higher MgO, and the highest values are in the Kuusamo belt with MgO lower than 5 wt.%.
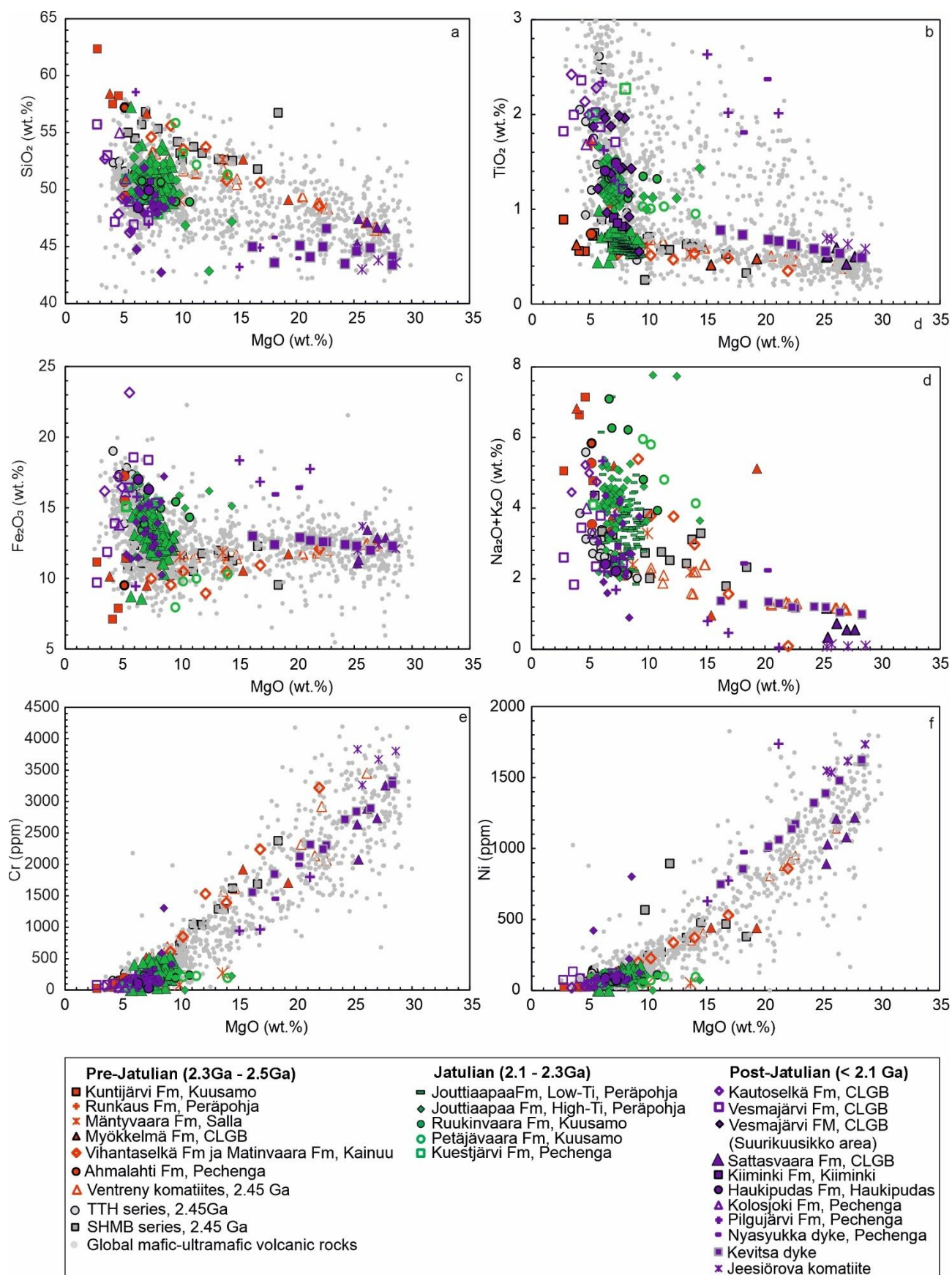
Fig. 22. Selected major element oxides plotted against MgO for mafic-ultramafic volcanic rocks from NE Fennoscandia. Grey dots indicate global database from Barnes and Fiorentini (2012).

54
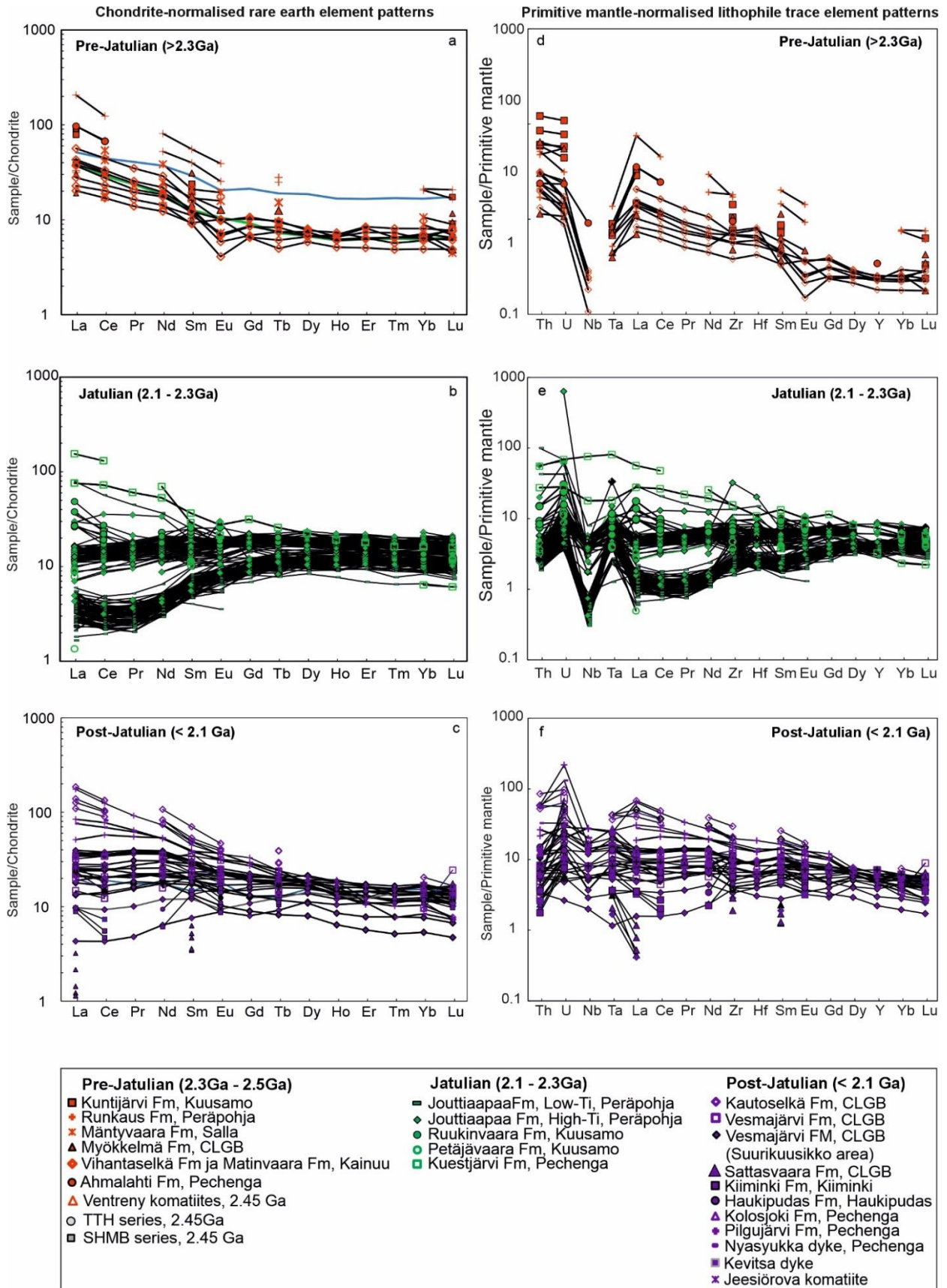
Fig. 23. Chondrite-normalised REE patterns and primitive mantle-normalised trace element patterns for mafic-ultramafic volcanic rocks from NE Fennoscandia. Grey dots indicate global database from Barnes and Fiorentini (2012).

55
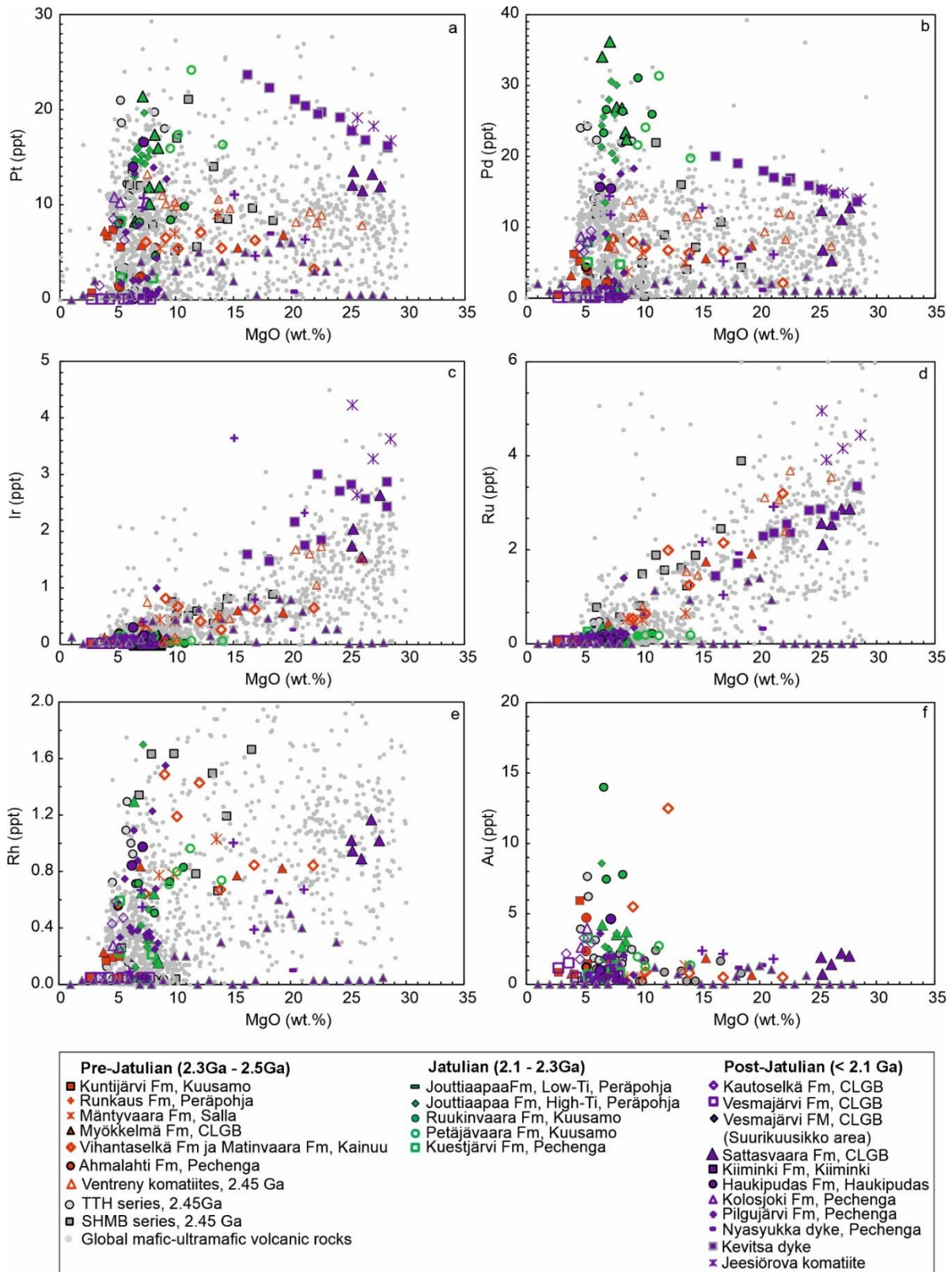
Fig. 24. Plots of Pt, Pd, Ir, Ru against MgO for mafic-ultramafic volcanic rocks from NE Fennoscandia. Grey dots indicate global database from Barnes and Fiorentini (2012).

56
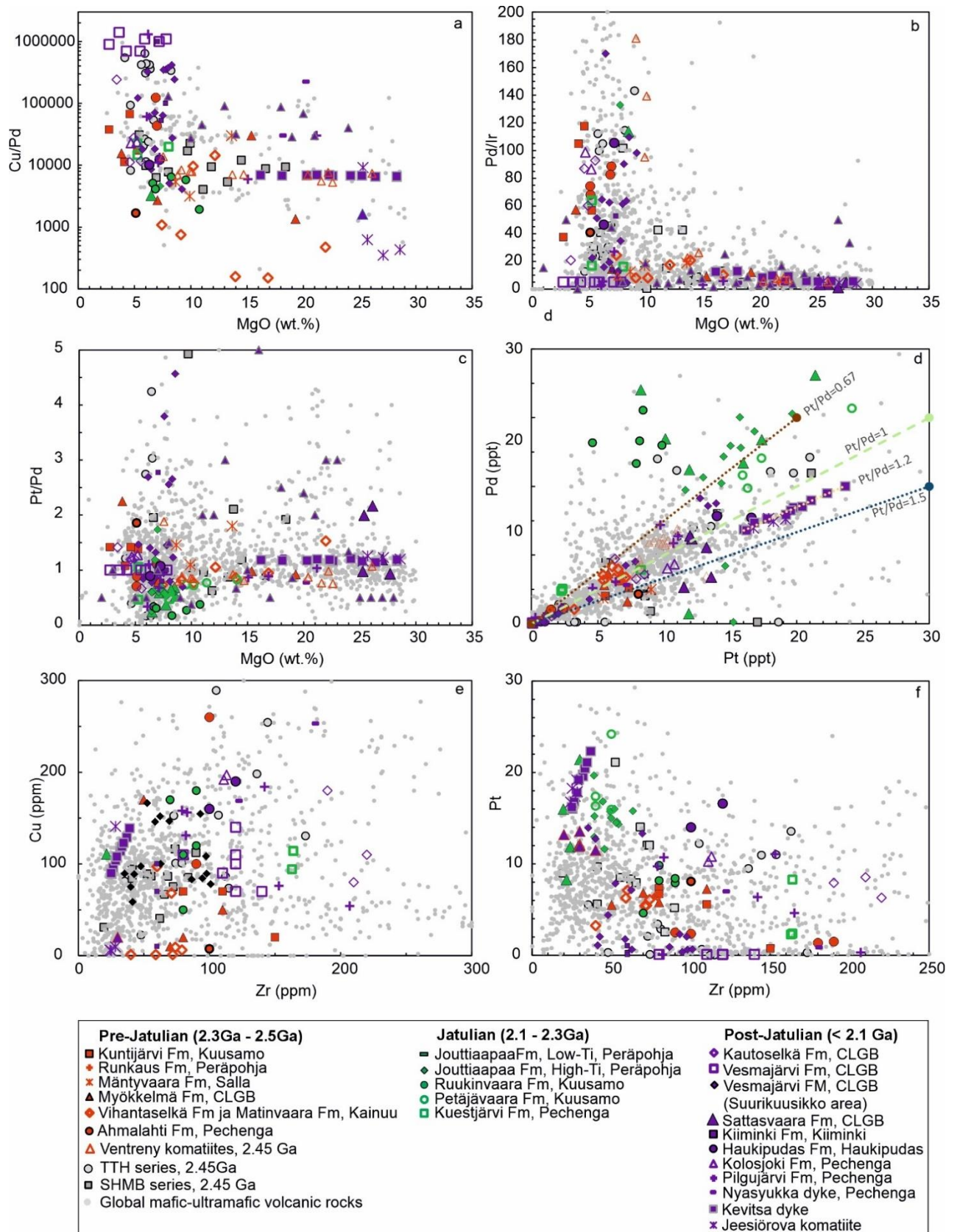
Fig. 25. Plots of Cu/Pd, Pd/Ir, and Pt/Pd ratio vs. MgO and Pd vs. Pt, Cu vs. Zr, Pt vs. Zr for mafic ultramafic volcanic rocks from NE Fennoscandia.

The middle-stage rifting (2.3–2.06 Ga, Jatulian stage)

The middle-stage rifting volcanic rocks are contemporaneous with mafic dyke swarms occurring across the Karelian, Superior, Wyoming and Hearne cratons (Stepanova et al., 2014; Davey et al., 2022). The middle-stage rifting volcanic rocks from three belts have been studied, including the Jouttiaapa Formation in the Peräpohja belt, the Petäjävaara and Ruukinvaara Formations in the Kuusamo belt, and the Kuetsjärvi Formation in the Pechenga belt. The basaltic rocks have moderate MgO contents mainly from 5 to 10 wt.% and can be divided into the low-Ti and high-Ti series (Fig. 22). They show variation in REE patterns with either depletion in LREE or flat LREE, to slight LREE enrichment in LREE (Fig. 23), probably reflecting diverse mantle sources, which have experienced variable extents of earlier melt extraction. Different degrees of partial melting may have also contributed to the diversity of geochemical compositions.

Compared with global volcanic rocks, one striking feature of the Jatulian volcanic rocks is their unusually high Pt and Pd content. Kyläkoski et al. (2007) analysed samples from the Jouttiaapa Formation and found high Pt and Pd contents up to 37 ppb. In the present project, 18 additional samples were re-analysed, resulting in Pt concentrations of 15–25 ppb and Pd concentrations of 20–32 ppb (with one sample having >50 ppb Pd). There is no systematic difference in the PGE contents between the low-Ti and high-Ti series (Fig. 24). Interestingly, the Petäjävaara and Ruukinvaara Formations of the Kuusamo belt, which have been assigned to the Jatulian volcanic rocks, also show relatively high contents of Pd and Pt. In the case of the Petäjävaara Formation, both the Pd (20–31 ppb) and Pt (16–24 ppb) contents are similar to those of the Jouttiaapa Formation. This is also true for Pd in the Ruukinvaara Formation (23–31 ppb), but the Pt concentrations of this Formation are lower than those the Jouttiaapa Formation, falling in the range of 4.6 to 9.8 ppb. Both the Jouttiaapa and Petäjävaara Formations show good positive correlation between Pt and Pd, with Pt/Pd ratio of 0.7 (Fig. 25). However, samples from the Ruukinvaara Formation show much lower and variable Pt/Pd ratios from 0.2 to 0.4 (Fig. 25). These data confirm that unusually high Pd and Pt contents do not only occur in the Peräpohja belt, but also at Kuusamo, and they may share a similar PGE-rich mantle source. However, both the Jouttiaapa and Petäjävaara Formations have relatively low Au contents, in most samples below 5 ppb, whereas samples from the Ruukinvaara Formation show higher, though variable Au contents (7–28 ppb, with one sample having 102 ppb). None of these three formations show unusually high Rh contents, ranging from 0.04 to 1.70 ppb. Both the low-Ti and high-Ti basalts of the Jouttiaapa Formation from Peräpohja show high Pt/Ir and Pd/Ir, consistent with their evolved nature. Most samples of

this stage show mantle-like Cu/Pd ratios (3000−7000), indicating that no significant sulphide saturation occurred in these belts at this stage.

Late rifting stage (2.06–1.98 Ga, post-Jatulian stage)

The studied komatiite samples from the Sattasvaara Formation in the CLGB are rather homogeneous and represent the most MgO-rich (25.2−27.7 wt.%) volcanic rocks in our sample suite (Fig. 22). These samples also have the highest compatible element contents including Cr (2080−2890 ppm) and Ni (893−1220 ppm). The two Formations analysed from the Kiiminki belt, the Kiiminki and Haukipudas Formations, have similar major elements contents with a limited range of MgO (6.3−7.8 wt.%), Cr (34−334 ppm) and Ni (73.7−110 ppm). The Kolosjoki and Pilgujärvi Formation samples from the Pechenga belt are tholeiitic basalts (MgO 4.7, 7.2 wt.%, Cr 46 ppm, and Ni 42 ppm) and ferropicrites (MgO 6.09 to 21.2 wt.%, Cr 49−1800 ppm, and Ni 69−1738 ppm), respectively. The Pilgujärvi ferropicrites also have unusually high Fe_2O_{3tot} (up to 18.4 wt.%) and TiO_2 contents (up to 2.63 wt.%). The youngest samples in our dataset are the two ferropicritic samples from the ca. 1.94 Ga Nyasyukka dyke from the Archaean basement just east of the Pechenga belt. They have similar compositions with MgO contents of 18.0 and 19.3 wt.%, Cr (1453−1996 ppm) and Ni (973−991 ppm). The basalts of the Vesmajärvi and Kautoselkä Formations in the CLGB are mostly relatively evolved rocks, with MgO ranging from 3.3 to 6.9 wt.% and low Cr (34−259 ppm) and Ni (18.9−132 ppm).

In the post-Jatulian stage, the volcanic units differ much in their trace element characteristics. The Sattasvaara Formation shows hump-shaped REE patterns with depletion in both LREE and HREE relative to MREE (Fig. 23). The Kiiminki and Haukipudas Formations show near flat, MORB-like REE patterns, with $(La/Yb)_{CN}$ ratios from 0.8 to 1.8 (Fig. 23). The two formations of the Kittilä suite, the Kautoselkä and Vesmajärvi Formations, show enrichment in LREE and flat REE patterns, respectively. The post-Jatulian volcanic rocks in the Pechenga belt generally show variable enrichment in LREE (Fig. 23). These features are consistent with either depleted or enriched mantle source.

The volcanic rocks in the different belts show variable contents of Pt and Pd. Some samples show moderately high Pt and Pd contents and mantle-like Cu/Pd ratios (e.g., the Haukipudas formation in the Kiiminki, the Kolosjoki and Pilgujärvi Volcanic Formations in the Pechenga belt), consistent with normal sulphide-undersaturated magmas. However, extremely low PGE concentrations (below 1 ppb or below detection limits) and variable and high Cu/Pd ratios occur widely, indicating

a wide occurrence of sulphide saturation both in early stages of magma fractionation in primitive magmas and later in evolved magmas with intensive fractionation.

One prominent feature is the clearly high Pt and Pd contents in the Sattasvaara Formation of the CLGB compared to global database. This is consistent with the recently reported high Pt and Pd in co-eval Jeesiörova komatiites and Kevitsa komatiitic dykes (Puchtel et al., 2020). In contrast to the Pt- and Pd-rich magmas of the middle-rifting stage, these rocks have higher Pt/Pd ratios varying from from 0.93 to 2. Basaltic or ferropicritic rocks in other belts show normal Pt and Pd contents, probably derived from a different mantle source with 'normal' PGE.

In the Kittilä suite, most samples show relatively low but rather variable PPGE and Au contents (Pt 0.35−7.85 ppb, Pd 0.24−9.07 ppb, Rh 0.25−0.88 ppb, Au 0.24−2.06 ppb) (Fig. 24). However, there are three samples from the Vesmajärvi Formation (Suurikuusikko area) with MgO varying from 6.48 to 9.22 wt.% that have clearly higher PPGE contents (Pt 12.7−13.9 ppb, Pd 17.1−18.3 ppb, Rh 1.09−1.55 ppb, Au 0.24−0.67 ppb) (Fig. 17). These three samples show consistent Pt/Pd ratios from 0.70 to 0.79, moderate Pd/Ir ratios of 114−219, and Cu/Pd ratios of 4094−8557 (Fig. 25).

Most samples from the Vesmajärvi Formation in the Kittilä suite show the lowest PGE contents of the post-Jatulian group, with all PGE plotting below 0.1 ppb, but Au levels from 0.5 to 1.53 ppb (Fig. 24). These samples thus show extremely high Cu/Pd ratios from 1400k to 700k and very low Pd/Ir ratios of ~5. Samples from the Kautoselkä Formation have moderate PGE and Au contents (e.g., Pt 1.52−8.54 ppb, Pd 1.07−9.45 ppb, Rh 0.05−0.59 ppb, Au 1.78−3.29 ppb) and variably high Cu/Pd ratios of 112k to 242k and Pd/Ir ratios of 29 to 104 (Fig. 25). All these features are consistent with a PGE-rich parental magma that has locally undergone sulphide saturation in the crust.

7. Discussion

7.1 Archaean greenstone belts

Komatiites host some of the world's most important Ni sulphide deposits, notably in the Yilgarn craton (Mudd and Jowitt, 2014). Smaller Ni deposits also occur in komatiites of the Zimbabwe craton and the Abitibi greenstone belt in Canada (Barnes and Fiorentini, 2012, and references therein). Crustal contamination is an important factor in the formation of komatiite-hosted sulphide deposits, by increasing the S content of the magma through addition of external S and by decreasing the sulphur solubility in magma through addition of Si and other crustal components

(Lightfoot and Hawkesworth, 1997; Lesher and Keays, 2002; Arndt et al., 2008; Barnes et al., 2011; Barnes and Fiorentini, 2008, 2012). In the Vedlozero-Segozero greenstone belt, most samples show flat or slightly LREE-enriched patterns with weak negative Nb-Ta anomalies on primitive mantle-normalised multi-element plots (Fig. 9). In the Tikshozero greenstone belt, a group of samples from the Khizovaara area shows a LREE-enriched chemical signature, which is accompanied by negative Nb-Ta anomalies (Fig. 9). These features can be explained by crustal contamination (Arndt and Jenner, 1986).

As komatiites are generally sulphur undersaturated during eruption, contamination with S-bearing crustal rocks is considered an important, if not essential factor in the formation of komatiitic Ni-sulphide deposits (e.g., Keays and Lightfoot, 2010; Barnes and Fiorentini, 2012). Archaean sulphide-bearing BIF have been reported to be present in the Ilomantsi and Kostomuksha greenstone belts (Sorjonen-Ward and Luukkonen, 2005; Kuleshevich and Gor'kovets, 2008), which could potentially have provided external sulphur to the komatiites to form sulphide deposits. In the Sovdozero area of the Vedlozero-Segozero greenstone belt, BIF occurs above the komatiite rocks in the upper part of the volcano-sedimentary sequence and was thus formed later than the major komatiitic magmatism. This is consistent with the slightly older age of the komatiites in the Vedlozero-Segozero belt compared with that of the Ilomantsi and Kostomuksha belt komatiites. There are no reports of the occurrence of BIF in the Tikshozero greenstone belt. Accordingly, in the Vedlozero-Segozero and Tikshozero greenstone belts, the absence of sulphide-rich sedimentary rocks could imply a relatively low prospectivity for Ni-Cu sulphide mineralisation.

Traditionally, chalcophile element depletion in mafic-ultramafic lavas has been used in the evaluation of the Ni prospectivity of greenstone belts (Lesher and Keays, 2002; Lesher and Barnes, 2009; Barnes and Fiorentini, 2012), as it is a useful indicator of sulphide saturation. On the Pd vs. MgO diagram (Fig. 9), the samples of this study show a considerable scatter, with three samples from the Vedlozero-Segozero belt plotting above the rest of the data. However, most of the samples follow a negative trend on the Pt and Pd vs. MgO diagrams with only a few komatiite and basalt samples being depleted in Pt and Pd (Fig. 11). Komatiite samples from both Russian Karelia and Finland plot within the global field of barren komatiites, being clearly different from well mineralised komatiites. Consequently, these data suggest that the komatiites in Russian Karelia did not undergo extensive sulphide liquid saturation, which is not a good indication for the presence of Ni sulphide mineralisation.

In komatiitic lava flows, olivine-rich cumulates are interpreted to represent channelised lava conduits where relatively unevolved, hot, and turbulently flowing lava is particularly effective in eroding the substrate, assimilating external sulphur, and precipitating sulphides in flow dynamic traps, thereby facilitating ore formation (e.g., Arndt et al., 2008; Barnes and Fiorentini, 2012). Komatiite sequences with the thickest cumulate package are favoured for the formation of Ni sulphide ores as they may reflect a particularly high magma influx, probably resulting from the presence of craton-scale, deep lithospheric structures (Barnes and Fiorentini, 2012).

The komatiite samples from the Vedlozero-Segozero and Tikshozero greenstone belts have similar MgO contents to those of the komatiites in eastern Finland, but they seem to be less magnesian than most mineralised komatiite fields elsewhere (e.g., Abitibi and Kalgoorlie) (Maier et al., 2013). The lower MgO content could result from a lower degree of mantle melting or more advanced fractionation.

In the Vedlozero-Segozero and Tikshozero greenstone belts, another potential explanation for the paucity of Ni-Cu mineralisation is the lack of olivine-rich cumulate units and the dominance of sheet flows, including spinifex-textured komatiites, breccia-textured komatiites, and pillow basalts. Only small serpentinite bodies that may represent lava channels occur in the Sovdozero, Koikary, and Palaselga areas. This is a significant difference compared with the komatiites in the Kalgoorlie area, which contain abundant thick (up to km scale) olivine-rich adcumulates (Fiorentini et al., 2004; Barnes and Fiorentini, 2012). The scarcity of olivine-rich cumulates suggests a low magma flux rate, representing relatively unfavourable conditions to form large and extensive channelised lava tubes, which can efficiently erode their substrate and form Ni-Cu sulphide mineralisation.

The age of the Vedlozero-Segozero greenstone belt is estimated to be ca. 2.92 Ga (Svetov et al., 2001), i.e., similar to the ages of 2916 ± 117 and 2892 ± 130 Ma obtained for the komatiites in the Sumozero–Kenozero greenstone belt using the Sm-Nd and Pb-Pb methods, respectively (Puchtel et al., 1999). On the other hand, these ages are slightly older than the age of ca. 2.8 Ga determined for the Kostomuksha greenstone belt (Puchtel et al., 1998, 2005), the age of 2.82 Ga reported for the TKS greenstone belts in eastern Finland (Huhma et al., 2012), and the age of 2.8 Ga for the Tikshozero greenstone belt. These multiple generations of komatiitic magmatism in the Fennoscandian Shield are clearly older than the global Neoarchaean peak in mantle plume magmatism and Ni-Cu sulphide mineralisation at around 2.7 Ga (Arndt et al., 2008, and references therein). For reasons presently not well understood, it appears that the slightly older magma influx has less potential to form major Ni sulphide ore deposits (Weihed et al., 2005; Hanski, 2015).

However, as the available database is relatively limited, it is difficult to assess the Ni sulphide prospectivity of these belts accurately. Future exploration work should focus on the identification of relatively prospective lava channel-facies rocks (i.e., olivine mesocumulate and adcumulates) in Archaean greenstone belts.

7.2 Magmatism related to the early-stage rifting

7.2.1 Mantle sources of the 2.45 Ga dyke groups

The nature of the mantle source to the 2.45 Ga magmatism in the Karelian craton remains under debate. The available isotope and lithophile trace element data from the dyke suites provide new constraints on these models. The SHMB and GBNO dykes have negative initial εNd values, relatively high initial $^{87}Sr/^{86}Sr$ ratios, negative Ta-Nb anomalies, relatively high La/Sm and Ce/Yb and low Nb/La ratios (Fig. 16, 17). I argue that these data are more readily explained by crustal contamination of asthenospheric magma than melting of subcontinental lithospheric mantle (SCLM) for the following reasons. First, magmas derived from the SCLM would be expected to mix efficiently during ascent through the SCLM, resulting in a relatively constant enriched geochemical compositions (Arndt, 2013, and references therein). In Fennoscandia, the lithophile trace element composition of the SHMB and GBNO dykes is highly heterogenous, showing an up to 3-fold variation. In addition, La/Sm displays a strong positive correlation with Ce/Yb and a negative correlation with Nb/La, consistent with variable degrees of crustal contamination (Fig. 16). Similar variation has been reported for coeval komatiites in the Vetreny belt in Russian Karelia (Puchtel et al., 1996, 1997) and interpreted as a result of AFC processes affecting a komatiitic magma derived from a mantle plume. Our SHMB and GBNO dykes display a much larger compositional variation, with the Vetreny belt komatiites plotting near the lower end of the variation trend (Fig. 16). This feature suggests that the Vetreny belt komatiite experienced less crustal contamination compared to our SHMB and GBNO dyke magmas. Compared with the SHMB and GBNO dykes, the low-Ti tholeiitic and Fe-tholeiitic dykes exhibit no or weaker Ta-Nb anomalies, higher initial εNd values (from -0.3 to +1.7) (Vuollo and Huhma, 2005), and lower initial $^{87}Sr/^{86}Sr$ ratios (~0.7022) (Fig. 17). These features are best interpreted to be derived from a long-term depleted asthenospheric mantle component, with a minor amount of crustal contamination.

Another potential approach to constrain the mantle source to magmas is to consider their PGE contents and ratios (Maier and Barnes, 2004). Relative to the primitive mantle with the estimated

Pt and Pd concentration of 7 and Pd of 4 ppb, respectively (Maier and Barnes, 1999), the SCLM is generally depleted in Pt and Pd by ca. 50–70% (ca. 4 ppb Pt, 2 ppb Pd) due to dissolution of most mantle sulphides during large degrees of partial melting that normally occur during the SCLM formation (Pearson et al., 2003; Pearson, 2004; Maier et al., 2012, 2015; Barnes et al., 2015; Lorand and Luguet, 2016). All the dyke groups studied in the present project show relatively high PPGE contents and high Pd/Ir and Pd/Pt ratios, thus not supporting derivation from a SCLM source.

The relationship between the relatively MgO-rich SHMB and GBNO dykes and the relatively MgO-poor tholeiitic dykes (LTTH and FTH) remains enigmatic. It is interesting to note that other LIPs and layered intrusions also contain both SHMB and tholeiitic magma suites (Fig. 18) (e.g., Belomorian belt in Russia, Lobach-Zhuchenko et al., 1998; the Bushveld magmatic event on the Kaapvaal craton in South Africa, B1and B2/B3 magmas, Sharpe et al., 1981, Barnes et al., 2010; the Stillwater Complex of Montana, Helz, 1995; Lambert and Simmons, 1987, 1988). The variation in the major element compositions of the Karelian SHMB and GBNO dykes is similar to that of the SHMB dykes in the Belomorian belt and the Vetreny belt komatiites, whereas the Karelian tholetiitic dykes display similar variation as the tholeiitic dykes in the Kola and Belomorian belts (Fig. 18). One possibility is that the two contrasting magma types were derived from a common mantle plume source, but the SHMB/GBNO group experienced a higher degree of crustal contamination than the tholeiitic group. The contamination elevated the SiO_2 and alkali contents and considerably influenced the isotope and incompatible trace element ratios of the SHMB/GBNO group (Fig. 18). To test this hypothesis, I conducted thermodynamically constrained major element modelling using the Magma Chamber Simulator (MCS) software (Bohrson et al., 2020).

I chose an average composition of seven relatively primitive tholeiite dyke samples from the Karelian and Belomorian cratons and then added equilibrium liquidus olivine in 1 wt.% steps until the calculated melt was in equilibrium with forsteritic mantle olivine (Fo_{92}). After adding 43 wt.% of olivine, the melt reached a komatiitic composition with ~21 wt.% MgO, which I used as the parental magma composition. The initial oxidation state of iron is assumed to be at $Fe^{2+}/Fe^{tot} = 0.88$, but not forced through the runs, and the H_2O content is assumed to be 0.5 wt.% based on the recent H_2O content estimation for Archaean komatiites by Sobolev et al. (2019). For the crustal contaminant, I chose a sample from the Surmansuo porphyritic granite (A2128, Mikkola et al., 2014) from the Archaean basement near the Suomussalmi belt, a representative rock type for wall rocks of most Karelian mafic dykes and layered intrusions. The modelling results suggests that the SHMB and GBNO dykes experienced an AFC process at a relatively deep crustal level (300 MPa),

followed by a FC process in a shallower crust, whereas the LTTH and FTH dykes experienced mainly a FC process with a very low degree of crustal contamination (Fig. 18). On the other hand, a model in which the SHMB suite magma was derived from the SCLM and the tholeiitic suite magma from a plume mantle is inconsistent with the modelling.

7.2.2 Distribution and origin of 2.44 Ga siliceous high-Mg basalts in NE Fennoscandia

The 2.44 Ga plume-related mafic dyke swarms are divided into two main groups based on geochemistry, siliceous high-magnesium basalt (SHMB) and tholeiite (Guo et al., 2023). The SHMB group is considered to be parental magma to many coeval PGE-mineralised mafic layered intrusions (e.g., Penikat, Portimo), and the tholeiite group may be the parental magma to the Tspringa intrusion which has minor PGE mineralisation (Guo et al., 2023). In this study, I found that the older generation of pre-Jatulian mafic volcanic rocks generally show clear LREE enrichment, similar to the 2.44 Ga mafic dyke swarms (Fig. 23). For major elements, most of these volcanic rocks from different supracrustal belts (e.g., Salla and Myökkelmä areas in the CLGB, Suollavaara in the Kuusamo belt, and Ahmalahti in the Pechenga belt, and Jaurakkajärvi in the Kainuu belt) show high SiO_2 and high alkali contents, consistent with a SHMB affinity, with only two basalt samples from the Salla belt showing a tholeiitic affinity (Fig. 22). This indicates that the 2.44 Ga SHMB-type magma occurs across much of the Karelian and Kola cratons, i.e. over a much larger area than the tholeiitic magma. This is in line with the observation that most mafic layered intrusions coeval with the mafic dykes have SHMB rather than a tholeiitic affinity.

7.2.3 Relationship between 2.45 Ga mafic dykes and layered intrusions

A genetic relationship between the dyke suites and the coeval and spatially associated layered intrusions has long been assumed, based mainly on Nd isotope evidence. One common feature of many Fennoscandian 2.45 Ga layered intrusions, including the intrusions of the Tornio-Näränkävaara belt (Fig. 5), is that their upper parts tend to have a much lower Cr content than the lower portions (Halkoaho et al., 1990; Iljina, 1994; Alapieti and Halkoaho, 1995; Maier et al., 2018). Based on mineralogical and bulk-rock geochemical data, it has been suggested that this reflects injection of two parental magma types, one high in Cr (>1000 ppm) and the other low in Cr (<600 ppm) (Alapieti et al., 1990; Vogel et al., 1998; Iljina and Hanski, 2005). The authors argue that the high-Cr magma has a similar composition to that of SHMB dykes, with an elevated SiO_2 content and fractionated REE pattern, whereas the low-Cr magma, featuring a less fractionated REE pattern, is related to the tholeiitic dykes.

Regarding the relationship between the tholeiitic dykes and the Fennoscandian intrusions, the dykes have positive initial εNd values, which are distinct from the negative initial εNd values of the upper parts of the Penikat, Koitelainen and Akanvaara intrusions (εNd from -1.3 to -2.4, Hanski et al., 2001b; Maier et al., 2018). Also, plagioclase grains from the tholeiitic dykes show low initial $^{87}Sr/^{88}Sr$ ratios of ~0.7024 (Fig. 17), clearly lower than in plagioclase from the Penikat intrusion (0.7027–0.7032) (Rivas, 2022), which are more consistent with the initial $^{87}Sr/^{88}Sr$ ratios of the SHMB and GBNO dykes (0.7030–0.7037, Fig. 17). Maier et al. (2018) proposed that the upper part of the Penikat intrusion may have been derived from an evolved SHMB magma that ascended from a deeper staging magma chamber and had a low Cr content due to extensive crystal fractionation. This model is consistent with the large variation of composition in the SHMB dykes with variable MgO and Cr contents.

7.2.4 Sulphide saturation history and implications for PGE exploration

The SHMB and GBNO dyke samples have PGE-undepleted mantle-normalised siderophile element patterns (Figs. 21a, b), with Pd contents of up to 22 ppb and mostly mantle-like Cu/Pd ratios (Fig. 20b), indicating that the magma was sulphur undersaturated during high-degree partial melting of the mantle and remained so *en route* to the upper crust. Similarly, the coeval SHMB-like volcanic rocks display moderate PGE contents, with Pt and Pd ranging from 5 to 15 ppb for the most primitive rocks (22 to 8 wt.% MgO, e.g., Kainuu belt, CLGB, Salla), i.e. PGE levels that are broadly comparable to the Vetreny komatiites with Pd ranging from 11 to 14 ppb at MgO of 9 to 14 wt.% (Puchtel et al., 2001). This renders the magmas prospective to form PGE deposits (e.g., Naldrett, 2004). In these rocks, Pt and Pd correlated negatively MgO, indicating that fractionation of a silicate magma played a significant role in controlling the contents of Pt, Pd and Rh. However, one SHMB and two GBNO dyke samples with a relatively low MgO content (<7 wt.%) and several coeval volcanic rocks show low PGE concentrations (Pt, Pd < 3 ppb). In addition, there is a decrease both in the Cu content in the more evolved magmas (MgO, 5–10 wt.%), and an increase in Cu/Pd ratios (Fig. 20a, b), suggesting that these relatively evolved magmas reached saturation in sulphide melt. Notably, PGE reefs occur in both primitive and relatively differentiated portions of the 2.45 Ga layered intrusions (e.g., Penikat, Portimo, Koillismaa) (Barkov et al., 1999; Maier and Hanski, 2017; Maier et al., 2018), but the latter tends to be richer.

Regarding the tholeiitic dykes, the most primitive samples (LTTH) have broadly mantle-like Cu/Pd ratios (Fig. 20b) indicating that the magmas did not reach sulphide saturation during the early stage of their differentiation. Some of the LTTH samples show high Pd contents ranging

from 20 to 24 ppb, which are close to the highest values reported for basaltic rocks worldwide (Fiorentini et al., 2010). The high PGE contents of these samples are unlikely a result from re-mobilisation of metals during low-T alteration as they also show the highest Pt contents of 10–20 ppb (Fig. 19). In the more differentiated members of the tholeiitic dyke suite (MgO = 4−6 wt.%), PGE and Cu show large variation, with Pt and Pd contents ranging from <1 ppb to 20 ppb, indicating that sulphide melt saturation was reached during an advanced stage of fractionation. From the above discussion, it appears that all magma types occurring in the 2.45 Ga dyke suites are fertile in terms of the concentration of PGE at a relatively unevolved stage. Depletion in PGE is restricted to some of the most evolved samples, suggesting that sulphide melt saturation was reached during advanced fractionation, which is commonly observed in flood basalt provinces. In the SHMB suite, sulphide melt saturation occurred at a slightly earlier stage (7–8 wt.% MgO) than in the tholeiitic suites (5 wt.% MgO), possibly because the former underwent more crustal contamination. The obtained data on these 2.45 Ga dyke suites suggest that all stratigraphic levels of the coeval layered intrusions have potential to host PGE mineralisation.

7.2.5 Low PGE potential for the 2.31 Ga magmatism

The slightly younger generation of rift-related magmatism at ~2.31 Ga was relatively less wide-spread, but dyke swarms dated at 2.31 Ga were recently reported in Russian Karelia, and it is possible that the scale of this generation of magmatism is underestimated (Stepanova et al., 2015). In the Peräpohja belt in Finland, the Runkaus Formation is estimated to have an age of 2.2–2.44 Ga based on cross cutting relationships of mafic sills (Nykänen et al., 1994; Hanski et al., 2010; Stepanova et al., 2015). These Runkaus rocks show similar trace element characteristics as the 2.31 Ga dyke swarms in Russia Karelia (Stepanova et al., 2015). This group of basalt has relatively low PGE contents and high Ni/Pt ratios, indicating that the magma has equilibrated with sulphide, either in the source mantle due to a relatively low degree of partial melting in upwelling asthenosphere or during magma ascent through the crust. As all the rocks generally show low MgO contents, we favour control of PGE contents by a low degree of partial mantle melting. Hence, this pulse of magma may have relatively low potential to form economic PGE deposits.

7.3 Magmatism related to the middle-stage of rifting (2.3–2.06 Ga) (Jatulian)

The Jatulian stage of the Fennoscandian magmatism contains some of the most PGE-rich basaltic magmas on Earth, as manifested by the Jouttiaapa Formation of the Peräpohja belt and the Petäjävaara Formation in the Kuusamo belt (Fig. 5), suggesting that PGE enrichment is a characteristic feature of the Jatulian magmatism. The Jouttiaapa and Petäjävaara samples generally

define a positive correlation between Pd and Pt (Fig. 7), confirming that the high Pt and Pd contents are a primary magmatic feature of these magmas. The Ruukinvaara Formation of the Kuusamo belt share similarly high Pd contents (23.3−31.1 ppb) with the Petäjävaara Formation, but its Pt content is moderate (4.62−9.84 ppb). As a result, it has the highest and most variable Pd/Pt ratios (2.6−5.7) among all our samples, whereas the Jouttiaapa Formation shows an average Pt/Pd ratio of 0.67. The reason for the variation in Pt/Pd remains unclear. Barnes and Liu (2012) suggested that Pd is more mobile during alteration. This could cause enhanced variation in Pt/Pd, but arguably should result in wide spread Pd depletion across the Ruukinvaara Formation. Also, in terms of LOI values (0.9−6.2 vs. 4.1−6.9), the alteration degree of the Ruukinvaara Formation is generally lower than that of the Petäjävaara Formation, and thus the mobility of Pd may not be the key factor. On the Pd vs. Zr diagram, the Ruukinvaara Formation samples plot well in the field of samples from the Jouttiaapa and Petäjävaara Formations, showing a positive correlation due to the incompatibility of both elements during fractionation. However, on the Pt vs. Zr diagram, the Ruukinvaara Formation samples plot well below the main trend of the Jouttiaapa and Petäjävaara Formation samples (Fig. 25). Possibly, the magma lost some Pt during fractionation (cf. Momme et al., 2002; Lightfoot and Keays, 2005; Park et al. 2017).

All Jatulian basalts show relatively low contents of IPGE and Rh, likely reflecting their relatively evolved composition (Fig. 24). The Kuestijärvi Formation of the Pechenga belt shows relatively low Pt and Pd contents which may be the result of some sulphide segregation (discussed below).

The samples from the Jouttiaapa, Ruukinvaara and Petäjävaara Formations all show mantle-like Cu/Pd ratios (mostly 4000−7000) (Fig. 25), indicating that sulphide saturation has not been achieved during magma fractionation, even for the most evolved members of the suites. On the Cu vs. Zr, and Pt vs. Zr diagram, these samples generally define a positive trend (except the samples from Ruukinvaara). However, the samples from the Kuestijärvi Formation in Pechenga show much lower Pt and Pd contents, and higher Cu/Pd ratios (14500−22500), indicating that sulphide saturation occurred in the Pechenga belt. One possible reason for the absence of sulphide saturation in the Peräpohja and Kuusamo belts may be that there were no large magma chambers at this stage to allow protracted fractionation of magma and attainment of sulphide saturation, probably because the supercontinent has almost broken up during the middle−stage of rifting, and the continental crust was becoming too weak to store the magma to form large magma chambers. In an analogous manner, the 2.2 Ga mafic sills in Fennoscandia formed thin sills with a strike length of more than 10 km, but with thicknesses of less than 300 meters (e.g., Koli intrusion; Hanski et al., 2010).

7.4 Magmatism related to the late-stage of rifting (2.06–1.98 Ga) (post-Jatulian)

The occurrence of large volumes of ca. 2.06 Ga komatiites in the CLGB has been attributed to mantle plume activity (Hanski et al., 2001a; Törmänen et al., 2016; Puchtel et al., 2020). These komatiites show strong depletion in LREE and strongly positive initial εNd values (+4.2), consistent with a long-term depletion in the mantle source. However, there are also coeval Ti-enriched picrites in both the CLGB in Finland and the Karasjok greenstone belt in Norway, which may have been derived from an OIB-like enriched mantle source (Barnes and Often, 1990; Hanski et al., 2001a; Orvik et al., 2022 a,b). Similar Fe-Ti rich picrites also occur in the slightly younger 1.98 Ga Pechenga belt (Hanski and Smolkin, 1995; Hanski et al., 2014), and the Onega Basin in Russian Karelia (Puchtel et al. 1998; Hanski et al., 2001a). The Sattasvaara samples in this study are depleted in LREE, and thus comparable with the regional komatiites in the CLGB (e.g., Jeesiörova, Hanski et al., 2001a; Kevitsa komatiitic dyke, Puchtel et al., 2020).

Unusually high PGE contents have been reported from komatiites at Jeesiörova, komatiitic dykes at Kevitsa, and komatiites at Lomalampi (Törmänen et al., 2016; Puchtel et al., 2020). Based on S-poor samples, the Pt and Pd contents of the primary silicate melt at Lomalampi are estimated to be 27 ppb and 10 ppb, respectively (Törmänen et al., 2016). Puchtel et al. (2020) found unusually high contents of Pt (16.8−19.2 ppb) and Pd (13.9−15.4 ppb) in 4 komatiite samples from Jeesiövaara (25.3−28.6% MgO), and even higher levels of Pt (16.0−23.7 ppb) and Pd (13.6−20.0 ppb) in the slightly less magnesian (18.1−28.3 wt.% MgO) Kevitsa dykes. In this study, we obtained 13 ppb Pt and 12 ppb Pd for the Sattasvaara komatiites (26 wt.% MgO), in the southern part of the CLGB. The PGE levels in the CLGB are amongst the highest recorded for komatiites, implying that relatively high PGE contents are a characteristic feature of the CLGB. Equally remarkable are the relatively high Pt/Pd ratios of the Jeesiövaara, Kevitsa and Sattasvaara komatiites, typically at 0.9−1.2. Platinum/Palladium ratios above unity are relatively rare amongst global magmas (see compilation of Maier and Mundl-Petermeier 2023). Notable exceptions include the Bushveld magmas, Emeishan picrites, Kerguelen lavas as well as Coppermine Mg-basalt. These authors showed that Pt/Pd is controlled by a range of processes, including mantle heterogeneity, fractionation, as well as hydrothermal and low-T alteration. Considering that high Pt/Pd appears to be a regional feature in the CLGB (it is also found at the Kevitsa and Sakatti sulphide deposits, Mutanen, 1997; Le Vaillant et al., 2016), I propose that it reflects the heterogeneity of the post-Jatulian source mantle.

The Cu/Pd ratios of the Sattasvaara, Jeesiovaara and Kevitsa komatiites and Mg-basalts is typically around 7000 (Puchtel et al., 2020), suggesting that these rocks have not equilibrated with

significant sulphide. However, sulphide saturation clearly has occurred in unevolved magmas at Lomalampi (Törmänen et al., 2016), Pulju (Konnunaho et al., 2015), and Sakatti (Makkonen et al., 2017; Brownscombe et al., 2015; Moilanen et al., 2021; Fröhlich et al., 2021), and also in somewhat more evolved magmas at Kevitsa (Mutanen, 1997; Luolavirta et al., 2018). This strong regional variation amongst the CLGB magmas to attain sulphide saturation likely reflects the availability of sulphur-bearing sedimentary rocks with which the magmas could react.

In contrast to the komatiitic rocks of the CLGB, the ferropicritic rocks of the Pechenga belt are interpreted to be derived from an enriched plume mantle source with high FeO and TiO_2 contents (Hanski et al., 1995, 2011). The unevolved ferropicrites of the Pilgujärvi Volcanic Formation and the Nyasyukka dyke, and basalt of the Kolosjoki Volcanic Formation, have moderate Pt and Pd contents at a given MgO content (15.1−21.2 wt.%), plotting well within the global dataset, but below the trend of the CLGB (Fig. 24). This indicates that the source mantle of the Pechenga ferropicrite is relatively "normal" in terms of PGE, but different compared with the CLGB, though the two pulses of magmatism are rather similar in age (1.98 Ga vs. 2.06 Ga), representing the final-stage of continental break-up. One ferropicritic sample from the Pilgujärvi Volcanic Formation has a mantle-like Cu/Pd ratios (about 6000), indicating sulphur undersaturated condition. However, another ferropircrite sample from the Pilgujärvi Volcanic Formation and the Nyasyukka dyke have Cu/Pd ratios from 30000 to 220,000, indicating sulphide saturation at a relatively early stage of magma fractionation. The basalt samples from Pechenga also show variable and high values of Cu/Pd ranging from 11000 to 1310000, indicating that sulphide saturation was wide-spread, due to interaction with sulphide bearing sedimentary rocks, as previously suggested by Brügmann et al. (2000), Barnes et al. (2001) and Hanski et al. (2011).

The basalts in the Kiiminki and Haukipudas Formations on the SW margin of the Karelia craton show flat REE patterns or weak enrichment in LREE, respectively, and moderate to high TiO_2 (0.9 to 1.4 wt.%) and MgO from 6.67 to 7.74 wt.%. It is possible that the source mantle of the Kiiminki and Haukipudas Formation basalts is a mixing product of the depleted and enriched mantle discussed above. The Haukipudas Formation shows moderate to high Pt (14.0−16.6 ppb) and Pd (15.5−15.7 ppb) contents, and a positive correlation between Pt and Zr (Figs. 24, 25), indicating sulphide undersaturated conditions, though relatively high Cu/Pd ratios (10200−12300). In contrast, the Kiiminki Formation samples have very low Pt and Pd contents (both below 1.3 ppb) and high Cu/Pd ratios (52700−1000000), clearly indicating that the magmas equilibrated with sulphide melt. So far no Ni-Cu-PGE sulphide mineralisation has been identified in these SW Karelian formations, but the combination of high PGE contents in the Haukipudas Formation and

the sulphide-saturated nature of the Kiiminki Formation lavas could suggest potential for such deposits in this region.

In contrast to all the rocks discussed above, most basalts from the Kittilä allochthon are believed to have an affinity of oceanic plateau basalt or EMORB (Lehtonen et al., 1998; Hanski and Huhma, 2005). These rocks generally show rather large variation in terms of their PGE contents. Three samples from the Suurikuusikko basalt (belonging to the Vesmajärvi Formation) display moderately high Pt (12.7−13.9 ppb) and Pd (17.1−18.3 ppb) contents, whereas most of the Kautoselkä Formation samples have moderately low Pt (6.30−8.54 ppb) and Pd contents (6.54−9.45 ppb), but clearly higher levels than MORB basalts which generally have Pt and Pd below 2 ppb (Yang et al., 2014), indicating a relatively high degree of mantle melting consistent with an oceanic plateau basalt affinity. As samples from the Vesmajärvi Formation have very low Pt and Pd contents below 0.03 ppb and highly variable Cu/Pd ratios (4000−1000000), I argue that sulphide saturation did not occur during mantle melting, but during magma fractionation in the crust.

7.5 Origin of the high-PGE magmas

To explain the variable PGE content of the studied magmas, including the unusual PGE enrichment in some of the Jatulian and post-Jatulian magmas, four models are considered below: (i) Variable degree of partial melting of sub-lithospheric (plume) mantle followed by fractional crystallisation and sulphide saturation, (ii) contribution of SCLM in generating PGE-rich magmas, (iii) assimilation of PGE-rich crust, and (iv) melting of mantle containing preserved domains of PGE-rich late veneer.

(i) Variable degree of partial melting of sub-lithospheric (plume) mantle followed by fractional crystallisation and sulphide saturation. Törmänen et al. (2016) suggest that the melting degree for komatiitic basalts in the CLGB was generally lower than that for normal komatiites (e.g., Archaean komatiites), and hence the PGE and Cu were not diluted by further melting of mantle after consumption of all sulphides. This could explain the relatively low Ni tenor and high Cu and PGE tenors in the Lomalampi sulphide ore. However, Puchtel et al. (2020) estimated that the source mantle of komatiitic magma in the CLGB had 9.54 ± 0.22 ppb Pt and 8.13 ± 0.19 ppb Pd, which are about 20% higher than the concentrations in the bulk silicate earth composition. Based on the positive εNd and εHf values and LREE-depleted patterns of komatiites in the CLGB, it is proposed that the mantle source of komatiites in the CLGB experienced an earlier, relatively low degree melt extraction event (Hanski et al., 2001a; Puchtel et al., 2020). If the earlier melting failed to

dissolve all the sulphur in the source mantle, the generated magma was S saturated and metal depleted, such as typical MORBs which have Pt generally lower than 1 ppb and Pd lower than 1.5 ppb coupled with high Cu/Pd ratios ranging from 50,000 to 400,000 (Yang et al., 2014). Mass balance dictates that the residual mantle should be enriched in PGE.

Huhma et al. (1990) suggest a relatively high degree of partial melting of a highly depleted asthenospheric mantle for the low-TiO_2 Jouttiaapa basalts and a lower degree partial melting of mantle for the high-TiO_2 Jouttiaapa basalts. However, the modelling suggests that if the two types of magma are derived from the same mantle source, the melting degree for the high-Ti basalts will be just 1%, which is unreasonable. Another possibility is that the mantle source to the high-Ti basalt may have experienced a lesser amount of earlier melt extraction, which resulted in less depletion in incompatible trace elements. If earlier melt extraction is the key factor for PGE-enriched mantle source, it would be expected that the low-Ti basalts should have higher PGE content than the high-Ti basalts, which is not consistent with our data.

(ii) Contributions of SCLM in generating PGE rich magmas. There has been considerable debate whether PGE-rich magmas need a contribution of metals from the sub-continental lithospheric mantle (Griffin et al. 2013; Maier et al. 2016). One important observation is that PGE-rich ore deposits generally occur in cratonic settings rather than at craton margins (e.g., Bushveld, Stillwater, Great Dyke, and Finnish intrusions in NE Fennoscandia, Maier et al., 2013a, 2015; Maier and Hanski, 2017). Yang et al. (2016) argue that the near chondritic γOs of LIPs is inconsistent with a significant contribution of SCLM. In addition, a compilation of global mantle xenoliths shows that the SCLM is relatively depleted in Pt and Pd. Also, Group II kimberlitic magmas generated by melting of SCLM are highly PGE depleted (Maier et al., 2012). In the case of the PGE-rich Jouttiaapa formation basalts and the komatiitic rocks in the CLGB, the highly positive εNd values and LREE-depleted REE patterns indicate a depleted asthenospheric mantle source without notable interaction with the continental crust or the metasomatised SCLM (Hanski et al., 2001b; Stepanova et al., 2014; Puchtel et al., 2020). These data are more consistent with an origin via late rifting when the Fennoscandian continental lithosphere and crust was thinned near the final break-up of the Kenorland super continent.

(iii) Assimilation of PGE-rich crustal contamination. Several studies have postulated that assimilation of crustal magmatic protosulphide may be the cause for elevated the PGE contents of mafic magmas and associated ore deposits, including the Kevitsa deposit (e.g., Naldrett et al., 2009; Li et al., 2009; Maier et al., 2011; Yang et al., 2013; Maier et al., 2023). In the case of the Jouttiaapa basalt (Peräpohja belt) and the Ruukinvaara and Petäjävaara Formation basalts in the Kuusamo

belt, no older or coeval Ni-Cu-(PGE) sulphide mineralisation has yet been identified, but this could be a reflection a lack of exposure. On the other hand, coeval Ni-Cu-PGE sulphide mineralisation exists in the CLGB.

Alternatively, the elevated PGE content of the post-Jatulian komatiites in the CLGB could be explained by assimilation of black shale with elevated PGE (cf. Jiang et al., 2007). Unfortunately, though there are many occurrences of black shale in Fennoscandia, so far few PGE data are available for these rocks. However, the high εNd values do not support extensive interaction with black shale for these mafic-ultramafic igneous rocks.

(iv) Melting of mantle containing preserved domains of PGE-rich late veneer. Maier et al. (2009) show that the PGE contents of Archaean komatiites increases with decreasing age. The authors proposed that this is the result of progressive in-mixing of late veneer into the Archaean mantle. Puchtel et al. (2020) proposed that late accretion of a fragment of a differentiated planetesimal core, or material from the Earth's core, both of which have higher Pt/Os and Re/Os ratios than the bulk mantle, may best explain the decoupling of lithophile and chalcophile isotope systematics in the CLGB komatiites. Modelling suggests that only 0.2% addition of iron meteorite to the primitive mantle (Cook et al., 2004) may account for the unusually high PGE contents in the komatiite of the CLGB. A similar model was considered for Bushveld by Maier et al. (2016) and Maier and Mundl-Petermaier (2023). If this model is correct for the PGE-rich Palaeoproterozoic magmas in Fennoscandia and the Bushveld province, homogenisation of late veneer in the Earth's mantle may have taken much longer than previously thought.

It is worth noting that the enrichment of Pd in the Jatulian-stage magmas is even higher than that in komatiites in the CLGB, plotting above the trend defined by komatiites from Kevitsa and Jeesiörova. On the other hand, Pt plots slightly below the trend of the CLGB, though still above the global trend (Fig. 5). Compared to the PGE-rich Bushveld B1 SHMB (Barnes et al., 2010; Maier et al., 2016), the Jatulian-stage magmas have a comparable Pt content, but clearly higher Pd with lower Pt/Pd. Considering the diverse types of iron meteorite with some having either higher or lower Pt/Pd ratios than unity (Cook et al., 2004; Worsham et al., 2016), I propose that different types of planetesimal core material have been concentrated in the Fennoscandian sub-lithosphehric mantle.

7.6 Implications for sulphide saturation and the criteria of mineralisation

One important feature in the Karelian craton is that large mafic layered intrusions only occur in the earliest stage of Palaeoproterozoic rifting (2.44−2.5 Ga). Layered intrusions of broadly similar

age are also found on the Kola craton in NW Russia and the Superior craton in Canada (Ernst and Bleeker, 2010), which are believed to have formed during a common mantle plume event at the initial stage of continental breakup. This is probably because the continental crust was still rather thick and the magma could be stored in large magma chambers before continuing its ascent into the uppermost crust and to the surface (Fig. 26A). This model is consistent with the observation that large layered intrusions tend to occur in the central portions of cratons (Maier and Groves, 2011). On the other hand, almost no large layered intrusions have been identified in the middle stage of rifting (Jatulian) in NE Fennoscandia. One could argue that there was not sufficient magma supply in the Jatulian stage. However, a number of mafic intrusions have been identified at 2.13 and 2.22 Ga both in the Fennoscandian and Superior cratons. Together with the occurrence of thick (several hundred meters) basaltic formations (e.g., Jouttiaapa Formation), and many sills with up to more than 10 kms length this indicates a considerable amount of magma supply during the Jatulian rifting phase. One possible explanation may be that when the continental crust is thinning, it is easier for the magma to reach the surface, but more difficult to pond in the crust to form large magma chambers which will eventually form large mafic layered intrusions (Fig. 26B).

I further argue that magmas in large intrusions can more readily reach sulphide saturation via crystal fractionation, magma mixing, and/or crustal contamination than magmas in small intrusions or lava flows (Naldrett, 2010; Maier et al., 2013a), due largely to slower cooling rates of the large intrusions. This may explain the chalcophile element depletion in volcanic rocks and related mafic dyke swarms in the early rifting stage at 2.45 Ga (Guo et al., 2023; this study). In contrast, in the Jatulian middle stage of rifting (e.g., Jouttiaapa Formation in Peräpohja belt, Petäjävaara and Ruukinvaara Formations in Kuusamo belt), there are few signs of sulphide saturation.
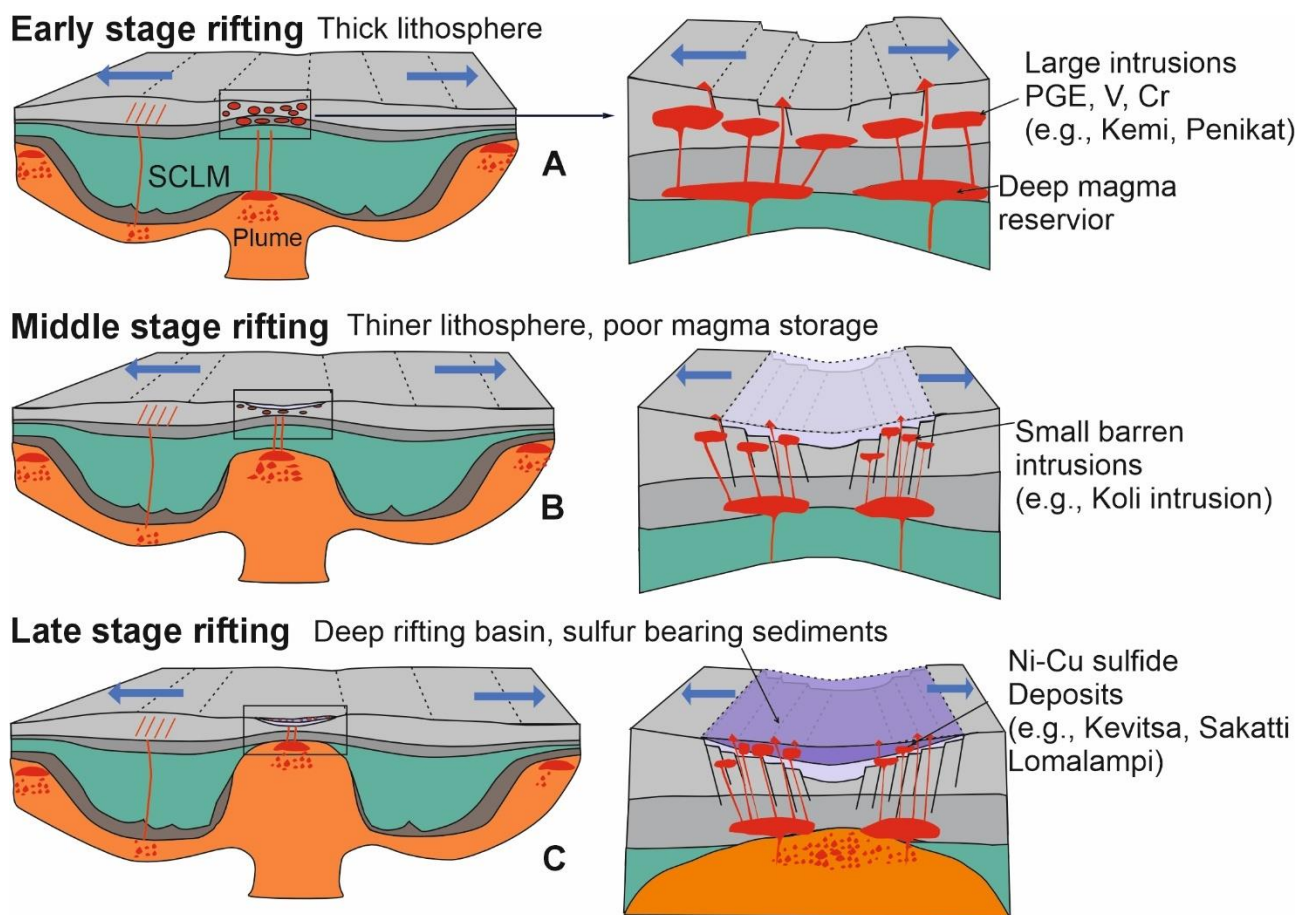
Fig. 26. Correlation between different types of mineralisation at different tectonic settings from early-stage to late-stage rifting.

This concept cannot explain the observation that the late-stage rifting-related magmatism (2.06 Ga, 1.98 Ga) did not form large layered intrusions, and generally show PGE depletion (e.g., Pechenga, Kiiminki). They are coeveal with conduit-type Ni-Cu sulphide deposits in Finland and Russia (e.g., Kevitsa, Sakatti, Lomalampi, Pechenga). Different from the 2.44 Ga magmas, in which sulphide saturation mainly occurred in fractionated magmas with MgO lower than 8 wt.%, sulphide saturation in the late rifting stage occurred in relatively primitive magmas (Pechenga ferropicrites, komatiites in the CLGB). This is likely because sulphur-rich sediments, including black shales, had been deposited during the late rifting stage in deep sedimentary basins, and assimilation of these sediments by the post-Jatulian magmas could trigger sulphide saturation (Fig. 26C).

Thus, I suggest that the earliest stage of rifting is favourable to form large layered intrusion-hosted Cr-PGE-V-(Ni-Cu-Co) deposits. The late-rifting stage is more favourable to generation of conduit-type Ni-Cu-(PGE-Co) deposits. The middle-stage magmatic events seem to have less potential for both of these deposit types because of a poorer magma storage capability and the lack of sulphur in the associated sediments.

Magmatic Ni-Cu sulphide deposits occur in continental rift settings or in orogenic belts during the subduction or collision stage (Barnes et al., 2016). Our new data from the Kittilä area suggest that it may be possible to have PGE-rich magma and sulphide saturation in an oceanic environment (e.g., oceanic plateau).

8 Conclusions

The studied komatiitic lavas from two Archaean greenstone belts in Russian Karelia are relatively evolved (mostly <25 wt.% MgO) and their PGE contents are within the range of other unmineralised komatiites globally. The absence of sulphide-rich sedimentary rocks in the studied greenstone belts, the lack of PGE-enriched or depleted samples, the relatively differentiated magma composition compared with sulphide-mineralised komatiites globally, and the paucity of olivine adcumulates suggest a relatively low prospectivity for Ni sulphide mineralisation, though localised crustal contamination and sulphide saturation seem to have occurred. However, as the available database is relatively limited, the Ni sulphide prospectivity of the studied belts remains incompletely understood, and future exploration should focus on the identification of prospective lava channel-facies rocks.

During the early Palaeoproterozoic era (2.45–2.5 Ga), northern Fennoscandia has seen a large amount of basaltic and komatiitic magmatism, exposed in dykes, layered intrusions and lava flows. The SHMB-group dykes were likely derived via AFC from a komatiitic parent melt, followed by FC at a relatively low pressure, whereas tholeiitic dykes represent less contaminated magmas generated dominantly by crystal fractionation. The lower portions of most of the Finnish PGE-mineralised layered intrusions (e.g., Penikat, Portimo) appear to have crystallised from a primitive SHMB-like magma with high MgO and Cr contents, whereas the upper portions of the intrusions crystallised from fractionated SHMB magma with lower MgO and Cr contents. One exception is the Tspringa intrusion, the parental magma of which shows tholeiitic affinity. There is currently no clear evidence to suggest that individual layered intrusions crystallised from hybrid SHMB-tholeiitic magmas. Most of the mafic dykes and volcanic rocks are undersaturated in sulphides and fertile in PGE, but several of the most differentiated samples have evidently reached sulphide saturation, indicating a high potential for PGE deposits. The slightly younger pulse of magmatism at 2.3 Ga shows generally low PGE contents and thus has lower ore potential, possibly due to a low degree of mantle melting.

The volcanic rocks of the middle stage of rifting (i.e., the Jatulian stage, 2.2−2.1 Ga) show diverse geochemical features. Some of the belts show unusually high PGE contents, namely Peräpohja

and Kuusamo. Most magmas do not appear to have experienced sulphide saturation, possibly because the lithosphere had become relatively weak and thin, resulting in a low magma storage capability and few large magma chambers. The magmatism related to the late stage of rifting (post-Jatulian, i.e., younger than ~2.06 Ga) also shows unusually high Pt and Pd contents, though the PGE contents in the 1.98 Ga event are normal. Sulphide saturation occurred widely at this stage, probably due to interaction of magmas with sulphide-bearing sedimentary rocks, deposited as wide-spread black shales at the late rifting stage.

The unusually PGE-rich magmas of the Fennoscandian mid- and late-rifting stages remain enigmatic. One model could be that the sub-lithospheric mantle below Fennoscandia contained poorly digested, PGE-rich late veneer materials with diverse composition.

References

Alard, O., Griffin, W.L., Lorand, J.P., Jackson, S.E. and O'Reilly, S.Y., 2000. Non-chondritic distribution of the highly siderophile elements in mantle sulphides. Nature, 407, 891–894. https://doi.org/10.1038/35038049

Alapieti, T., 1982. The Koillismaa layered igneous complex, Finland – its structure, mineralogy and geochemistry, with emphasis on the distribution of chromium. Geological Survey of Finland, Bulletin 319, 1–116.

Alapieti, T.T., Filén, B.A., Lahtinen, J.J., Lavrov, M.M., Smolkin, V.F., Voitsekhovsky, S.N., 1990. Early Proterozoic layered intrusions in the northeastern part of the Fennoscandian Shield. Mineralogy and Petrology 42, 1–22. https://doi.org/10.1007/BF01162681

Alapieti, T.T., Halkoaho, T.A.A., 1995. Cryptic variation of augite in the Penikat layered intrusion, Northern Finland, with reference to megacyclic units and PGE-enriched zones. Mineralogy and Petrology 54, 11–24. https://doi.org/10.1007/BF01162754

Amelin, Yu.V., Heaman, L.M., Semenov, V.S., 1995. U-Pb geochronology of layered mafic intrusions in the eastern Baltic Shield: implications for the timing and duration of Paleoproterozoic continental rifting. Precambrian Research 75, 31–46. https://doi.org/10.1016/0301-9268(95)00015-W

Arestova, N.A., Chekulaev, V.P., Matveeva, L.V, Kucherovskii, G.A., Lepekhina, E.N., Sergeev, S.A., 2012. New age data on the Archaean rocks of the Vodlozero domain, Baltic Shield, and their significance for geodynamic reconstructions. Doklady Earth Sciences 442, 1–8. doi: 10.1134/S1028334X12010023

Arguin, J.-P., Pagé, P., Barnes, S.-J., Yu, S.-Y., Song, X.-Y., 2016. The effect of chromite crystallization on the distribution of osmium, iridium, ruthenium and rhodium in picritic magmas: an example from the Emeishan Large Igneous Province, southwestern China. Journal of Petrology 57, 1019–1048. https://doi.org. /10.1093/petrology/egw033

Arndt, N., 2003. Komatiites, kimberlites, and boninites. Journal of Geophysical Research: Solid Earth 108. https://doi.org/10.1029/2002JB002157

Arndt, N., 2013. The lithospheric mantle plays no active role in the formation of orthomagmatic ore deposits. Economic Geology 108, 1953–1970. https://doi.org/10.2113/econgeo.108.8.1953

Arndt, N., Jenner, G., 1986. Crustally contaminated komatiites and basalts from Kambalda, Western Australia. Chemical Geology 56, 229-255 doi:10.1016/0009-2541(86)90006-9

Arndt, N., Czamanske, G.K., Walker, R.J., Chauvel, C., Fedorenko, V.A., 2003. Geochemistry and origin of the intrusive hosts of the Noril'sk-Talnakh Cu-Ni-PGE sulphide deposits. Economic Geology 98, 495–515. https://doi.org/10.2113/gsecongeo.98.3.495

Arndt, N., Lesher, C.M., Barnes, S.J., 2008. Komatiite. Cambridge University Press, Cambridge. 467p. https://doi.org/10.1017/CBO9780511535550

Ballhaus, C., Tredoux, M., Späth, A., 2001. Phase relations in the Fe–Ni–Cu–PGE–S system at magmatic temperature and application to massive sulphide ores of the Sudbury Igneous Complex. Journal of Petrology 42, 1911–1926. https://doi.org/10.1093/petrology/42.10.1911

Barkov, A.Y., Halkoaho, T., Roberts, A.C., Criddle, A.J., Martin, R.F., Papunen, H., 1999. New Pd-Pb and Pb-V oxides from a bonanza-type PGE-rich, nearly BMS-free deposit in the Penikat layered complex, Finland. Canadian Mineralogist 37, 1507–1524. https://doi.org/10.2113/gscanmin.43.5.1663

Barnes, S.-J., Lightfoot, P.C., 2005. Formation of magmatic nickel-sulphide deposits and processes affecting their copper and platinum-group element contents, in: Hedenquist, J.W., Thompson, J.F.H., Goldfarb, R.J., Richards, J.P. (Eds.), Economic Geology 100th Anniversary Volume, pp. 179–213. https://doi.org/10.5382/AV100.08

Barnes, S.-J., Often, M., 1990. Ti-rich komatiites from northern Norway. Contributions to Mineralogy and Petrology 105, 42–54. https://doi.org/10.1007/BF00320965

Barnes, S.-J., Makovicky, E., Makovicky, M., Rose-Hansen, J., Karup-Moller, S., 1997. Partition coefficients for Ni, Cu, Pd, Pt, Rh, and Ir between monosulphide solid solution and sulphide liquid and the formation of compositionally zoned Ni-Cu sulphide bodies by fractional crystallization of sulphide liquid. Canadian Journal of Earth Sciences 34, 366–374. https://doi.org/10.1139/e17-032

Barnes, S.-J., Melezhik, V.A., Sokolov, S.V., 2001. The composition and mode of formation of the Pechenga nickel deposits, Kola Peninsula, northwestern Russia. The Canadian Mineralogist, 39, 447–471. https://doi.org/10.2113/gscanmin.39.2.447

Barnes, S.-J., Maier, W.D., Curl, E.A., 2010. Composition of the marginal rocks and sills of the Rustenburg Layered Suite, Bushveld Complex, South Africa: Implications for the formation of the platinum-group element deposits. Economic Geology 105, 1491–1511. https://doi.org/10.2113/econgeo.105.8.1491

Barnes, S.-J., Francis, D., 1995. The distribution of platinum-group elements, nickel, copper, and gold in the Muskox layered intrusion, Northwest Territories, Canada. Economic Geology 90, 135–154. https://doi.org/10.2113/gsecongeo.90.1.135

Barnes, S.J., Fiorentini, M.L., 2008. Iridium, ruthenium and rhodium in komatiites: Evidence for iridium alloy saturation. Chemical Geology 257, 44–58. https://doi.org/10.1016/j.chemgeo.2008.08.015

Barnes, S.J., Fiorentini, M.L., 2012. Komatiite magmas and sulphide nickel deposits: A comparison of variably endowed Archaean terranes. Economic Geology 107, 755–780. https://doi.org/10.2113/econgeo.107.5.755

Barnes, S.J., Liu, W., 2012. Pt and Pd mobility in hydrothermal fluids: evidence from komatiites and from thermodynamic modelling. Ore Geology Reviews 44, 49–58. https://doi.org/10.1016/j.oregeorev.2011.08.004

Barnes, S.J., Fiorentini, M.L., Duuring, P., Grguric, B.A., Perring, C.S., 2011. The Perseverance and Mount Keith nickel deposits of the Agnew-Wiluna belt, Yilgarn Craton, Western Australia, in: Li, C., Ripley, E.M. (Eds.), Magmatic Ni-Cu and PGE Deposits: Geology, Geochemistry, and Genesis. Reviews in Economic Geology 17, 51–88. https://doi.org/10.5382/Rev.17.02

Barnes, S.J., Mungall, J.E., Maier, W.D., 2015. Platinum group elements in mantle melts and mantle samples. Lithos 232, 395–417. https://doi.org/10.1016/j.lithos.2015.07.007

Barnes, S.J., Cruden, A.R., Arndt, N., Saumur, B.M., 2016. The mineral system approach applied to magmatic Ni–Cu–PGE sulphide deposits. Ore Geology Reviews 76, 296–316. https://doi.org/10.1016/j.oregeorev.2015.06.012

Barnes, S.J., Yao, Z.-S., Mao, Y.-J., Jesus, A.P., Yang, S., Taranovic, V., Maier, W.D., 2023. Nickel in olivine as an exploration indicator for magmatic Ni-Cu sulphide deposits: A data review and re-evaluation. American Mineralogist 108, 1–17. https://doi.org/10.2138/am-2022-8327

Bayanova, T., Korchagin, A., Mitrofanov, A., Serov, P., Ekimova, N., Nitkina, E., Kamensky, I., Elizarov, D., Huber, M., 2019. Long-lived mantle plume and polyphase evolution of Palaeoproterozoic PGE intrusions in the Fennoscandian Shield. Minerals 9, 59. https://doi.org/10.3390/min9010059

Bédard, J.H., 2001. Parental magmas of the Nain Plutonic Suite anorthosites and mafic cumulates: a trace element modelling approach. Contributions to Mineralogy and Petrol 141, 747–771. https://doi.org/10.1007/s004100100268

Bibikova, E.V., Krylov, I.N., 1983. Isotopic age of acid volcanics from Karelia. Doklady Akademii Nauk SSSR 268, 1231–1235.

Bibikova, E.V., Samsonov, A.V., Shchipansky, A.A., Bogina, M.M., Gracheva, T.V., Makarov, A., 2003. The Hisovaara structure in the Tikshozero greenstone belt as a Late Archaean accreted island arc: isotopic geochronological and petrological evidence. Petrology 11, 261–290.

Bohrson, W.A., Spera, F.J., Heinonen, J.S., Brown, G.A., Scruggs, M.A., Adams, J.V., Takach, M.K., Zeff, G., Suikkanen, E., 2020. Diagnosing open-system magmatic processes using the Magma Chamber Simulator (MCS): part I—major elements and phase equilibria. Contributions to Mineralogy and Petrology 175, 104. https://doi.org/10.1007/s00410-020-01722-z

Boudreau, A.E., McCallum, I.S., 1992. Concentration of platinum-group elements by magmatic fluids in layered intrusions. Economic Geology 87, 1830–1848. https://doi.org/10.2113/gsecongeo.87.7.1830

Brownscombe, W., Ihlenfeld, C., Coppard, J., Hartshorne, C., Klatt, S., Siikaluoma, J.K., Herrington, R.J., 2015. The Sakatti Cu-Ni-PGE sulphide deposit in northern Finland, in: Maier, W.D., Lahtinen, R., O'Brien, H. (Eds.), Mineral Deposits of Finland. Elsevier, Amsterdam, pp. 211–252. https://doi.org/10.1016/B978-0-12-410438-9.00009-1

Brügmann, G.E., Hanski, E.J., Naldrett, A.J., Smolkin, V.F., 2000. Sulphide segregation in ferropicrites from the Pechenga Complex, Kola Peninsula, Russia. Journal of Petrology 41, 1721–1742. https://doi.org/10.1093/petrology/41.12.1721

Cabri, L.J., 1973. New data on phase relations in the Cu-Fe-S system. Economic Geology 68, 443–454. https://doi.org/10.2113/gsecongeo.68.4.443

Campbell, I.H., Naldrett, A.J., 1979. The influence of silicate:sulphide ratios on the geochemistry of magmatic sulphides. Economic Geology 74, 1503–1506. https://doi.org/10.2113/gsecongeo.74.6.1503

Chai, G., Naldrett, A.J., 1992. The Jinchuan ultramafic intrusion: Cumulate of a high-Mg basaltic magma. Journal of Petrology 33, 277–303. https://doi.org/10.1093/petrology/33.2.277

Cook, D.L., Walker, R.J., Horan, M.F., Wasson, J.T. and Morgan, J.W., 2004. Pt-Re-Os systematics of group IIAB and IIIAB iron meteorites. Geochimica et Cosmochimica Acta, 68, 1413–1431. https://doi.org/10.1016/j.gca.2003.09.017

Davey, S., 2020. Testing the paleogeography of late Archaean supercraton Superia using pre-breakup 2.51–1.98 Ga dyke and sill provinces–with a focus on the relationship between the Karelia-Kola and Superior cratonic fragments. Doctoral dissertation, Carleton University. 313 p.

Davey, S.C., Bleeker, W., Kamo, S.L., Ernst, R.E., Cousens, B.L., Vuollo, J. and Huhma, H., 2022. Evidence for a single large igneous province at 2.11 Ga across Supercraton Superia. Journal of Petrology 63, egac038. https://doi.org/10.1093/petrology/egac038

Eckstrand, O.R., 1996. Nickel-copper sulphides, in: Eckstrand, O.R., Sinclair, W.D., Thorpe, R.I. (Eds.), Geology of Canadian Mineral Deposit Types. Geological Survey of Canada, pp. 584–605. https://doi.org/10.1130/DNAG-GNA-P1

Ernst, R., Bleeker, W., 2010. Large igneous provinces (LIPs), giant dyke swarms, and mantle plumes: significance for breakup events within Canada and adjacent regions from 2.5 Ga to the Present. Canadian Journal of Earth Sciences 47, 695–739. https://doi.org/10.1139/E10-025

Ezad, I.S., Blanks, D.E., Foley, S.F., Holwell, D.A., Bennett, J. and Fiorentini, M.L., 2024. Lithospheric hydrous pyroxenites control localisation and Ni endowment of magmatic sulfide deposits. Mineralium Deposita, 59, 1–10. https://doi.org/10.1007/s00126-023-01238-z

Farquhar, J., Bao, H., Thiemens, M., 2000. Atmospheric influence of Earth's earliest sulfur cycle. Science 289, 756–758.

Fiorentini, M.L., Stone, W.E., Beresford, S.W., Barley, M.E., 2004. Platinum-group element alloy inclusions in chromites from Archaean mafic-ultramafic units: evidence from the Abitibi and the Agnew-Wiluna Greenstone Belts. Mineralogy and Petrology 82, 341–355. https://doi.org/10.1007/s00710-004-0044-6

Fiorentini, M.L., Beresford, S.W., Deloule, E., Hanski, E., Stone, W.E., Pearson, N.J., 2008. The role of mantle-derived volatiles in the petrogenesis of Palaeoproterozoic ferropicrites in the Pechenga Greenstone Belt, northwestern Russia: Insights from in-situ microbeam and nanobeam analysis of hydromagmatic amphibole. Earth and Planetary Science Letters 268, 2–14. https://doi.org/10.1016/j.epsl.2007.12.018

Fiorentini, M.L., Barnes, S.J., Lesher, C.M., Heggie, G.J., Keays, R.R., Burnham, O.M., 2010. Platinum group element geochemistry of mineralized and nonmineralized komatiites and basalts. Economic Geology 105, 795–823. https://doi.org/10.2113/gsecongeo.105.4.795

Fiorentini, M.L., Bekker, A., Rouxel, O., Wing, B.A., Maier, W., Rumble, D., 2012. Multiple sulfur and iron isotope composition of magmatic Ni-Cu-(PGE) sulphide mineralization from eastern Botswana. Economic Geology 107, 105–116. https://doi.org/10.2113/econgeo.107.1.105

Fleet, M.E., Chryssoulis, S.L., Stone, W.E., Weisener, C.G., 1993. Partitioning of platinum-group elements and Au in the Fe−Ni−Cu−S system: experiments on the fractional crystallization of sulphide melt. Contributions to Mineralogy and Petrology 115, 36–44. https://doi.org/10.1007/BF00712976

Fröhlich, F., Siikaluoma, J., Osbahr, I. and Gutzmer, J., 2021. Genesis of sulfide vein mineralization at the Sakatti Ni-Cu-PGE deposit, Finland. Canadian Mineralogist 59, 1485–1510. https://doi.org/10.3749/canmin.2100020

Godel, B., 2015. Platinum-group element deposits in layered intrusions: Recent advances in the understanding of the ore forming processes, in: Charlier, B., Namur, O., Latypov, R., Tegner, C. (Eds.), Layered Intrusions. Springer Netherlands, Dordrecht, pp. 379–432. https://doi.org/10.1007/978-94-017-9652-1_9

Godel, B., Barnes, S.-J., Maier, W.D., 2007. Platinum-group elements in sulphide minerals, platinum-group minerals, and whole-rocks of the Merensky Reef (Bushveld Complex, South Africa): Implications for the formation of the reef. Journal of Petrology 48, 1569–1604. https://doi.org/10.1093/petrology/egm030

Griffin, W.L., Begg, G.C., O'Reilly, S.Y., 2013. Continental-root control on the genesis of magmatic ore deposits. Nature Geosciences 6, 905–910. https://doi.org/10.1038/ngeo1954

Groshev, N.Y., Rundkvist, T.V., Karykowski, B.T., Maier, W.D., Korchagin, A.U., Ivanov, A.N. and Junge, M., 2019. Low-sulfide platinum–palladium deposits of the Paleoproterozoic Fedorova–Pana layered complex, Kola Region, Russia. Minerals 9, 764. https://doi.org/10.3390/min9120764

Guo, F.-F., Svetov, S., Maier, W.D., Hanski, E., Yang, S.H. and Rybnikova, Z., 2020. Geochemistry of komatiites and basalts in Archaean greenstone belts of Russian Karelia with emphasis on platinum-group elements. Mineralium Deposita 55, 971–990. https://doi.org/10.1007/s00126-019-00909-0

Guo, F.-F., Maier, W.D., Heinonen, J.S., Hanski, E., Vuollo, J., Barnes, S.-J., Lahaye, Y., Huhma, H., Yang, S., 2023. Geochemistry of 2.45 Ga mafic dykes in northern Finland: Constraints on the petrogenesis and PGE prospectivity of coeval layered intrusions. Lithos 452–453, 107206. https://doi.org/10.1016/j.lithos.2023.107206

Halkoaho, T.A.A., Alapieti, T.T., Lahtinen, J.J., Lerssi, J.M., 1990. The Ala-Penikka PGE reefs in the Penikat layered intrusion, Northern Finland. Mineralogy and Petrology 42, 23–38. https://doi.org/10.1007/BF01162682

Hanski, E., 1980. Komatiitic and tholeiitic metavolcanics of the Siivikkovaara area in the Archaean Kuhmo greenstone belt, eastern Finland. Bulletin of the Geological Society of Finland 52, 67–100. https://doi.org/10.17741/bgsf/52.1.004

Hanski, E., 2015. Synthesis of the geological evolution and metallogeny of Finland, in: Maier, W.D., Lahtinen, R., O'Brien, H. (Eds.), Mineral Deposits of Finland. Elsevier, Amsterdam, pp. 39–71. https://doi.org/10.1016/B978-0-12-410438-9.00002-9

Hanski, E.J., Smolkin, V.F., 1995. Iron- and LREE-enriched mantle source for early Proterozoic intraplate magmatism as exemplified by the Pechenga ferropicrites, Kola Peninsula, Russia. Lithos 34, 107–125. https://doi.org/10.1016/0024-4937(95)90015-2

Hanski, E., Huhma, H., Rastas, P., Kamenetsky, V.S., 2001a. The Palaeoproterozoic komatiite-picrite association of Finnish Lapland. Journal of Petrology 42, 855–876. https://doi.org/10.1093/petrology/42.5.855

Hanski, E., Walker, R.J., Huhma, H., Suominen, I., 2001b. The Os and Nd isotopic systematics of c. 2.44 Ga Akanvaara and Koitelainen mafic layered intrusions in northern Finland. Precambrian Research 109, 73–102. https://doi.org/10.1016/S0301-9268(01)00142-5

Hanski, E., Huhma, H., Vuollo, J., 2010. SIMS zircon ages and Nd isotope systematics of the 2.2 Ga mafic intrusions in northern and eastern Finland. Bulletin of the Geological Society of Finland 82, 31–62. https://doi.org/10.17741/bgsf/82.1.002

Hanski, E.J., Luo, Z.-Y., Oduro, H., Walker, R.J., 2011. The Pechenga Ni-Cu sulphide deposits, northwestern Russia: A review with new constraints from the feeder dykes, in: Li, C., Ripley, E.M. (Eds.), Magmatic Ni-Cu and PGE Deposits: Geology, Geochemistry, and Genesis. Society of Economic Geologists, 17, 145–162. https://doi.org/10.5382/Rev.17.05

Hanski, E.J., Huhma, H. and Melezhik, V.A., 2014. New isotopic and geochemical data from the Palaeoproterozoic Pechenga Greenstone Belt, NW Russia: implication for basin development and duration of the volcanism. Precambrian Research 245, 51–65. https://doi.org/10.1016/j.precamres.2014.01.008

Hawkesworth, C.J., Lightfoot, P.C., Fedorenko, V.A., Blake, S., Naldrett, A.J., Doherty, W., Gorbachev, N.S., 1995. Magma differentiation and mineralisation in the Siberian continental flood basalts. Lithos 34, 61–88. https://doi.org/10.1016/0024-4937(95)90011-X

Helz, R.T., 1995. The Stillwater Complex, Montana; a subvolcanic magma chamber? American Mineralogist 80, 1343–1346. https://doi.org/10.2138/am-1995-11-1225

Hickey, R.L. and Frey, F.A., 1982. Geochemical characteristics of boninite series volcanics: implications for their source. Geochimica et Cosmochimica Acta 46, 2099–2115. https://doi.org/10.1016/0016-7037(82)90188-0

Honkamo, M., 1987. Geochemistry and tectonic setting of early Proterozoic volcanic rocks in northern Ostrobothnia, Finland. Geological Society, London, Special Publications 33, 59–68. https://doi.org/10.1144/GSL.SP.1987.033.01.05

Huhma, H., Cliff, R.A., Perttunen, V., Sakko, M., 1990. Sm-Nd and Pb isotopic study of mafic rocks associated with early Proterozoic continental rifting: the Peräpohja schist belt in northern Finland. Contributions to Mineralogy and Petrology 104, 369–379. https://doi.org/10.1007/BF00321491

Huhma, H., Mänttäri, I., Peltonen, P., Kontinen, A., Halkoaho, T., Hanski, E., Hokkanen, T., Hölttä, P., Juopperi, H., Konnunaho, J., Lahaye, Y., Luukkonen, E., Pietikäinen, K., Pulkkinen, A., Sorjonen-Ward, P., Vaasjoki, M., Whitehouse, M., 2012. The age of the Archaean greenstone belts in Finland. Geological Survey of Finland, Special Paper 54, 74–175.

Huhma, H., Hanski, E., Kontinen, A., Vuollo, J., Mänttäri, I, Lahaye, Y., 2018. Sm-Nd and U-Pb isotope geochemistry of the Palaeoproterozoic mafic magmatism in eastern and northern Finland. Bulletin of the Geological Society of Finland 405, 150 p.

Huhtelin, T., 2015. The Kemi chromite deposit, in: Maier, W.D., Lahtinen, R., O'Brien, H. (Eds.), Mineral Deposits of Finland. Elsevier, Amsterdam, pp. 165–178. https://doi.org/10.1016/B978-0-12-410438-9.00006-6

Huppert, H.E., Sparks, R.S.J., 1989. Chilled margins in igneous rocks. Earth and Planetary Science Letters 92, 397–405. https://doi.org/10.1016/0012-821X(89)90063-0

Hölttä, P., Heilimo, E., Huhma, H., Juopperi, H., Kontinen, A., Konnunaho, J., Lauri, L., Mikkola, P., Paavola, J., Sorjonen-Ward, P., 2012. Archaean complexes of the Karelia Province in Finland. Geological Survey of Finland, Special Paper 54, 9–20.

Iacono-Marziano, G., Ferraina, C., Gaillard, F., Di Carlo, I., Arndt, N.T., 2017. Assimilation of sulfate and carbonaceous rocks: Experimental study, thermodynamic modeling and application to the Noril'sk-Talnakh region (Russia). Ore Geology Reviews 90, 399–413. https://doi.org/10.1016/j.oregeorev.2017.04.027

Iljina, M., 1994. The Portimo layered igneous complex: with emphasis of diverse sulphide and platinum-group element deposits. Doctoral dissertation, University of Oulu, 158 p.

Iljina, M., Hanski, E., 2005. Layered mafic intrusions of the Tornio-Näränkävaara belt, in: Lehtinen, M., Nurmi, P.A., Rämö, O.T. (Eds.), Precambrian Geology of Finland – Key to the Evolution of the Fennoscandian Shield. Elsevier, pp. 101–137. https://doi.org/10.1016/S0166-2635(05)80004-0

Iljina, M., Maier, W.D., Karinen, T., 2015. PGE-(Cu-Ni) deposits of the Tornio-Näränkävaara belt of intrusions (Portimo, Penikat, and Koillismaa), in: Mineral Deposits of Finland. Elsevier, Amsterdam, pp. 133–164. https://doi.org/10.1016/B978-0-12-410438-9.00005-4

Jahn, B.-M., Vidal, P., Tilton, G.R., Bailey, D.K., Tarney, J., Dunham, K.C., 1980. Archaean mantle heterogeneity: evidence from chemical and isotopic abundances in Archaean igneous rocks. Philosophical Transactions of the Royal Society 297, 353–364. https://doi.org/10.1098/rsta.1980.0221

Jiang, S.Y., Yang, J.H., Ling, H.F., Chen, Y.Q., Feng, H.Z., Zhao, K.D. and Ni, P., 2007. Extreme enrichment of polymetallic Ni–Mo–PGE–Au in Lower Cambrian black shales of South China: an Os isotope and PGE geochemical investigation. Palaeogeography, Palaeoclimatology, Palaeoecology 254, 217–228.

Jowitt, S.M., Williamson, M.-C., Ernst, R.E., 2014. Geochemistry of the 130 to 80 Ma Canadian High Arctic Large Igneous Province (HALIP) event and implications for Ni-Cu-PGE prospectivity. Economic Geology 109, 281–307. https://doi.org/10.2113/econgeo.109.2.281

Junge, M., Wirth, R., Oberthür, T., Melcher, F., Schreiber, A., 2015. Mineralogical siting of platinum-group elements in pentlandite from the Bushveld Complex, South Africa. Mineralium Deposita 50, 41–54. https://doi.org/10.1007/s00126-014-0561-0

Järvinen, V., Halkoaho, T., Konnunaho, J., Heinonen, J., Karinen, T., Rämö, T., 2022. Petrogenesis of the Paleoproterozoic Näränkävaara layered intrusion, northern Finland, Part I: The northern peridotites and their relationships with the layered series and recharge events. Bull Geol Soc Finland 94, 23–52. https://doi.org/10.17741/bgsf/94.1.002

Karhu, J.A., 1993. Paleoproterozoic evolution of the carbon isotope ratios of sedimentary carbonates in the Fennoscandian Shield. Geological Survey of Finland, Bulletin 371, 87 p.

Karinen, T., 2010. The Koillismaa intrusion, northeastern Finland: evidence for the PGE reef forming processes in the layered series Geological Survey of Finland, Bulletin 404, 176 p.

Karinen, T., Hanski, E., Taipale, A., 2015. The Mustavaara Fe-Ti-V oxide deposit, in: Mineral Deposits of Finland. Elsevier, Amsterdam, pp. 179–194. https://doi.org/10.1016/B978-0-12-410438-9.00007-8

Karykowski, B.T., Maier, W.D., Groshev, N.Y., Barnes, S.-J., Pripachkin, P.V., McDonald, I., 2018a. Origin of reef-style PGE mineralization in the Paleoproterozoic Monchegorsk Complex, Kola Region, Russia. Economic Geology 113, 1333–1358. https://doi.org/10.5382/econgeo.2018.4594

Karykowski, B.T., Maier, W.D., Groshev, N.Y., Barnes, S.-J., Pripachkin, P.V., McDonald, I., Savard, D., 2018b. Critical controls on the formation of contact-style PGE-Ni-Cu mineralization: Evidence from the Paleoproterozoic Monchegorsk Complex, Kola Region, Russia. Economic Geology 113, 911–935. https://doi.org/10.5382/econgeo.2018.4576

Keays, R.R., 1995. The role of komatiitic and picritic magmatism and S-saturation in the formation of ore deposits. Lithos 34, 1–18. https://doi.org/10.1016/0024-4937(95)90003-9

Keays, R.R., Lightfoot, P.C., 2010. Crustal sulfur is required to form magmatic Ni–Cu sulphide deposits: evidence from chalcophile element signatures of Siberian and Deccan Trap basalts. Mineralium Deposita 45, 241–257. https://doi.org/10.1007/s00126-009-0271-1

Keays, R.R., Tegner, C., 2015. Magma chamber processes in the formation of the low-sulphide magmatic Au–PGE mineralization of the Platinova Reef in the Skaergaard intrusion, East Greenland. Journal of Petrology 56, 2319–2340. https://doi.org/10.1093/petrology/egv075

Konnunaho, J.P., Hanski, E.J., Bekker, A., Halkoaho, T.A.A., Hiebert, R.S., Wing, B.A., 2013. The Archaean komatiite-hosted, PGE-bearing Ni-Cu sulphide deposit at Vaara, eastern Finland: evidence for assimilation of external sulfur and post-depositional desulfurization. Mineralium Deposita 48, 967–989. https://doi.org/10.1007/s00126-013-0469-0

Konnunaho, J., Halkoaho, T., Hanski, E., Törmänen, T., 2015. Komatiite-hosted Ni-Cu-PGE deposits in Finland, in: Maier, W.D., Lahtinen, R., O'Brien, H. (Eds.), Mineral Deposits of Finland. Elsevier, Amsterdam, pp. 93–131. https://doi.org/10.1016/B978-0-12-410438-9.00004-2

Konnunaho, J. P, Hanski, E. J., Wing, B., Bekker, A., Lukkari, S., Halkoaho, T., 2016. The Hietaharju PGE-enriched komatiite-hosted sulfide deposit in the Archaean Suomussalmi greenstone belt, eastern Finland. Ore Geology Reviews 72 (1), 641−658. https://doi.org/10.1016/j.oregeorev.2015.08.022

Kozhevnikov, V.N., 1992. Geology and Geochemistry of the Archaean North Karelian Greenstone Structures. Karelian Research Center, Russian Academy of Sciences, Petrozavodsk. (in Russian).

Kuleshevich, L.V., Gor'kovets, V.Ya., 2008. Mineralogy of the Precambrian southern Kostomuksha gold prospect in Karelia. Geology Ore Deposits 50, 599–608. https://doi.org/10.1134/S1075701508070118

Kullerud, G., Yund, R.A., Moh, G.H., 1969. Phase relations in the Cu-Fe-S, Cu-Ni-S, and Fe-Ni-S systems, in: Wilson, H.D.B. (Ed.), Magmatic Ore Deposits. Economic Geology Monograph Series 4, 323–343. https://doi.org/10.5382/Mono.04.23

Kyläkoski, M., 2007. Nickel, Copper and Platinum-Group Element Ore Potential of the Jouttiaapa Formation, a ca. 2.1 Ga Continental Flood Basalt Sequence in the Peräpohja Belt, Northwestern Finland. Licentiate Thesis, Department of Geosciences, University of Oulu. In Finnish with English abstract. 204 p.

Kyläkoski, M., Hanski, E., Huhma, H., 2012. The Petäjäskoski Formation, a new lithostratigraphic unit in the Paleoproterozoic Peräpohja Belt, northern Finland. Bulletin of the Geological Society of Finland 84, 85–120. https://doi.org/10.17741/bgsf/84.2.001

Köykkä, J., Lahtinen, R., Manninen, T., 2022. Tectonic evolution, volcanic features and geochemistry of the Paleoproterozoic Salla belt, northern Fennoscandia: From 2.52 to 2.40 Ga LIP stages to ca. 1.92–1.90 Ga collision. Precambrian Research 371, 106597. https://doi.org/10.1016/j.precamres.2022.106597

Lambert, D.D. and Simmons, E.C., 1987. Magma evolution in the Stillwater Complex, Montana; I, Rare-earth element evidence for the formation of the Ultramafic Series. American Journal of Science, 287, 1–32. https://doi.org/10.2475/ajs.287.1.1

Lambert, D.D. and Simmons, E.C., 1988. Magma evolution in the Stillwater Complex, Montana; II, Rare earth element evidence for the formation of the JM Reef. Economic Geology 83, 1109–1126. https://doi.org/10.2113/gsecongeo.83.6.1109

Lesher, C.M., Barnes, S.J., 2009. Komatiite-associated Ni-Cu-PGE deposits., in: Li, C., Ripley, E.M. (Eds.), New Developments in Magmatic Ni-Cu and PGE Deposits. Geological Publishing House, Beijing, pp. 27–120.

Lesher, C.M., Keays, R.R., 2002. Komatiite-associated Ni-Cu-PGE deposits: Geology, mineralogy, geochemistry and genesis, in: Cabri, L. (Eds.), The Geology, Geochemistry, Mineralogy and Mineral Beneficiation of the Platinum-Group Elements. Canadian Institute Mineral Metallurgy Petroleum, Special Volume 54, pp.579–618. https://doi.org/10.2113/gsecongeo.97.7.1609

Lesher, C.M., Stone, W.E., 1996. Exploration geochemistry of komatiites. In Igneous Trace Element Geochemical Applications for Massive Sulphide Exploration. Edited by D.A. Wyman. Geological Association of Canada, Short Course Notes, 12, pp. 153–204.

Le Vaillant, M., Barnes, S.J., Fiorentini, M.L., Santaguida, F. and Törmänen, T., 2016. Effects of hydrous alteration on the distribution of base metals and platinum group elements within the Kevitsa magmatic nickel sulphide deposit. Ore Geology Reviews 72, 128–148. https://doi.org/10.1016/j.oregeorev.2015.06.002

Li, C., Naldrett, A.J., 1993. Sulphide capacity of magma; a quantitative model and its application to the formation of sulphide ores at Sudbury, Ontario. Economic Geology 88, 1253–1260. https://doi.org/10.2113/gsecongeo.88.5.1253

Li, C., Naldrett, A.J., 1999. Geology and petrology of the Voisey's Bay intrusion: reaction of olivine with sulphide and silicate liquids. Lithos 47, 1–31. https://doi.org/10.1016/S0024-4937(99)00005-5

Li, C., Ripley, E.M., 2005. Empirical equations to predict the sulfur content of mafic magmas at sulfide saturation and applications to magmatic sulfide deposits. Mineralium Deposita, 40, 218–230. https://doi.org/10.1007/s00126-005-0478-8

Li, C., Ripley, E.M., 2010. The relative effects of composition and temperature on olivine-liquid Ni partitioning: Statistical deconvolution and implications for petrologic modeling. Chemical Geology 275, 99–104. https://doi.org/10.1016/j.chemgeo.2010.05.001

Li, C., Ripley, E.M., Naldrett, A.J., 2003. Compositional variations of olivine and sulfur isotopes in the Noril'sk and Talnakh intrusions, Siberia: Implications for ore-forming processes in dynamic magma conduits. Economic Geology 98, 69–86. https://doi.org/10.2113/gsecongeo.98.1.69

Li, C., Xu, Z., de Waal, S.A., Ripley, E.M., Maier, W.D., 2004. Compositional variations of olivine from the Jinchuan Ni–Cu sulphide deposit, western China: implications for ore genesis. Mineralium Deposita 39, 159–172. https://doi.org/10.1007/s00126-003-0389-5

Li, C., Ripley, E.M., Naldrett, A.J., 2009. A new genetic model for the giant Ni-Cu-PGE sulphide deposits associated with the Siberian flood basalts. Economic Geology 104, 291–301. https://doi.org/10.2113/gsecongeo.104.2.291

Lightfoot, P.C., Hawkesworth, C.J., 1997. Flood basalts and magmatic Ni, Cu, and PGE sulphide mineralization: Comparative geochemistry of the Noril'sk (Siberian Traps) and West Greenland sequences, in: Large Igneous Provinces: Continental, Oceanic, and Planetary Flood Volcanism. American Geophysical Union (AGU), pp. 357–380. https://doi.org/10.1029/GM100p0357

Lightfoot, P.C., Keays, R.R., 2005. Siderophile and chalcophile metal variations in flood basalts from the Siberian trap, Noril'sk region: Implications for the origin of the Ni-Cu-PGE sulfide ores. Economic Geology, 100, 439–462. https://doi.org/10.2113/gsecongeo.100.3.439

Lightfoot, P.C., Naldrett, A.J., Gorbachev, N.S., Doherty, W., Fedorenko, V.A., 1990. Geochemistry of the Siberian Trap of the Noril'sk area, USSR, with implications for the relative contributions of crust and mantle to flood basalt magmatism. Contributions to Mineralogy Petrology 104, 631–644. https://doi.org/10.1007/BF01167284

Lobach-Zhuchenko, S.B., Arestova, N.A., Chekulaev, V.P., Levsky, L.K., Bogomolov, E.S., Krylov, I.N., 1998. Geochemistry and petrology of 2.40–2.45 Ga magmatic rocks in the north-western Belomorian Belt, Fennoscandian Shield, Russia. Precambrian Research 92, 223–250. https://doi.org/10.1016/S0301-9268(98)00076-X

Lorand, J.-P., Luguet, A., 2016. Chalcophile and siderophile elements in mantle rocks: trace elements controlled by trace minerals. Reviews in Mineralogy and Geochemistry 81, 441–488. https://doi.org/10.2138/rmg.2016.81.08

Lorand, J.-P., Luguet, A., Alard, O., 2013. Platinum-group element systematics and petrogenetic processing of the continental upper mantle: A review. Lithos 164–167, 2–21. https://doi.org/10.1016/j.lithos.2012.08.017

Luolavirta, K., Hanski, E., Maier, W. and Santaguida, F., 2018. Whole-rock and mineral compositional constraints on the magmatic evolution of the Ni-Cu-(PGE) sulfide ore-bearing Kevitsa intrusion, northern Finland. Lithos 296, 37–53. https://doi.org/10.1016/j.lithos.2017.10.015

Maier, W.D., Barnes, S.-J., 1999. Platinum-group elements in silicate rocks of the Lower, Critical and Main Zones at Union Section, Western Bushveld Complex. Journal of Petrology 40, 1647–1671. https://doi.org/10.1093/petroj/40.11.1647

Maier, W.D., Barnes, S.-J., 2004. Pt/Pd and Pd/Ir ratios in mantle-derived magmas: A possible role for mantle metasomatism. South African Journal of Geology 107, 333–340. https://doi.org/10.2113/107.3.333

Maier, W.D, Barnes, S.-J., 2005. Application of lithogeochemistry to exploration for PGE deposits, in: Mungall, J. (Eds.), Exploration for Platinum-Group Elements Deposits, Mineralogical Association of Canada, Short Course Series 35, 537 p.

Maier, W.D., Groves, D.I., 2011. Temporal and spatial controls on the formation of magmatic PGE and Ni–Cu deposits. Mineralium Deposita 46, 841–857. https://doi.org/10.1007/s00126-011-0339-6

Maier, W.D., Hanski, E.J., 2017. Layered mafic–ultramafic intrusions of Fennoscandia: Europe's treasure chest of magmatic metal deposits. Elements 13, 415–420. https://doi.org/10.2138/gselements.13.6.415

Maier, W.D., Mundl-Petermeier, A., 2023. Controls on Pt/Pd ratios in Bushveld magmas and cumulates: a review complemented by new W isotope data. Mineralium Deposita 58, 553–568. https://doi.org/10.1007/s00126-022-01141-z

Maier, W.D., Barnes, S.-J., Gartz, V., Andrews, G., 2003. Pt-Pd reefs in magnetitites of the Stella layered intrusion, South Africa: A world of new exploration opportunities for platinum group elements. Geology 31, 885–888. https://doi.org/10.1130/G19746.1

Maier, W.D, Barnes, S., Campbell, I.H., Fiorentini M.L., Peltonen P., Barnes S.-J., Smithies, R.H., 2009. Progressive mixing of meteoritic veneer into the early Earth's deep mantle. Nature 460, 620–623. https://doi.org/10.1038/nature08205

Maier, W.D., Peltonen, P., McDonald, I., Barnes, S.J., Barnes, S.-J., Hatton, C., Viljoen, F., 2012. The concentration of platinum-group elements and gold in southern African and Karelian kimberlite-hosted mantle xenoliths: Implications for the noble metal content of the Earth's mantle. Chemical Geology 302–303, 119–135. https://doi.org/10.1016/j.chemgeo.2011.06.014

Maier, W.D., Barnes, S.-J., Groves, D.I., 2013a. The Bushveld Complex, South Africa: formation of platinum–palladium, chrome- and vanadium-rich layers via hydrodynamic sorting of a mobilized cumulate slurry in a large, relatively slowly cooling, subsiding magma chamber. Mineralium Deposita 48, 1–56. https://doi.org/10.1007/s00126-012-0436-1

Maier, W.D., Peltonen, P., Halkoaho, T., Hanski, E., 2013b. Geochemistry of komatiites from the Tipasjärvi, Kuhmo, Suomussalmi, Ilomantsi and Tulppio greenstone belts, Finland: Implications for tectonic setting and Ni sulphide prospectivity. Precambrian Research 228, 63–84. https://doi.org/10.1016/j.precamres.2012.12.004

Maier, W.D., Määttä, S., Yang, S., Oberthür, T., Lahaye, Y., Huhma, H., Barnes, S.-J., 2015. Composition of the ultramafic–mafic contact interval of the Great Dyke of Zimbabwe at Ngezi mine: Comparisons to the Bushveld Complex and implications for the origin of the PGE reefs. Lithos 238, 207–222. https://doi.org/10.1016/j.lithos.2015.09.007

Maier, W.D., Barnes, S.-J., Karykowski, B.T., 2016. A chilled margin of komatiite and Mg-rich basaltic andesite in the western Bushveld Complex, South Africa. Contributions to Mineralogy and Petrology 171, 57. https://doi.org/10.1007/s00410-016-1257-5

Maier, W.D., Halkoaho, T., Huhma, H., Hanski, E., Barnes, S.-J., 2018. The Penikat intrusion, Finland: Geochemistry, geochronology, and origin of platinum–palladium reefs. Journal of Petrology 59, 967–1006. https://doi.org/10.1093/petrology/egy051

Maier, W.D., Barnes, S.-J., Smith, W.D., 2023.Petrogenesis of the Mesoarchaean Stella layered intrusion, South Africa: implications for the origin of PGE reefs in the upper portion of layered intrusions. Mineralium Deposita, 58, 1477–1497. https://doi.org/10.1007/s00126-023-01189-5

Makkonen, H.V., Halkoaho, T., Konnunaho, J., Rasilainen, K., Kontinen, A., Eilu, P., 2017. Ni-(Cu-PGE) deposits in Finland – Geology and exploration potential. Ore Geology Reviews 90, 667–696. https://doi.org/10.1016/j.oregeorev.2017.06.008

Manninen, T., 1991. Volcanic rocks in the Salla area, northeastern Finland. Geological Survey of Finland, Report of Investigation 104, 97 p.

Mansur, E., Barnes, S.-J., Janasi, V., Henrique-Pinto, R., Alves, A., Marteleto, N.S., 2021. The distribution of platinum-group elements and Te, As, Bi, Sb and Se (TABS+) in the Paraná Magmatic Province: Effects of crystal fractionation, sulphide segregation and magma degassing. Lithos 400–401, 106374. https://doi.org/10.1016/j.lithos.2021.106374

Mavrogenes, J.A., O'Neill, H.St.C., 1999. The relative effects of pressure, temperature and oxygen fugacity on the solubility of sulphide in mafic magmas. Geochimica et Cosmochimica Acta 63, 1173–1180. https://doi.org/10.1016/S0016-7037(98)00289-0

McDonald, I., Holwell, D.A., 2011. Geology of the Northern Bushveld Complex and the Setting and Genesis of the Platreef Ni-Cu-PGE Deposit. Reviews in Economic Geology 17, 297–327.

McDonough, W.F. and Sun, S.S., 1995. The composition of the Earth. Chemical geology 120, 223–253. https://doi.org/10.1016/0009-2541(94)00140-4

Melezhik, V.A., Hanski, E.J., 2012. 4.2 The Pechenga greenstone belt, in: Melezhik, Victor A., Prave, A.R., Fallick, A.E., Kump, L.R., Strauss, H., Lepland, A., Hanski, E.J. (Eds.), Reading the Archive of Earth's Oxygenation: Volume 1: The Palaeoproterozoic of Fennoscandia as Context for the Fennoscandian Arctic Russia – Drilling Early Earth Project, Frontiers in Earth Sciences. Springer, Berlin, Heidelberg, pp. 289–385. https://doi.org/10.1007/978-3-642-29682-6_8

Melezhik, V.A., Fallick, A.E., Martin, A.P., Condon, D.J., Kump, L.R., Brasier, A.T., Salminen, P.E., 2013. The Palaeoproterozoic perturbation of the global carbon cycle: The Lomagundi-Jatuli isotope excursion, in: Melezhik, V., Kump, L., Fallick, A., Strauss, H., Hanski, E., Prave, A., Lepland, A. (Eds.), Reading the Archive of Earth's Oxygenation. Volume 3: Global Events and the Fennoscandian Arctic Russia – Drilling Early Earth Project, Springer-Verlag, Berlin, Heidelberg, pp. 1111–1150. https://doi.org.10.1007/978-3-642-29670-3_3

Mikkola, P., Huhma, H., Heilimo, E., Whitehouse, M., 2011. Archaean crustal evolution of the Suomussalmi district as part of the Kianta Complex, Karelia: Constraints from geochemistry and isotopes of granitoids. Lithos 125, 287–307. https://doi.org/10.1016/j.lithos.2011.02.012

Miller, J.D., 2002. Stratiform PGE mineralization in the tholeiitic layered intrusions of the Midcontinent rift, northeastern Minnesota: Known examples and potential Targets. 9th International Platinum Symposium Abstracts, Montana

Mitrofanov, F.P., Bayanova, T.B., Ludden, J.N., Korchagin, A.U., Chashchin, V.V., Nerovich, L.I., Serov, P.A., Mitrofanov, A.F. and Zhirov, D.V., 2019. Origin and exploration of the Kola PGE-bearing province: New constraints from geochronology, in: Decrée, S., Robb, L. (Eds.), Ore Deposits: Origin, Exploration, and Exploitation. Geophysical Monograph Series. Wiley, Hoboken, NJ, USA, pp. 3–36.

Moilanen, M., Hanski, E. and Yang, S.H., 2021. Re-Os isotope geochemistry of the Palaeoproterozoic Sakatti Cu-Ni-PGE sulphide deposit in northern Finland. Ore Geology Reviews 132, 104044. https://doi.org/10.1016/j.oregeorev.2021.104044

Mokrushin, A.V., Smol'kin, V.F., 2021. Chromite mineralization in the Sopcheozero deposit (Monchegorsk layered intrusion, Fennoscandian Shield). Minerals 11, 772. https://doi.org/10.3390/min11070772

Momme, P., Tegner, C., Brooks, K.C. and Keays, R.R., 2002. The behaviour of platinum-group elements in basalts from the East Greenland rifted margin. Contributions to Mineralogy and Petrology 143, 33–153.

Mudd, G.M. and Jowitt, S.M., 2014. A detailed assessment of global nickel resource trends and endowments. Economic Geology 109, 1813-1841. https://doi.org/10.1007/s00410-001-0338-1

Mungall, J.E. and Brenan, J.M., 2014. Partitioning of platinum-group elements and Au between sulfide liquid and basalt and the origins of mantle-crust fractionation of the chalcophile elements. Geochimica et Cosmochimica Acta 125, 265–289. https://doi.org/10.1016/j.gca.2013.10.002

Mutanen, T., 1997. Geology and ore petrology of the Akanvaara and Koitelainen mafic layered intrusions and the Keivitsa-Satovaara layered complex, northern Finland. Geological Survey of Finland, Bulletin 395, 233 p.

Naldrett, A.J., 1989. Magmatic Sulphide Deposits. Oxford Monographs on Geology and Geophysics. Oxford University Press, Oxford, New York, 186 p.

Naldrett, A.J., 1992. A model for the Ni-Cu-PGE ores of the Noril'sk region and its application to other areas of flood basalt. Economic Geology 87, 1945–1962. https://doi.org/10.2113/gsecongeo.87.8.1945

Naldrett, A.J., 1994. The Sudbury-Noril'sk symposium, an overview. Ontario Geological Survey, Special Publication 5, 3–10.

Naldrett, A.J., 2004. Magmatic Sulphide Deposits. Geology, Geochemistry and Exploration. Springer, Berlin, Heidelberg, 728 p. https://doi.org/10.1007/978-3-662-08444-1

Naldrett, A.J., 2010. Secular variation of magmatic sulphide deposits and their source magmas. Economic Geology 105, 669–688. https://doi.org/10.2113/gsecongeo.105.3.669

Naldrett, A.J., Wilson, A., Kinnaird, J., Chunnett, G., 2009. PGE tenor and metal ratios within and below the Merensky Reef, Bushveld Complex: Implications for its genesis. Journal of Petrology 50, 625–659. https://doi.org/10.1093/petrology/egp015

Nykänen, V.M., Vuollo, J.I., Liipo, J.P., Piirainen, T.A., 1994. Transitional (2.1 Ga) Fe-tholeiitic-tholeiitic magmatism in the Fennoscandian Shield signifying lithospheric thinning during Palaeoproterozoic extensional tectonics. Precambrian Research 70, 45–65. https://doi.org/10.1016/0301-9268(94)90020-5

Orvik, A.A., Slagstad, T., Hansen, H., Nilsson, L.P., Sørensen, B.E., 2022a. The Palaeoproterozoic Gallujavri ultramafic intrusion, Karasjok greenstone belt; Petrogenesis of a trans-crustal magma system. Journal of Petrology 63, egac008. https://doi.org/10.1093/petrology/egac008

Orvik, A.A., Slagstad, T., Sørensen, B.E., Millar, I., Hansen, H., 2022b. Evolution of the Gállojávri ultramafic intrusion from U-Pb zircon ages and Rb-Sr, Sm-Nd and Lu-Hf isotope systematics. Precambrian Research 379, 106813. https://doi.org/10.1016/j.precamres.2022.106813

Papunen, H., Halkoaho, T., Luukkonen, E., 2009. Archaean evolution of the Tipasjärvi-Kuhmo-Suomussalmi greenstone complex, Finland. Geological Survey of Finland, Bulletin 403, 68 p.

Park, J.W., Kamenetsky, V., Campbell, I., Park, G., Hanski, E. and Pushkarev, E., 2017. Empirical constraints on partitioning of platinum group elements between Cr-spinel and primitive terrestrial magmas. Geochimica et Cosmochimica Acta 216, 393–416.

Pearson, D.G., 2004. Re-Os and Lu-Hf isotope constraints on the origin and age of pyroxenites from the Beni Bousera Peridotite Massif: Implications for mixed peridotite-pyroxenite mantle sources. Journal of Petrology 45, 439–455. https://doi.org/10.1093/petrology/egg102

Pearson, D.G., Canil, D., Shirey, S.B., 2003. Mantle samples included in volcanic rocks: Xenoliths and diamonds, in: Holland, H.D., Turekian, K.K. (Eds.), Treatise on Geochemistry. Pergamon, Oxford, pp. 171–275. https://doi.org/10.1016/B0-08-043751-6/02005-3

Pripachkin, P., Rundkvist, T. and Groshev, N., 2023. Paleoproterozoic East Pana layered intrusion (Kola Peninsula, Russia): Geological structure, petrography, geochemistry and Cu-Ni-PGE mineralization. Minerals 13, 681. https://doi.org/10.3390/min13050681

Puchtel, I., Humayun, M., 2000. Platinum group elements in Kostomuksha komatiites and basalts: implications for oceanic crust recycling and core-mantle interaction. Geochimica et Cosmochimica Acta 64, 4227–4242. https://doi.org/10.1016/S0016-7037(00)00492-0

Puchtel, I.S., Hofmann, A.W., Mezger, K., Shchipansky, A.A., Kulikov, V.S., Kulikova, V.V., 1996. Petrology of a 2.41 Ga remarkably fresh komatiitic basalt lava lake in Lion Hills, central Vetreny Belt, Baltic Shield. Contributions to Mineralogy and Petrology 124, 273–290. https://doi.org/10.1007/s004100050191

Puchtel, I.S., Haase, K.M., Hofmann, A.W., Chauvel, C., Kulikov, V.S., Garbe-Schönberg, C.-D., Nemchin, A.A., 1997. Petrology and geochemistry of crustally contaminated komatiitic basalts from the Vetreny Belt, southeastern Baltic Shield: Evidence for an early Proterozoic mantle plume beneath rifted Archaean continental lithosphere. Geochimica et Cosmochimica Acta 61, 1205–1222. https://doi.org/10.1016/S0016-7037(96)00410-3

Puchtel, I.S., Hofmann, A.W., Mezger, K., Jochum, K.P., Shchipansky, A.A., Samsonov, A.V., 1998. Oceanic plateau model for continental crustal growth in the Archaean: A case study from the Kostomuksha greenstone belt, NW Baltic Shield. Earth and Planetary Science Letters 155, 57–74. https://doi.org/10.1016/S0012-821X(97)00202-1

Puchtel, I.S., Hofmann, A.W., Amelin, Yu.V., Garbe-Schönberg, C.-D., Samsonov, A.V., Shchipansky, A.A., 1999. Combined mantle plume-island arc model for the formation of the 2.9 Ga Sumozero-Kenozero greenstone belt, SE Baltic Shield: isotope and trace element constraints. Geochimica et Cosmochimica Acta 63, 3579–3595. https://doi.org/10.1016/S0016-7037(99)00111-8

Puchtel, I.S., Brügmann, G.E., Hofmann, A.W., 2001. [187]Os-enriched domain in an Archaean mantle plume: evidence from 2.8 Ga komatiites of the Kostomuksha greenstone belt, NW Baltic Shield. Earth and Planetary Science Letters 186, 513–526. https://doi.org/10.1016/S0012-821X(01)00264-3

Puchtel, I.S., Brandon, A.D., Humayun, M., Walker, R.J., 2005. Evidence for the early differentiation of the core from Pt–Re–Os isotope systematics of 2.8-Ga komatiites. Earth and Planetary Science Letters 237, 118–134. https://doi.org/10.1016/j.epsl.2005.04.023

Puchtel, I.S., Humayun, M., Walker, R.J., 2007. Os–Pb–Nd isotope and highly siderophile and lithophile trace element systematics of komatiitic rocks from the Volotsk suite, SE Baltic Shield. Precambrian Research 158, 119–137. https://doi.org/10.1016/j.precamres.2007.04.004

Puchtel, I.S., Mundl-Petermeier, A., Horan, M., Hanski, E.J., Blichert-Toft, J., Walker, R.J., 2020. Ultra-depleted 2.05 Ga komatiites of Finnish Lapland: Products of grainy late accretion or core-mantle interaction? Chemical Geology 554, 119801. https://doi.org/10.1016/j.chemgeo.2020.119801

Puustinen, K., Saltikoff, B., Tontti, M., 1995. Distribution and metallogenic types of nickel deposits in Finland. Geological Survey of Finland, Report of Investigations 132, 38 p.

Qi, L., Wang, C.Y., Zhou, M.-F., 2008. Controls on the PGE distribution of Permian Emeishan alkaline and peralkaline volcanic rocks in Longzhoushan, Sichuan Province, SW China. Lithos 106, 222–236. https://doi.org/10.1016/j.lithos.2008.07.012

Ripley, E.M., Li, C., 2003. Sulfur isotope exchange and metal enrichment in the formation of magmatic Cu-Ni-(PGE) deposits. Economic Geology 98, 635–641. https://doi.org/10.2113/gsecongeo.98.3.635

Rivas de la Torre, I., 2022. Sr isotope stratigraphy across the Paasivaara PGE reef of the Penikat intrusion, Northern Finland: insights into the genesis of reef-type PGE mineralization. Master's thesis, University of Oulu. 125 p.

Samalens, N., Barnes, S.-J., Sawyer, E.W., 2017. The role of black shales as a source of sulfur and semimetals in magmatic nickel-copper deposits: Example from the Partridge River Intrusion, Duluth Complex, Minnesota, USA. Ore Geology Reviews 81, 173–187. https://doi.org/10.1016/j.oregeorev.2016.09.030

Savard, D., Barnes, S.J. and Meisel, T., 2010. Comparison between nickel-sulfur fire assay Te co-precipitation and isotope dilution with high-pressure asher acid digestion for the determination of platinum-group elements, rhenium and gold. Geostandards and Geoanalytical Research 34, 281–291. https://doi.org/10.1111/j.1751-908X.2010.00090.x

Schissel, D., Tsvetkov, A.A., Mitrofanov, F.P., Korchagin, A.U., 2002. Basal platinum-group element mineralization in the Federov Pansky layered mafic intrusion, Kola Peninsula, Russia. Economic Geology 97, 1657–1677. https://doi.org/10.2113/gsecongeo.97.8.1657

Seat, Z., Beresford, S.W., Grguric, B.A., Waugh, R.S., Hronsky, J.M.A., Gee, M.A.M., Groves, D.I., Mathison, C.I., 2007. Architecture and emplacement of the Nebo–Babel gabbronorite-hosted magmatic Ni–Cu–PGE sulphide deposit, West Musgrave, Western Australia. Mineralium Deposita 42, 551–581. https://doi.org/10.1007/s00126-007-0123-9

Sharpe, M.R., Bahat, D., Gruenewaldt, G.V., 1981. The concentric elliptical structure of feeder sites to the Bushveld complex and possible economic implications. Transactions of the Geological Society of South Africa 84, 239–244. https://hdl.handle.net/10520/AJA10120750_2879

Shimizu, K., Nakamura, E., Maruyama, S., 2005. The geochemistry of ultramafic to mafic volcanics from the Belingwe greenstone belt, Zimbabwe: Magmatism in an Archaean continental large igneous province. Journal of Petrology 46, 2367–2394 https://doi.org/10.1093/petrology/egi059

Smith, W.D., Maier, W.D., 2021. The geotectonic setting, age and mineral deposit inventory of global layered intrusions. Earth-Science Reviews 220, 103736. https://doi.org/10.1016/j.earscirev.2021.103736

Sobolev, A.V., Asafov, E.V., Gurenko, A.A., Arndt, N.T., Batanova, V.G., Portnyagin, M.V., Garbe-Schönberg, D., Wilson, A.H., Byerly, G.R., 2019. Deep hydrous mantle reservoir provides evidence for crustal recycling before 3.3 billion years ago. Nature 571, 555–559. https://doi.org/10.1038/s41586-019-1399-5

Sorjonen-Ward, P., Luukkonen, E.J., 2005. Archaean rocks, in: Lehtinen, M., Nurmi, P.A., Rämö, O.T. (Eds.), Precambrian Geology of Finland – Key to the Evolution of the Fennoscandian Shield. Elsevier, Amsterdam, pp. 19–99. https://doi.org/10.1016/S0166-2635(05)80003-9

Stepanova, A.V., Samsonov, A.V., Salnikova, E.B., Puchtel, I.S., Larionova, Yu.O., Larionov, A.N., Stepanov, V.S., Shapovalov, Y.B., Egorova, S.V., 2014. Palaeoproterozoic continental MORB-type tholeiites in the Karelian Craton: Petrology, geochronology, and tectonic setting. Journal of Petrology 55, 1719–1751. https://doi.org/10.1093/petrology/egu039

Stepanova, A.V., Salnikova, E.B., Samsonov, A.V., Egorova, S.V., Larionova, Y.O., Stepanov, V.S., 2015. The 2.31 Ga mafic dykes in the Karelian Craton, eastern Fennoscandian shield: U–Pb age, source characteristics and implications for continental break-up processes. Precambrian Research 259, 43–57. https://doi.org/10.1016/j.precamres.2014.10.002

Svetov, S.A., 2005. Magmatic Systems in the Ocean-Continent Transition Zone in the Archaean of the Eastern Fennoscandian Shield. Karelian Research Center, Russian Academy of Sciences, Petrozavodsk, 230 p. (in Russian)

Svetov, S.A., Smolkin, V.F., 2003. Model P-T conditions of high-magnesia magma generation in the Precambrian of the Fennoscandian Shield. Geochemistry International 41, 799–812

Svetov, S.A., Svetova, A.I., Huhma, H., 2001. Geochemistry of the komatiite-tholeiite rock association in the Vedlozero-Segozero Archaean greenstone belt, Central Karelia. Geochemistry International 39, 24–38

Svetov, S.A., Svetova, A.I., Nazarova, T.N., 2010. Vedlozero-Segozero greenstone belt, Central Karelia: new age data and interpretation of the results. Geology of Useful Minerals of Karelia 13, 5–12 (in Russian)

Tredoux, M., Davies, G., McDonald, I., Lindsay, N.M., 1995. The fractionation of platinum-group elements in magmatic systems, with the suggestion of a novel causal mechanism. South African Journal of Geology 98, 157–167. https://doi.org/10.10520/EJC-929c57f03

Törmänen, T., Konnunaho, J.P., Hanski, E., Moilanen, M., Heikura, P., 2016. The Paleoproterozoic komatiite-hosted PGE mineralization at Lomalampi, Central Lapland Greenstone Belt, northern Finland. Mineralium Deposita 51, 411–430. https://doi.org/10.1007/s00126-015-0615-y

Vogel, D.C., Vuollo, J.I., Alapieti, T.T., James, R.S., 1998. Tectonic, stratigraphic, and geochemical comparisons between ca. 2500–2440 Ma mafic igneous events in the Canadian and Fennoscandian Shields. Precambrian Research 92, 89–116. https://doi.org/10.1016/S0301-9268(98)00073-4

Vuollo, J., Huhma, H., 2005. Paleoproterozoic mafic dykes in NE Finland, in: Lehtinen, M., Nurmi, P.A., Rämö, O.T. (Eds.), Precambrian Geology of Finland – Key to the Evolution of the Fennoscandian Shield. Elsevier, Amsterdam, pp. 195–236. https://doi.org/10.1016/S0166-2635(05)80006-4

Wang, C.Y., Zhou, M.-F., Qi, L., 2007. Permian flood basalts and mafic intrusions in the Jinping (SW China)–Song Da (northern Vietnam) district: Mantle sources, crustal contamination and sulphide segregation. Chemical Geology 243, 317–343. https://doi.org/10.1016/j.chemgeo.2007.05.017

Wang, C.Y., Zhou, M.-F., Qi, L., 2011. Chalcophile element geochemistry and petrogenesis of high-Ti and low-Ti magmas in the Permian Emeishan large igneous province, SW China. Contributions to Mineralogy and Petrology 161, 237–254. https://doi.org/10.1007/s00410-010-0529-8

Weihed, P., Arndt, N., Billström, K., Duchesne, J.-C., Eilu, P., Martinsson, O., Papunen, H., Lahtinen, R., 2005. Precambrian geodynamics and ore formation: The Fennoscandian Shield. Ore Geology Reviews 27, 273–322. https://doi.org/10.1016/j.oregeorev.2005.07.008

Wendlandt, R.F., 1982. Sulphide saturation of basalt and andesite melts at high pressures and temperatures. American Mineralogist 67, 877–885.

Wilson, A.H., Naldrett, A.J., Tredoux, M., 1989. Distribution and controls of platinum group element and base metal mineralization in the Darwendale subchamber of the Great Dyke, Zimbabwe. Geology 17, 649–652. https://doi.org/10.1130/0091-7613(1989)017<0649:DACOPG>2.3.CO;2

Worsham, E.A., Bermingham, K.R. and Walker, R.J., 2016. Siderophile element systematics of IAB complex iron meteorites: New insights into the formation of an enigmatic group. Geochimica et Cosmochimica Acta 188, 261-283. https://doi.org/10.1016/j.gca.2016.05.019

Yang, A.Y., Zhou, M.F., Zhao, T.P., Deng, X.G., Qi, L. and Xu, J.F., 2014. Chalcophile elemental compositions of MORBs from the ultraslow-spreading Southwest Indian Ridge and controls of lithospheric structure on S-saturated differentiation. Chemical Geology 382, 1-13. https://doi.org/10.1016/j.chemgeo.2014.05.019

Yang, S.H., Maier, W.D., Hanski, E.J., Lappalainen, M., Santaguida, F., Määttä, S., 2013. Origin of ultra-nickeliferous olivine in the Kevitsa Ni–Cu–PGE-mineralized intrusion, northern Finland. Contributions to Mineralogy and Petrology 166, 81–95. https://doi.org/10.1007/s00410-013-0866-5

Yang, S.H., Hanski, E., Li, C., Maier, W.D., Huhma, H., Mokrushin, A.V., Latypov, R., Lahaye, Y., O'Brien, H., Qu, W.-J., 2016. Mantle source of the 2.44–2.50-Ga mantle plume-related magmatism in the Fennoscandian Shield: evidence from Os, Nd, and Sr isotope compositions of the Monchepluton and Kemi intrusions. Mineralium Deposita 51, 1055–1073. https://doi.org/10.1007/s00126-016-0673-9

Zhang, M., O'Reilly, S.Y., Wang, K.-L., Hronsky, J., Griffin, W.L., 2008. Flood basalts and metallogeny: The lithospheric mantle connection. Earth-Science Reviews 86, 145–174. https://doi.org/10.1016/j.earscirev.2007.08.007

RES TERRAE

UNIVERSITY
OF OULU